

INSTITUTO TECNOLÓGICO Y DE ESTUDIOS
SUPERIORES DE MONTERREY

CAMPUS MONTERREY

GRADUATE PROGRAM IN MECHATRONICS AND
INFORMATION TECHNOLOGIES



TECNOLÓGICO
DE MONTERREY

MODELING THE EFFECTS OF EXERCISE ON BLOOD GLUCOSE
CONCENTRATION LEVEL AND THEIR COMPENSATION WITH THE
DESIGN OF A FEEDFORWARD PREDICTIVE CONTROL STRATEGY

THESIS

PRESENTED AS A PARTIAL FULFILLMENT OF THE
REQUIREMENTS FOR THE DEGREE OF
MASTER OF SCIENCE WITH MAJOR IN AUTOMATION

BY

LEON CANTU GARCIA

MONTERREY, N. L. DECEMBER 2009

**INSTITUTO TECNOLÓGICO Y DE ESTUDIOS
SUPERIORES DE MONTERREY**

CAMPUS MONTERREY

**GRADUATE PROGRAM IN MECHATRONICS AND
INFORMATION TECHNOLOGIES**



**TECNOLÓGICO
DE MONTERREY**

**MODELING THE EFFECTS OF EXERCISE ON BLOOD GLUCOSE
CONCENTRATION LEVEL AND THEIR COMPENSATION WITH THE
DESIGN OF A FEEDFORWARD PREDICTIVE CONTROL STRATEGY**

THESIS

**PRESENTED AS A PARTIAL FULFILLMENT OF THE
REQUIREMENTS FOR THE DEGREE OF
MASTER OF SCIENCE WITH MAJOR IN AUTOMATION**

BY

LEON CANTU GARCIA

MONTERREY, N. L. DECEMBER 2009

© León Cantú García, 2009

**INSTITUTO TECNOLÓGICO Y DE ESTUDIOS
SUPERIORES DE MONTERREY**

MONTERREY CAMPUS

**GRADUATE PROGRAM IN MECHATRONICS AND
INFORMATION TECHNOLOGIES**



**TECNOLÓGICO
DE MONTERREY®**

**MODELING THE EFFECTS OF EXERCISE ON BLOOD GLUCOSE
CONCENTRATION LEVEL AND THEIR COMPENSATION WITH THE
DESIGN OF A FEEDFORWARD PREDICTIVE CONTROL STRATEGY**

THESIS

**PRESENTED AS A PARTIAL FULFILLMENT OF THE REQUIREMENTS
FOR THE DEGREE OF**

MASTER OF SCIENCE WITH MAJOR IN AUTOMATION

BY

LEÓN CANTÚ GARCÍA

MONTERREY, N.L., MEXICO. DEC, 2009

**MODELING THE EFFECTS OF EXERCISE ON BLOOD GLUCOSE
CONCENTRATION LEVEL AND THEIR COMPENSATION WITH THE
DESIGN OF A FEEDFORWARD PREDICTIVE CONTROL STRATEGY**

BY

LEÓN CANTÚ GARCÍA

THESIS

**PRESENTED TO THE GRADUATE PROGRAM IN MECHATRONICS AND
INFORMATION TECHNOLOGIES**

**THIS THESIS IS A PARTIAL REQUIREMENT FOR THE DEGREE
OF MASTER OF SCIENCE WITH MAJOR IN**

AUTOMATION

**INSTITUTO TECNOLÓGICO Y DE ESTUDIOS
SUPERIORES DE MONTERREY**

MONTERREY CAMPUS

DECEMBER, 2009

To God, for standing always by my side.

To Mirtala and Francisco, for being my greatest support.

To Ismael, for sharing his medical knowledge.

To Celina, for her company and love.

To AECR, for being an unconditional friend.

For the Town boys, for making the stress to go away.

To myself.

To my teachers, for sharing their knowledge.

Abstract

Diabetes Mellitus disease is the principle cause of death in Mexico since year 2000, especially for the different complications that arise from this illness, such as heart, kidney, and hepatic failure. The principal risk factors that highly alter glucose concentration level in diabetic patients are carbohydrates consumption and prolonged exercise. This is due to a null insulin production in the Langerhans cells or to an increase of insulin resistance in the biochemical receptors of the body.

Today's treatments for controlling blood glucose level, which are the injection of insulin boluses and the following of a special nutritional regimen, are very susceptible to human errors, so there is a latent possibility that damage can be done to the patients health. Therefore, it is indispensable to regulate glucose concentration level in an automatic form.

In this research area, the scientist have mainly developed control strategies that impede glucose level to increase when the patients has a meal; successful results have been reported. However, no investigation was found concerned with the regulation of glucose level when physical activity is done, and which is an important factor, since prolonged exercise can cause hypoglycemic episodes that can lead to severe injuries in the person, even death.

In this thesis research, two major innovations were achieved: a nonlinear statistical mathematical model that represents the effects of exercise on blood glucose concentration and the design of a feedforward predictive compensator that impedes glucose decrement.

Successful simulations were obtained, since the proposed advanced control strategy regulated the blood glucose level when physical activity, limited to a duration of 120 minutes and from low to mid-high intensity, was performed. Also, it was demonstrated that this algorithm can be applied along with control strategies that react to an increase of glucose level due to postprandial conditions.

Table of contents

Abstract	1
Chapter 1	1
Introduction	1
1.1. Justification	2
1.2. Problem Statement	2
1.3. Objectives	2
1.4. Contents description	3
Chapter 2	4
Background	4
2.1. Biological sciences	4
2.1.1. Endocrinology basis	4
2.1.2. Glucose and its metabolism	5
2.1.2.1. Glucose structure	5
2.1.2.2. Glycolysis.....	6
2.1.3. Glucose regulation via insulin and glucagon hormones.....	11
2.1.3.1. Insulin effects.....	11
2.1.3.2. Glucagon effects	12
2.1.4. Diabetes Mellitus.....	12
2.1.5. Homeostasis changes during exercise.....	14
2.1.5.1. Effects on Heart Rate.....	14
2.1.5.2. Effects on Oxygen Uptake	14
2.1.5.3. Effects on Blood Flow	14
2.1.5.4. Effects on glucose and insulin plasma levels	15
2.2. Systems Identification and Control Theory	16
2.2.1. Systems Identification and Modeling.....	16
2.2.2. Control Theory.....	18

Chapter 3	20
State of the art	20
3.1. Glucose model development	20
3.1.1. Ackerman’s model.....	20
3.1.2. Sorensen’s model	22
3.1.2.1. Sorensen’s base model	22
3.1.2.2. Sorensen’s model with the addition of exercise as a disturbance	23
3.1.3. Bergman’s model.....	28
3.1.3.1. Bergman’s base model.....	28
3.1.3.2. Bergman’s base model with the addition of exercise as a disturbance	30
3.2. Glucose control strategies	35
3.2.1. Feedback strategy.....	36
3.2.1.1. Definition	36
3.2.1.2. Application to glucose-insulin system.....	36
3.2.2. Feedforward strategy	36
3.2.2.1. Definition	36
3.2.2.2. Disturbance modeling applied to the glucose – insulin system	36
3.2.3. Adaptive control strategy	39
3.2.3.1. Definition	39
3.2.3.2. Application to glucose-insulin system.....	39
3.2.4. Robust control strategy	40
3.2.4.1. Definition	40
3.2.4.2. Application to glucose-insulin system.....	41
3.2.5. Optimal control strategy	41
3.2.5.1. Definition	41
3.2.5.2. Application to glucose-insulin system.....	42
3.2.6. Intelligent materials applied to glucose-insulin system	43
3.3. Areas of opportunity	44
Chapter 4	45
Analytical modeling	45
4.1. Modeling exercise effects	45

4.1.1. Modification in Sorensen’s model.....	45
4.1.2. Simulation of modified Sorensen’s model	48
4.1.3. Simulation of the Bergman minimal order model.....	57
4.1.4. Combination of Bergman’s and Sorensen’s model	60
Chapter 5.....	65
Experiment design for statistical modeling.....	65
5.1. Criterion of the statistical experiment design	65
5.2. Data used in glucose system experiment	67
5.3. Data obtained in the experiment.....	70
Chapter 6.....	72
Statistical modeling	72
6.1. Hammerstein – Wiener modeling technique.....	72
6.1.1. Definition	72
6.1.2. System identification via Wiener technique	73
6.1.3. Wiener modeling advantages over other modeling methods	75
6.1.4. Wiener modeling applied to glucose regulation	76
6.1.4.1. Development of the Wiener model without normalization of data.....	77
6.1.4.2. Development of the Wiener model with normalized data ($N(\mu=0, \sigma^2=1)$).....	80
6.1.4.3. Development of the Wiener model with scaling of each input with respect to its maximum value and a sample time of 10 minutes.....	84
6.1.4.4. Development of the Wiener model with scaling of each input by dividing by its maximum value and a sample time of 5 minutes	88
6.1.4.5. Modifications in the chosen predictive model	91
6.1.4.6. Testing phase of the predictive model.....	94
Chapter 7.....	98
Predictive controller design	98
7.1. Model based predictive control strategy applied to glucose level regulation	98
7.2. Physical implementation of the feedforward predictive compensator	116
7.2.1. Disturbance measurement and sensor technology	117
7.2.2. Actuator and reservoir	118
Chapter 8.....	119
Conclusions	119

8.1. Discussion of results	119
8.1.1. Results from analytical modeling	119
8.1.2. Results from statistical modeling	120
8.1.3. Results from the predictive control implementation.....	121
8.2. Conclusions and future challenges	124
8.2.1. Conclusions.....	124
8.2.2. Future challenges	124
Works cited	159

List of tables

Table I. Comparison between aerobic and anaerobic glycolysis.....	6
Table II. Comparison between Diabetes Type I and Type II.	13
Table III. Relationship between blood flow (dL/min) in organs and exercise intensity (%).	15
Table IV. Parameters values of Bergman’s minimal order model.	29
Table V. Parameters values of modified Bergman’s minimal order model	31
Table VI. Parameters values of glycogenolysis depletion rate	33
Table VII. Values used in test I with Sorensen’s model.	48
Table VIII. Values used in test II with Sorensen model.....	53
Table IX. BBD experiment design input values.	66
Table X. Range of the inputs in the experiment design. (Deviation values).	68
Table XI. Initial conditions of the system prior to the experiment.	68
Table XII. New experiment design input values.	69
Table XIII. Parameters of the nonlinear model.	78
Table XIV. Parameters obtained for the linear ARX models without normalizing the data.....	79
Table XV. Parameters of the nonlinear model with $N(\mu=0, \sigma^2=1)$	80
Table XVI. Parameters obtained for the linear ARX models with $N(\mu=0, \sigma^2=1)$	82
Table XVII. Parameters of the nonlinear model dividing each input by to its maximum value.	84
Table XVIII. Parameters obtained for the linear ARX models normalizing each input respect to its maximum value.	86
Table XIX. Parameters of the nonlinear model dividing each input by its maximum value.....	88
Table XX. Parameters obtained for the linear ARX models dividing each input by its maximum value with a sample time of 5 minutes.	90
Table XXI. Parameters obtained for the linear ARX models scaling each input with its maximum value and using equation 6.17.	92
Table XXII. Testing trials of the selected models.....	94
Table XXIII. Initial conditions for PID controller test with exercise as output disturbance.....	99
Table XXIV. Parameters values of the discrete PID controller.	100
Table XXV. Test done in with the designed predictive regulator.	103
Table XXVI. Final test done, combining meal and exercise disturbances.	112
Table XXVII. Comparison in the system’s behavior when it is operated in manual and automatic mode.	116

List of figures

Figure 1. Linear and Hemiacetal ring D-Glucose structures.	6
Figure 2. Food to energy path.	7
Figure 3. Glycolysis reactions. Taken from Alberts.	9
Figure 4. Krebs Cycle. Taken from http://en.wikipedia.org/wiki/File:Citriccycle.svg	10
Figure 5. Oxidative phosphorylation process. Taken from Alberts.	11
Figure 6. Statistical identification of a system.	16
Figure 7. Block diagram of statistical modeling.	17
Figure 8. Control system block diagram. $R(t)$ is the reference signal,	19
Figure 9. Compartments in Sorensen's model	22
Figure 10. Peripheral glucose uptake by exercising muscle. Solid line is the prediction	25
Figure 11. Glucose response to a 30% PVO_2^{max} step. Dotted line represents	27
Figure 12. Glucose response to a 60% PVO_2^{max} step. Dotted line represents	27
Figure 13. Sorensen's model adding the effect of exercise.	28
Figure 14. Bergman's minimal order model of glucose-insulin interaction.	29
Figure 15. Dependence of glycogen depletion commencement time, t_{gly} on exercise intensity $u_3(t)$	32
Figure 16. Glucose (Top) dynamics due to exercise at intensity of 30% PVO_2^{max} ,	34
Figure 17. Glucose dynamics due to exercise at intensity of 60% PVO_2^{max} ,	34
Figure 18. Block diagram of glucose – insulin control system.	35
Figure 20. Glucose response prediction due to different inputs using H-W	37
Figure 19. Block diagram of Feedforward strategy.	37
Figure 21. Glucose response prediction due to different inputs. Using H-W method on a five days trial. .	38
Figure 22. Glucose response prediction due to different inputs. Using H-W method on	38
Figure 23. Block diagram of adaptive control strategy.	39
Figure 24. Results of glucose regulation using Run to run strategy.	40
Figure 25. Schematic of a system's model, $G_1(s)$, with parameters uncertainty addition	41
Figure 26. Block diagram of closed loop system for the regulation of	42
Figure 27. Glucose regulation using an optimal control strategy, with	43
Figure 28. Plasma glucose and insulin responses, using an intelligent	44
Figure 29. Schematic of the implementation of the global Sorensen's model.	49
Figure 30. Schematic of the compartments in Sorensen's model. Red lines limit glucose compartments; 49	49
Figure 31. Schematic of exercise effects in Sorensen's model: pancreatic glucose uptake and	50
Figure 32. Dynamic response of $\%PVO_2^{max}$ (blue) and 25% PAMM input (red).	50
Figure 33. Dynamic response of PGU_a (blue) with 25% PAMM or 30% PVO_2^{max}	51
Figure 34. Dynamic response of net HGP_a (blue) with 25% PAMM or 30% PVO_2^{max}	51
Figure 35. Dynamic responses of blood flows (L/min) for insulin transport in the	52
Figure 36. Dynamic responses of blood flows (dL/min) for glucose transport in the	52
Figure 37. Dynamic responses of glucose (green) (mg/dL) and insulin (red) (mU/L)	53
Figure 38. Dynamic response of $\%PVO_2^{max}$ (blue) and 59.1% PAMM input (red).	54

Figure 39. Dynamic response of PGU_o (blue) with 59.1% PAMM or 60% PVO_2^{max}	54
Figure 40. Dynamic response of net HGP_o (blue) with 59.1% PAMM or 60% PVO_2^{max}	55
Figure 41. Dynamic responses of blood flows (L/min) for insulin convective transport	55
Figure 42. Dynamic responses of blood flows (dL/min) for glucose convective transport.	56
Figure 43. Dynamic responses of glucose (green (mg/dL)) and insulin (red) (mU/L)	56
Figure 44. Global schematic of the implementation of Bergman.....	57
Figure 45. Compartments X (remote insulin), I (arterial insulin) and	58
Figure 46. Schematic of the compartments where PVO_2^{max} , PGU_o and net HGP_o are calculated.....	58
Figure 47. Response of glucose (blue)(mg/dL) and insulin (μ U/mL) arterial concentration with an	59
Figure 48. Response of glucose (blue)(mg/dL) and insulin (μ U/mL) arterial concentration with an	60
Figure 49. Schematic of the implementation of hepatic glucose production	62
Figure 50. Schematic of the combination of Sorensen's and.....	63
Figure 51. Response of glucose level (blue) (mg/dL) to external glucagon infusion rate step (green) (10^4 pg/min).	63
Figure 52. Glucose rate of change (mg/dL/min) response to a pulse input of 30 PAMM(%) from	67
Figure 53. Data obtained in the experiment: Glucose concentration (blue) (mg/dL) response to	70
Figure 54. Data obtained in the experiment: Glucose rate of change (blue) (mg/dL/min).	71
Figure 55. Block diagram of Wiener system for one output η_i	73
Figure 56. Performance of the system in the training and testing phases.....	76
Figure 57. Comparison between the predicted nonlinear steady state glucose concentration	78
Figure 58. Predicted glucose rate of change and its real value obtained in the experiment,	80
Figure 59. Comparison between the predicted nonlinear steady state glucose	82
Figure 60. Predicted glucose concentration rate of change and its real value obtained in the experiment,	84
Figure 61. Comparison between the predicted nonlinear steady state glucose concentration rates	86
Figure 62. Predicted glucose rate of change and its real value obtained in the experiment,	88
Figure 63. Comparison between the predicted nonlinear steady state glucose concentration rates	90
Figure 64. Predicted glucose concentration rate of change and its real value obtained in the experiment,	91
Figure 65. Predicted glucose concentration rate of change and its real value obtained in the experiment,	92
Figure 66. Comparison between the predicted and real glucose concentration rate in trial #1.	95
Figure 67. Comparison between the predicted and real glucose concentration rate in trial #2.	95
Figure 68. Comparison between the predicted and real glucose concentration rate rate in trial #3	96
Figure 69. Comparison between the predicted and real glucose concentration rate in trial #4.	96
Figure 70. Comparison between the predicted and real glucose concentration rate in trial #5.	97
Figure 71. Comparison between the predicted and real glucose concentration rate in trial #6.	97
Figure 72. Response of glucose level (mg/dL) (blue) in close loop, with	99
Figure 73. Flow chart of the predictive control algorithm for exercise effects compensation.	101
Figure 75. Implementation schematic of complete automatic system with predictive control strategy for compensation of exercise effects.	103

<i>Figure 74. Block diagram of complete glucose level control system with compensation of exercise effects</i>	102
<i>Figure 76. Performance of predictive control strategy, with 10% PAMM (blue) and</i>	105
<i>Figure 77. Performance of predictive control strategy, with 15% PAMM (blue) and</i>	105
<i>Figure 78. Performance of predictive control strategy, with 20% PAMM (blue) and</i>	106
<i>Figure 79. Performance of predictive control strategy, with 25% PAMM (blue) and</i>	106
<i>Figure 80. Performance of predictive control strategy, with 30% PAMM (blue) and</i>	107
<i>Figure 81. Performance of predictive control strategy, with 35% PAMM (blue) and</i>	107
<i>Figure 82. Performance of predictive control strategy, with 40% PAMM (blue) and</i>	108
<i>Figure 83. Performance of predictive control strategy, with 40% PAMM (blue) and</i>	108
<i>Figure 84. Performance of predictive control strategy, with 10% PAMM (blue) and</i>	109
<i>Figure 85. Performance of predictive control strategy, with 30% PAMM (blue) and</i>	109
<i>Figure 86. Performance of predictive control strategy, with 40% PAMM (blue) and</i>	110
<i>Figure 87. Performance of predictive control strategy, with 10% PAMM (blue) and</i>	110
<i>Figure 88. Performance of predictive control strategy, with 30% PAMM (blue) and</i>	111
<i>Figure 89. Performance of predictive control strategy, with 40% PAMM (blue) and</i>	111
<i>Figure 90. Performance of predictive control strategy, with 10% PAMM (blue) and</i>	112
<i>Figure 91. Performance of glucose level when meal and exercise disturbance excite the system</i>	113
<i>Figure 92. Manipulated variables of the feedback PID controller (external insulin in mU/min)(green) and feedforward predictive compensator (external glucagon in pg/min)(blue)</i>	114
<i>Figure 93. Response of blood glucose level when meal and exercise disturbance excite the system in manual mode</i>	115
<i>Figure 94. Performance of predictive control strategy. With 40% PAMM (blue) and a duration of 150 minutes. Glucose steady state level at 90 mg/dL(cyan).Glucose concentration response in red. Insulin concentration level in green.</i>	121
<i>Figure 95. Performance of predictive control strategy. With 45% PAMM (blue) and a duration of 100 minutes. Glucose steady state level at 90 mg/dL(cyan).Glucose concentration response in red. Insulin concentration level in green.</i>	122
<i>Figure 96. Performance of predictive control strategy. With 40% PAMM (blue) and a duration of 200 minutes. Glucose steady state level at 90 mg/dL(cyan).Glucose concentration response in red. Insulin concentration level in green.</i>	122
<i>Figure 97. Glucose rate of change (mg/dL/min)(blue) with 40% PAMM</i>	123

Chapter 1

Introduction

Nowadays, long term healthcare treatment of several diseases requires special and careful attention. Diabetes Mellitus disease is one of the multiple examples that can be cited. According to stats from INEGI (Mexican Government agency in charge of demographic statistics), diabetes has been the principle cause of death in Mexico since year 2000, especially for the different complications that arise from this disease, such as heart, kidney, and hepatic failure.

The care of this illness generally consists of applying a subcutaneous or intravenous injection of insulin, in an open loop way, meaning that the patient has to do it according to his previous experience or by measuring his actual glucose level in a manual form (Doyle, Jovanic, & Seborg, 2007). Nevertheless, there are several complications that can occur due to a mal-practice of the insulin shot, like hyper-hypo glycemic levels, causing from body ache to serious organ damage that could have decease as an outcome.

There are other risk factors that can modify plasma glucose level, these being carbohydrates intake and prolonged exercise the major ones; these, respectively, increase and decrease the level. This is the main reason, why human physiology during exercise will be taken into account, as well the effects that it produces on insulin and glucose metabolism.

Based on these reasons, as well as for patient comfort and safety, it is highly important to continue the pertinent research in automated systems that deliver an exact and precise quantity of insulin at the time the patient needs it. Insulin infusion pumps and glucose sensors have been the major technology issue for the last twenty year, a great number of control strategies that could be implemented for the regulation of the insulin-glucose physiologic system via negative feedback have been developed since 1960, such as PID, Run to Run, One step ahead and other feedback techniques (Doyle, Jovanic, & Seborg, 2007). However, because of the inherent integral action of these methods, an overdose of insulin might happen, resulting in a hypoglycemic episode for the user.

As control strategies for this system improved, mathematical models representing insulin and glucose dynamics were needed, so the regulation of blood glucose levels could be assured. Several analytical models were developed, such as the models by Sorensen (Parker, 2000), Bergman (Khou, 1999) and Havorka (Doyle, Jovanic, & Seborg, 2007) that quantify the glycemic and insulin levels as a function of external and initial conditions, like carbohydrates intake, external insulin bolus, basal glucose

and insulin level, etc. This is a priority when dealing with the automation of any system, knowing the response of the process depending on some conditions.

According to Doyle et al. (2007) diabetic people can control their glucose level by following a special low carbohydrate diet and exercising in a moderate way for a brief period of time. The main reason why they can only exercise for a short time is because after 30 to 40 minutes, their glucose level tends to decrease at a high rate, and given the condition that they use insulin shots, hypoglycemic state will appear. In the next chapters, more information about physiology during exercise will be discussed.

1.1. Justification

The principle motivations for this research are:

- Prolonged exercise can cause serious problems to the patient's safety if it is not regulated.
- There is not a control strategy that impedes glucose level changes caused by exercise.
- In the literature, a statistical physiological model was not found that suited glucose response due to exercise changes because of its nonlinear and unstable nature.
- Controlling glucose levels caused by different perturbations can help in the creation of an artificial pancreas, improving people's quality of life.

1.2. Problem Statement

Eventual or unintended increase in physical activity for relatively short periods of time, below 2 hours in a continuous form, makes glucose plasma level decrease, causing undesired symptoms that can put the patient's life in danger, especially the ones with Diabetes Mellitus. So it is necessary to compensate the negative effects of exercising at a high intensity.

1.3. Objectives

According to the needs stated in the justification section, the objectives of this thesis are

- Analysis of the response of glucose level when exercise is done.
- Combination of different analytical models, with the purpose of generating useful data that represent the system's behavior.
- Development of a statistical model that relates exercise intensity and glucose level.
- Design of a control strategy that compensates the effect of exercise on glucose level, without producing a hypo-hyper glyceemic state.
- Analysis of the combination of an exercise compensator and a PID control scheme.

1.4. Contents description

The organization of the contents of this dissertation are explained in the following paragraphs:

Chapter 2 is divided in two parts. The first section deals with biological aspects, like the explanation of glucose, insulin and glucagon physiology and their role and effects on the body, description of Diabetes Mellitus (its symptoms and its consequences) and finally, human physiology during exercise. In the second part, systems identification and control theory are explained.

In Chapter 3, the state-of-the-art of modeling and control of the glucose-insulin process is discussed.

Chapter 4 deals with fitting of clinical reported data with the mathematical models that are used in this thesis. Also a comparison between the models by Sorensen and Bergman models is shown, as well as how they can be combined.

Chapter 5 outlines the experiment design with the purpose of obtaining a statistical model that relates glucose rate of change with exercise, insulin and glucagon. It is explained why firstly Box-Behnken Design (BBD) experiment is chosen; also the reasons for the selected inputs and output ranges, and finally the decision of using glucose rate of change and not glucose itself will be discussed.

Chapter 6 presents the statistical model that fits the data generated by the simulated experiment. First the Hammerstein-Wiener modeling technique and its advantages are described; afterwards, the application of this method to the modeling of glucose rate of change is analyzed; and in the end, the methods of minimum square error for nonlinear systems and multiple regression used for obtaining the value of the parameters are mentioned.

Chapter 7 explains the compensation algorithm to prevent glucose level from decreasing, via glucagon application, this is done using the inputs of the model and the measurement of glucose itself.

Finally, Chapter 8 shows the results obtained using the exercise compensator and a PID controller in a close loop way and what can be done in order to improve the efficiency of the compensator; and the conclusions of this thesis.

Chapter 2

Background

This chapter is divided into two major parts: biological and control basics. The first part is an introduction to biological sciences, focused on the endocrinology of insulin and glucagon hormones, the definition of Diabetes Mellitus and its consequences, and the physiology during exercise. The second part summarizes modeling principles and presents the definitions of elements, variables, operation modes and types of control systems.

2.1. Biological sciences

2.1.1. Endocrinology basis

For an optimal performance of the human body, cardiovascular, neurological, nephrological and endocrinological systems, among others, must work in a perfect form. Because this investigation involves the usage of several hormones, it is important to remark that the Endocrinological system has the responsibility of keeping them in a level so life can be sustained.

According to Kronenberg (2002), an endocrinological hormone is a substance that is released by a glandule into the blood stream and has the capability of making the target organ to react, even if there is a long distance between them. The principal elements that form this structure are: hypothalamus, which is located in the front part of the brain; hypophysis, located underneath the hypothalamus; and glandules, like thyroid, testicles, ovaries, suprarenal, etc. The path how this system regulates the hormone levels is:

- The hypothalamus (functioning as a sensor) detects a low concentration of the hormone to be regulated and sends a signal, another hormone, to the hypophysis (acting as a controller), which in turn releases a secondary hormone to an specific glandule (working as an actuator), and this one discharges a last hormone to the target organ (that happens to be the plant).

As it can be seen, this path has a huge importance since it allows feedback (negative or positive) of the current hormone level. In medical terms, a positive feedback means incrementing the release of a hormone, and a negative feedback, decreasing it. This control mechanism impedes an unbalance of hormones in the body, due to a large or a low concentrations of them, that can provoke diseases like the Cushing Syndrome. The main reason of failure in this path is when a tumor arises in any of its elements.

It is important to remark the action mechanism and effects of the hormone released by a glandule in the target organ. The hormone anchors in specific receptors located in the cell membrane or in the nucleus and produces a desired reaction. If the receptors that detect the hormone are in the membrane, they generate a series of events, called second messengers, inside the cell, but if they are in the nucleus, their action consists on a modification of the DNA.

2.1.2. Glucose and its metabolism

2.1.2.1. Glucose structure

Glucose, also known as Dextrose, is the molecule that gives most of the energy that human body need. It is a monosaccharide classified as an aldohexose because it has an aldehyde group, $\overset{\text{O}}{\parallel}{\text{C}}-\text{H}$, with six carbon atoms, and it enter most of the cells via passive transport, but when dealing with digestive organs, it needs an active transport, meaning that it uses an hormone to allow its entrance.

According to McKee (2003), the roles of glucose in the organism are

- Principal source of energy in the body.
- Only source of energy of the brain and red cells.

Glucose can be obtained by two ways:

- Glycogenesis: deployment of complex carbohydrates, like lactose, maltose, etc., into glucose, and synthesis of glycogen from the excess of glucose.
- Gluconeogenesis: transformation of proteins and lipids into glucose.

Basically, there are two glucose isomers: D-glucose and L-glucose. The first enantiomer is the only one that can be used as a source of energy in cells. D-glucose can be found in two different structures, in a linear form and as a hemiacetal ring, the difference between them relies in their stability properties. Nevertheless, when glucose reacts with body fluids it does it in its open structure, but there can also be found hemiacetal ring structures (Ritter, 1996).

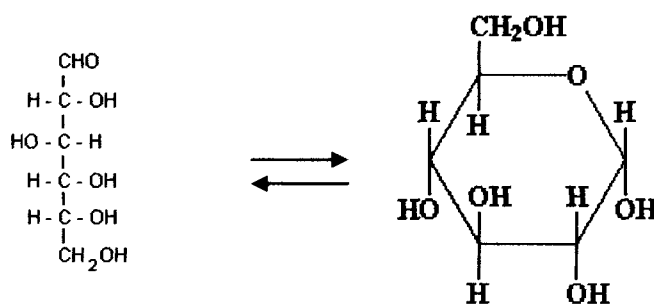


Figure 1. Linear and Hemiacetal ring D-Glucose structures.

2.1.2.2. Glycolysis

Metabolism is defined as the chemical reactions that occur in the body in order to obtain energy (Guyton & Hall, 2001). It can be divided in two major parts: catabolism and anabolism. The first one is the process of converting complex macromolecules into simple molecules; anabolism designates the reactions that make a macromolecule from simple elements.

Glycolysis is the metabolism of glucose. Depending on the organism and the cells specialization, there can be two types of glycolysis, which are aerobic and anaerobic. The usage of depends on the cardiovascular system's capacity of satisfying the oxygen and glucose uptake demands by the muscles (Alberts, 2002).

Pasteur classified the cells in charge of oxidizing glucose in three categories: strict aerobe cells that form CO₂ and H₂O; anaerobe strict cells that form lactic acid and facultative anaerobe cells that behaves as either of the other two types of cells (Murray, 1993).

Table I. Comparison between aerobic and anaerobic glycolysis.

	Glucose uptake	Lactic acid production	CO ₂ production
Aerobic	Low	None	High
Anaerobic	High	High	None

The conversion of glucose into energy has several biochemical steps that occur in the cells mitochondria, and takes different paths depending on the type of glycolysis.

The first step is transforming glucose into pyruvate, in medical terms this is known as glycolysis. It is important to acknowledge that aerobic and anaerobic glycolysis follow these same reactions and the total gain of this phase is 4 adenosine triphosphate (ATP) and 2 nicotinamide adenine dinucleotide (NADH) molecules; the second step is called Kreb's cycle or Citric acid cycle, which has the function of capturing H⁺ from the different reactions that happen inside the mitochondria; the third step has the main goal of generating ATPs from the hydrogen obtained in the NADH and FADH₂ molecules via the two

previous steps; Oxidative phosphorylation is the third step and is in charge, literally, of energy generation. This process occurs in the intermembrane space of the mitochondria.

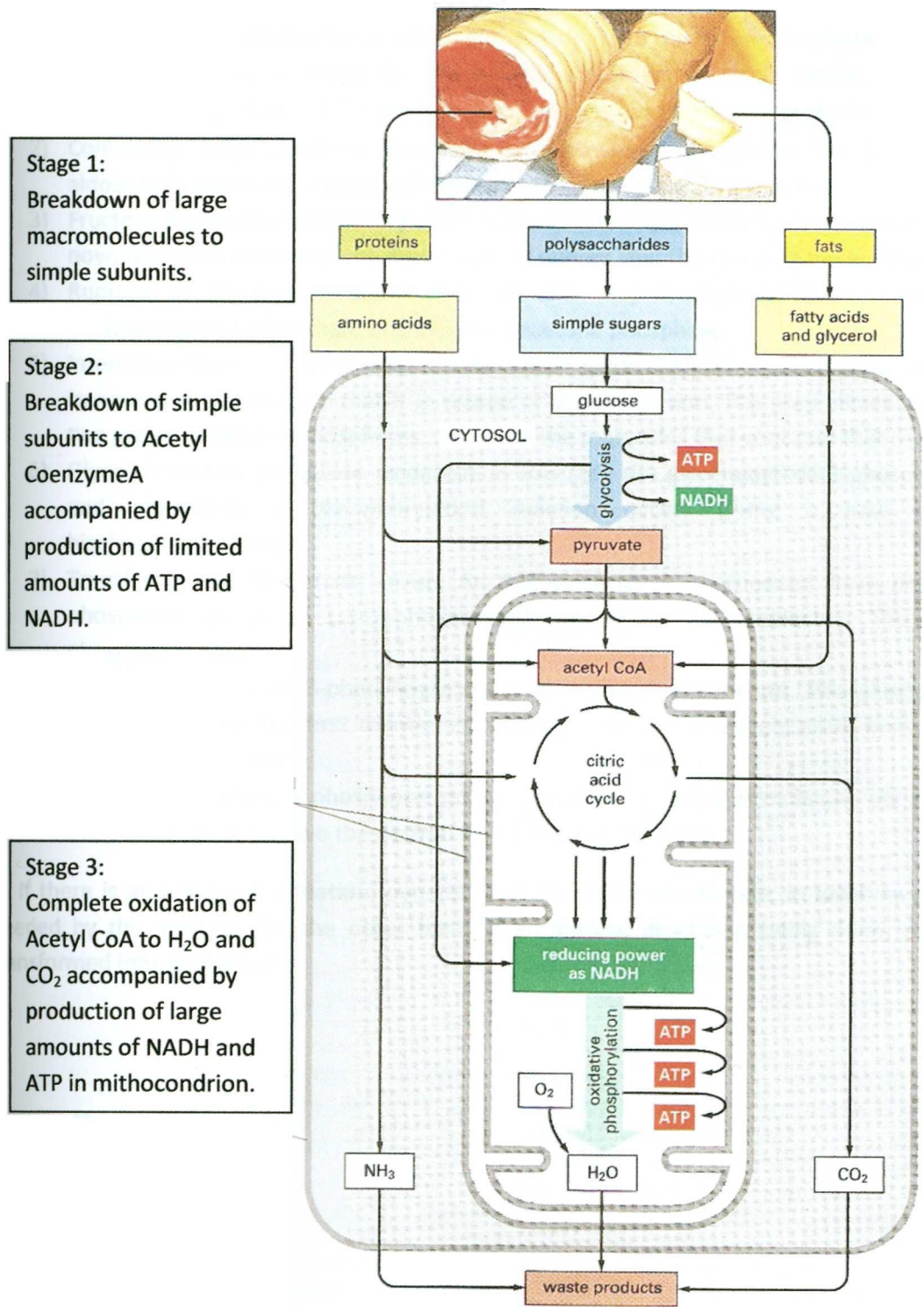


Figure 2. Food to energy path. Adapted from Albert (2002).

Following, the principle reactions in glycolysis are described:

- 1) Glucose-6-phosphate synthesis. When glucose enters to the cell, a phosphate group coming from an ATP molecule is added via the hexokinase enzyme. This is known as phosphorylation reaction. The purpose of this reaction is to keep the glucose molecule inside the cell.
- 2) Conversion from glucose-6-phosphate into fructose-6-phosphate. The glucose-6-phosphate aldose is changed into a fructose-6-phosphate ketose via an isomerization.
- 3) Fructose-6-phosphate phosphorylation. A phosphate from another ATP molecule is added. Until now, there has been only one investment of energy, and the resulting molecule is 6C-2P.
- 4) Rupture of fructose-1,6-biphosphate. In this step fructose-1,6-biphosphate is split into glyceraldehyde-3-phosphate and dihydroxyacetone phosphate.
- 5) Interconversion of dihydroxyacetone into glyceraldehyde-3-phosphate. Triosephosphate isomerase is the enzyme that is in charge of the conversion. This step allows the body to have two glyceraldehyde-3-phosphates, which are the molecules that continue that next steps.
- 6) Glyceraldehyde-3-phosphate oxidation. In this step the glyceraldehyde-3-phosphate is oxidized and afterwards a phosphorylation reaction occurs giving a new molecule, 1,3-bisphosphoglycerate.
- 7) Transfer of the phosphate group. An ATP molecule is synthesized from the transfer of a phosphoryl group of 1,3-bisphosphoglycerate to an ADP molecule. The product is 3-phosphoglycerate.
- 8) Interconversion from 3-phosphoglycerate to phosphoenolpyruvate. Phosphoglycerate mutase enzyme converts the first mentioned molecule into 2-phosphoglycerate and afterwards into phosphoenolpyruvate.
- 9) Pyruvate synthesis. A phosphoryl group is transfer to an ADP molecule via pyruvate kinase enzyme, in order to have the desired final molecule, pyruvate.

If there is an anaerobic situation, pyruvate will transform into lactate, in order to give the energy needed by the muscles. On the other hand, if an aerobic process is being done, pyruvate will be transformed into Acetyl CoA.

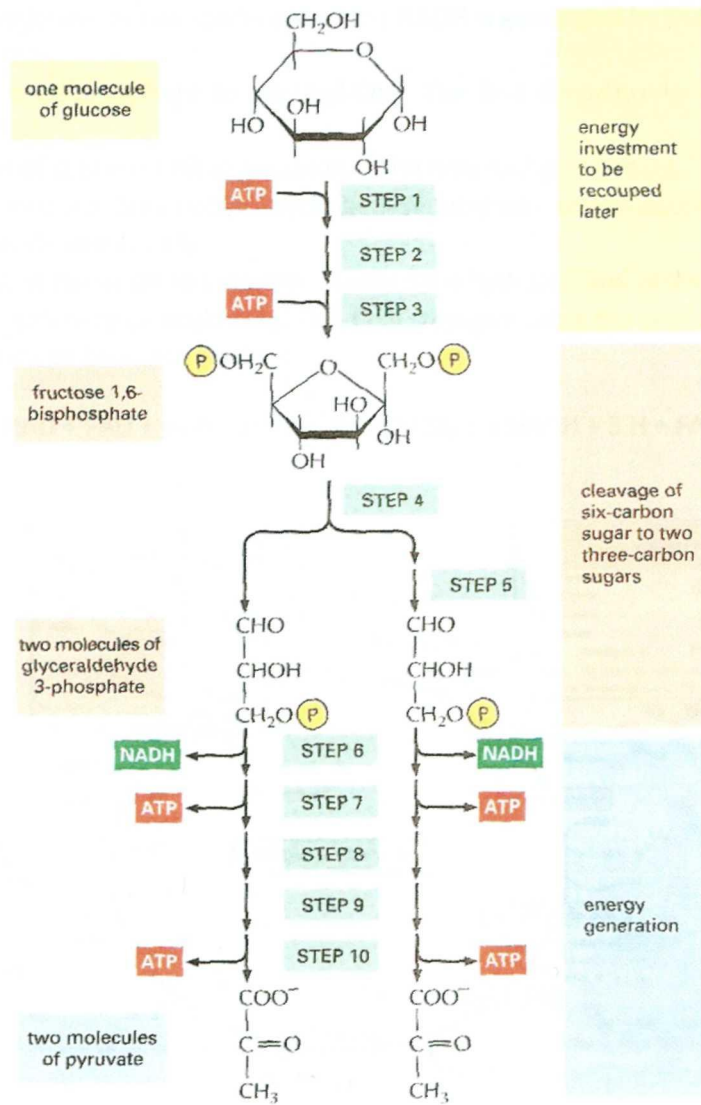


Figure 3. Glycolysis reactions. Taken from Alberts (202).

After glycolysis process ends, the next biochemical reactions that occur in the organism are known as the Krebs cycle.

This energy generation process occurs inside the mitochondria, and it has a net gain of 3 NADH, 1 FADH₂ and 1 ATP. Its main purpose is not the production of ATP but the attainment of hydrogen atoms. Citric acid cycle is divided in eight principal reactions (Alberts, 2002):

- 1) Conversion of acetyl CoA to citrate. The acetyl CoA combines with an oxaloacetate molecule and via the citrate synthase enzyme to form citrate.
- 2) Conversion of citrate into isocitrate and cis-aconitate.

- 3) Oxidation of isocitrate. In this reaction the first NADH is generated by the oxidation of isocitrate to α -ketoglutarate.
- 4) Conversion of α -ketoglutarate to succinyl-CoA. The first decarboxylation occurs and another NADH is obtained.
- 5) Transformation of succinyl-CoA to succinate. The only ATP gain occurs.
- 6) Oxidation of succinate. Succinate-dehydrogenase enzyme oxidizes succinate molecule, in order to obtain Fumarate and FADH_2
- 7) Transformation of fumarate to L-malate. Fumarate is hydrated and generates L-malate.
- 8) Oxidation of L-malate to oxaloacetate. This final step generates the final NADH molecule.

The reaction in this cycle can be summarized as:

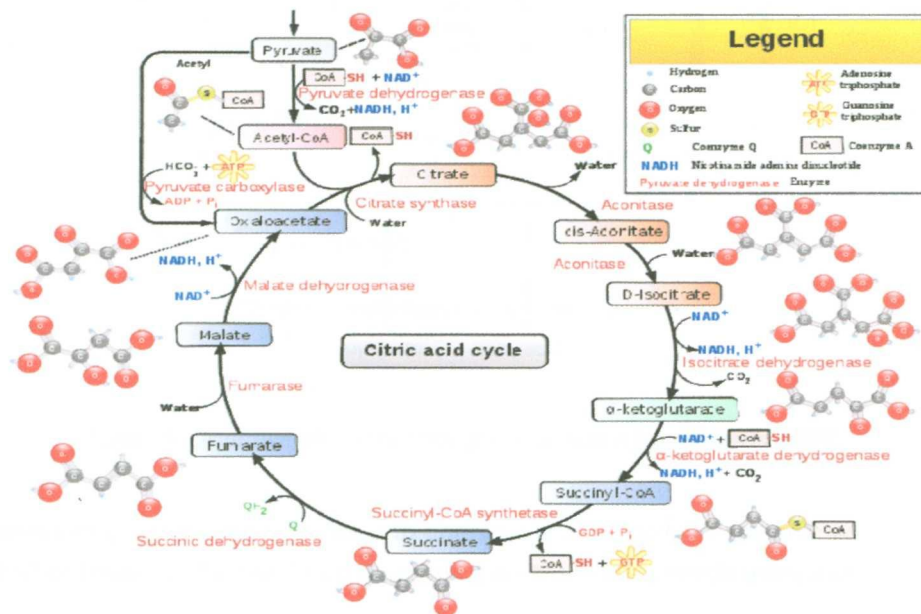
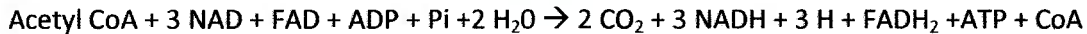


Figure 4. Krebs Cycle. Taken from <http://en.wikipedia.org/wiki/File:Citriccycle.svg>

Finally, the last group of reactions is known as oxidative phosphorylation, which is the most important step.

This process synthesizes ATP when electrons from NADH and FADH_2 are transferred to O_2 in the mitochondria's matrix. The total energy generation is in the order of 3 ATP / 1 NADH and 2 ATP / 1 FADH_2 .

The summary of this process is (Alberts, 2002):

- 1) NADH and FADH_2 are reduced by three enzyme electron complexes.
- 2) The electron transport chain pumps H^+ into the intermembrane space with the purpose of generating a H^+ gradient.
- 3) Due to a H^+ gradient increase in the intermembrane space, H^+ are returned to the mitochondria's matrix using an H^+ pump, also known as ATP pump.

- 4) For an ATP bomb can be used, the complex ADP + Pi (phosphate) must link to it. After the process is done, H⁺ returns to the mitochondria's matrix and a new product is formed, ATP.

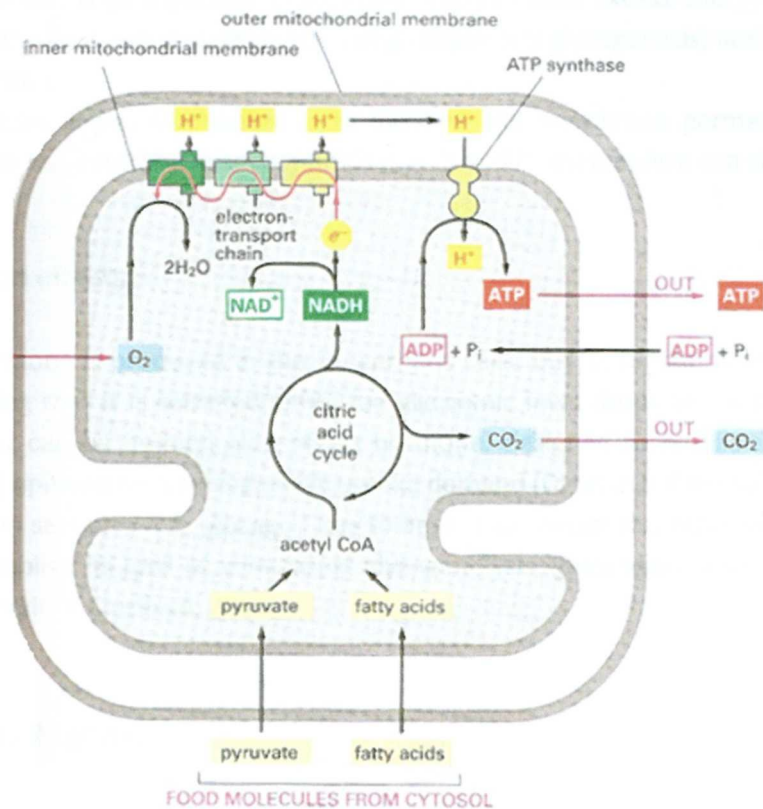


Figure 5. Oxidative phosphorylation process. Taken from Alberts (2002).

As it has been seen, conversion from food to energy is a very complex process, which involves a lot of reactions, but all of them can be regulated depending on the body's needs using enzymes.

2.1.3. Glucose regulation via insulin and glucagon hormones

According to Guyton (2001), the normal glycemic range in the plasma is 60 – 110 mg/dL. When the level drops or is increases beyond these values, the patient starts to feel illness, presenting symptoms, like lack of energy, paleness, headache, among others. It is in this situation when the endocrinology system starts its control with the goal of keeping glucose in the desired range. The two hormones involved in glycemic regulation are insulin and glucagon.

2.1.3.1. Insulin effects

Insulin is an essential life hormone secreted by the Langerhans cells in the pancreas. This hormone has hypoglycemic and protein anabolic effects (Dvorkin & Cardinali, 2003). Insulin secretion is associated

with energy abundance, that is, in presence of a meal bolus (especially carbohydrates) this hormone will be in charge of lowering glucose level.

Another aspect of insulin is its capability of inducing reserves from excess energy; it causes excess glucose to be stored in the liver and muscles in form of glycogen (via glycogenesis) and in adipocyte cells as fat (Guyton & Hall, 2001).

The goal of the insulin action mechanism is to increase the membrane permeability of cells to glucose, so this molecule can enter the mitochondria's matrix and its metabolism can start.

2.1.3.2. Glucagon effects

Like insulin, this hormone is produced in the Langerhans cells, but its functions are the opposite of those of insulin, meaning that it is secreted when the glycaemic level drops and with hyperglycaemic and catabolic effects. It can be defined as a stress hormone, designed to mobilize energy reservoir (glycogen, triglycerides) upon an increased glucose uptake demand (Dvorkin & Cardinali, 2003).

As it was explained in section 2.1.1, glucagon has to anchor to special receptors in the desired cells, so its effects can accomplish its goal of stimulating glycogenolysis, gluconeogenesis, ketogenesis and protein catabolism (Dvorkin & Cardinali, 2003).

2.1.4. Diabetes Mellitus

When there is a problem with insulin receptors or insulin hormone production, usually absence of Langerhans cells, glucose plasma level will increase because it won't be able to enter the target cells, causing diseases in the organism. This complication is called diabetes mellitus and also includes alteration of protein and fat metabolism.

Diabetes mellitus can be divided in two types, which are

- Type I, also known as insulin dependent diabetes.
This class of diabetes arises when there is a failure in insulin production in the Langerhans β -cells due to a genetic problem, virus infections or immune system disorders. According to Guyton (2001), its symptoms usually start in the age of 14 with three essential sequels: hyperglycemic level, increased fat metabolism and protein reduction. With this kind of diabetes, the glucose level increments to 300 – 1200 mg/dL.

Type I diabetes effects:

- Loss of glucose via the urine. When the glycemic level arises, more glucose is filtered to the renal tube than the quantity that can be absorbed, so part of the plasma glucose will end up in the urine.

- Dehydration. It occurs due to an increase of the osmotic pressure in the extracellular compartment, provoking water to flow outside the cell.
 - Tissue lesion. A chronic hyperglycemic level will have a negative impact in the blood vessels, causing a morphological change in them and poor irrigation of several organs. This syndrome will increment the possibility of myocardial infarction, ictus, lethal renal diseases, retina injure, blindness and limbs gangrene.
 - Usage of fat and protein as energy. The alteration of the carbohydrate metabolism will induced the usage of fat to satisfy the energy uptake demand. Nevertheless, the production of keto acids is greater than its consumption, this will provoke a metabolism acidosis that can take the patient to a diabetic coma. Also protein will be used for energy considerations, causing dystrophy in the organism tissues.
- Type II, also known as non-insulin dependence diabetes or insulin resistance.
In this kind of diabetes, there is insulin production but the cells sensitivity to this hormone is very low. As in type I, metabolism of carbohydrates, fats and proteins metabolism is altered, and symptoms are almost the same except for the high production of keto acids.
This is the most common type of Diabetes mellitus, since it includes 90% of this disease cases and it usually starts at the age of 50 (Guyton & Hall, 2001).

Type II Diabetes effects (Guyton & Hall, 2001):

- Increase of plasmatic insulin. Due to a lack of sensitivity in the insulin receptors, glycaemic level increments, this situation makes the β -Langerhans cells produce more of this hormone in order to lower the glucose level, but the response will not be the desired one because of receptors resistance to insulin.
- Obesity. There are two theories of how obesity and diabetes are related. One indicates that obese people have less insulin receptors in the muscles, liver and adipose tissue. The other expresses that there is an alteration in the activation signals on the insulin receptors.

Table II. Comparison between Diabetes Type I and Type II.

Data	Type I	Type II
Appearance age	<20 years	>40 years
Body mass	Reduced	Obesity
Plasmatic insulin	Reduced or absent	Raised
Plasmatic glucagon	Raised	Raised
Plasmatic glucose	Raised	Raised
Insulin sensitivity	Normal	Reduced

Treatment	External insulin	Diet, insulin, exercise
-----------	------------------	-------------------------

Depending on the type of diabetes the patient has, there are several treatments to follow. If it is type I, the only remedy is the external insulin shot, which is classified in two forms: the regular injection, for a basal one-day-long effect, and the supplementary injection, that is taken before a meal.

For type II, exercise and diet are the first treatment. According to Kronenberg (2002), exercise will increment insulin sensitivity in the cells, and glycemic level will decrease as consequence. If this fails, insulin shots have to be taken (Guyton & Hall, 2001)

2.1.5. Homeostasis changes during exercise

During exercise, the body's physiology suffers increased heart rate (HR), blood flow (Q), oxygen uptake (VO_2) and insulin sensitivity. Also plasma glucose and insulin levels decrease (Guyton & Hall, 2001; Firman 2005). Although these changes are beneficial to the organism because it improves the quality of life of people, if a patient has an illness, like Diabetes Mellitus, exercising at a high intensity or for a long time can provoke serious issues to his health.

2.1.5.1. Effects on Heart Rate

According to Firman (2005), the heart rate in an adult person is approximately 78 heart beats/min, but if a person is exercising, it will raise up to 200 heart beats / min, depending on the duration and intensity of the exercise.

Firman showed evidence that HR has a direct relation with oxygen uptake, that depends on the active muscles demand. Firstly there is not enough quantity to satisfy the needs, so a chemical stimulation is induced in order to increase the HR; as a second stage, the increment of the HR will also increase the heart and blood flow, allowing faster oxygen transportation to the active muscles.

2.1.5.2. Effects on Oxygen Uptake

In an adult person, the normal oxygen uptake is 250 mL/min, but it can rise up to 5100 mL/min, depending on the physical resistance. Additionally, this measure can vary due to the person's gender and age. Therefore, it is preferable to handle a percentage of maximum oxygen uptake ratio ($\text{PVO}_2^{\text{max}}$ or $\dot{\text{V}}\text{O}_2^{\text{max}}$), in order to make comparisons among people.

Fehlig and Wahren (1975) reported that $\text{PVO}_2^{\text{max}}$ has a basal value of is 8% and takes approximately from 4 to 5 minutes to reach its maximum.

2.1.5.3. Effects on Blood Flow

In basal conditions, the skeletal muscle only receives 15% of the total heart flow; also the arterioles that irrigate those muscles are closed. However, when exercise begins, the following reactions occur (Firman, 2005):

1. At the beginning of the exercise, as it was explained, heart rate and heart flow increase; this situation induces a reaction in the sympathetic nervous system that will open the arterioles in the skeletal muscles and close the ones in the abdominal region and skin, this is done with the purpose of pumping more blood to the active muscles.
2. The increase of metabolism waste products of skeletal muscles acts as a direct signal in the nervous system, so arteries nearby can dilate, allowing active muscles to receive the blood flow from other zones of the organism; the arterioles from those regions will be closed due to a signal sent by the sympathetic nervous system.

With the knowledge of these effects, Chapman & Mitchell (1965) realized a research pointing out the variations of blood flow in the organs during exercise. It is indispensable to remark that all of these changes are consequences of the active muscular mass, and this one is linked directly to an increase in PVO_2^{max} ; according to Andersen et al. (1985), this means that blood flow in active muscles is a linear function of exercise intensity.

Table III. Relationship between blood flow (dL/min) in organs and exercise intensity (%).

Organ	PVO_2^{max}			
	8%	30%	60%	90%
Brain	5.9	5.9	5.9	5.9
Liver	12.6	9.8	6.1	2.3
Kidneys	10.1	8.1	5.3	2.5
Periphery	15.1	50.6	99.1	147.5

2.1.5.4. Effects on glucose and insulin plasma levels

Firman (2005) indicates that during the first 15 minutes of exercise, glycogen stored in the muscles and plasma glucose is used to satisfy the energy needs; in a second phase, after 30 minutes of exercise had passed, liver glycogen is consumed; and after 40 to 90 minutes, fat metabolism is used in order to obtain energy. All this mechanism has the goal of giving the maximum energy to the active muscles so their demand is fulfill.

The risk that diabetic patients have when they exercise in a moderate or high intensity form is that their plasma glucose level will decrease in such a way that they will suffer of hypoglycemia, causing them several uncomfortable symptoms.

2.2. Systems Identification and Control Theory

2.2.1. Systems Identification and Modeling

According to Ogata (2002), a system is defined as a combination of components that act together and perform a certain objective. In order to fully comprehend any system found in nature, it is necessary to understand and represent how it responds to a known input variable or several inputs. This concept is known as system modeling.

The process of modeling a system can be done in an analytical form, this means that the mathematical model of the system is achieved through the use of laws of physics. Nevertheless, since most of the processes are nonlinear and complex this method is usually very difficult to follow. Hence, another technique is the statistical one, which basically is the adjustment of parameters in a firstly proposed model structure, using the inputs that excited the system and the consequently responses.

The major advantage of the last explained method is that it can be applied with successful results, even if the engineering does not know its internal elements, the only set back is that several times the adjustment techniques are so difficult that the identification can fail.

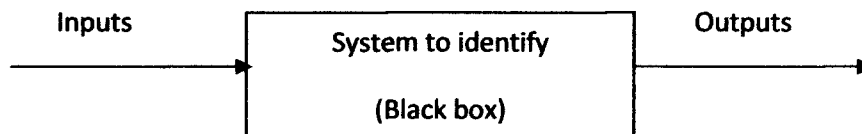


Figure 6. Statistical identification of a system.

Basically, the algorithm to identify a system via the statistical scheme is (Ljung, 1999):

1. **Experiment design.** This is an essential step because it has to be developed in such a way that it gathers all the system's dynamics. If the experiment is dysfunctional the data generated will not be reliable, causing lack of veracity of the identified model. There are several methods of designing an experiment, for further information look in (Montgomery, 1985).
2. **Obtained data.** All the inputs and outputs that resulted in the experiment must be recorded, because they will be needed in the adjustment of the model structure. Input and output variables were determined in the experiment design.
3. **Model structure proposal.** This is the most difficult stage in the algorithm and a special attention must be considered, because if the model structure selection is incorrect, it will not behave as the real plant and possibly the adjustment technique will fail.

4. Parameters adjustment criterion. In this section, a mathematical algorithm must optimize the parameters of the proposed model, in order that the response of the model would be the same as the system. Usually minimum square error method is used.
5. Model validation. After applying the same inputs to the system and the model, the responses will be compared, and if they are the same, the model is said to be reliable.

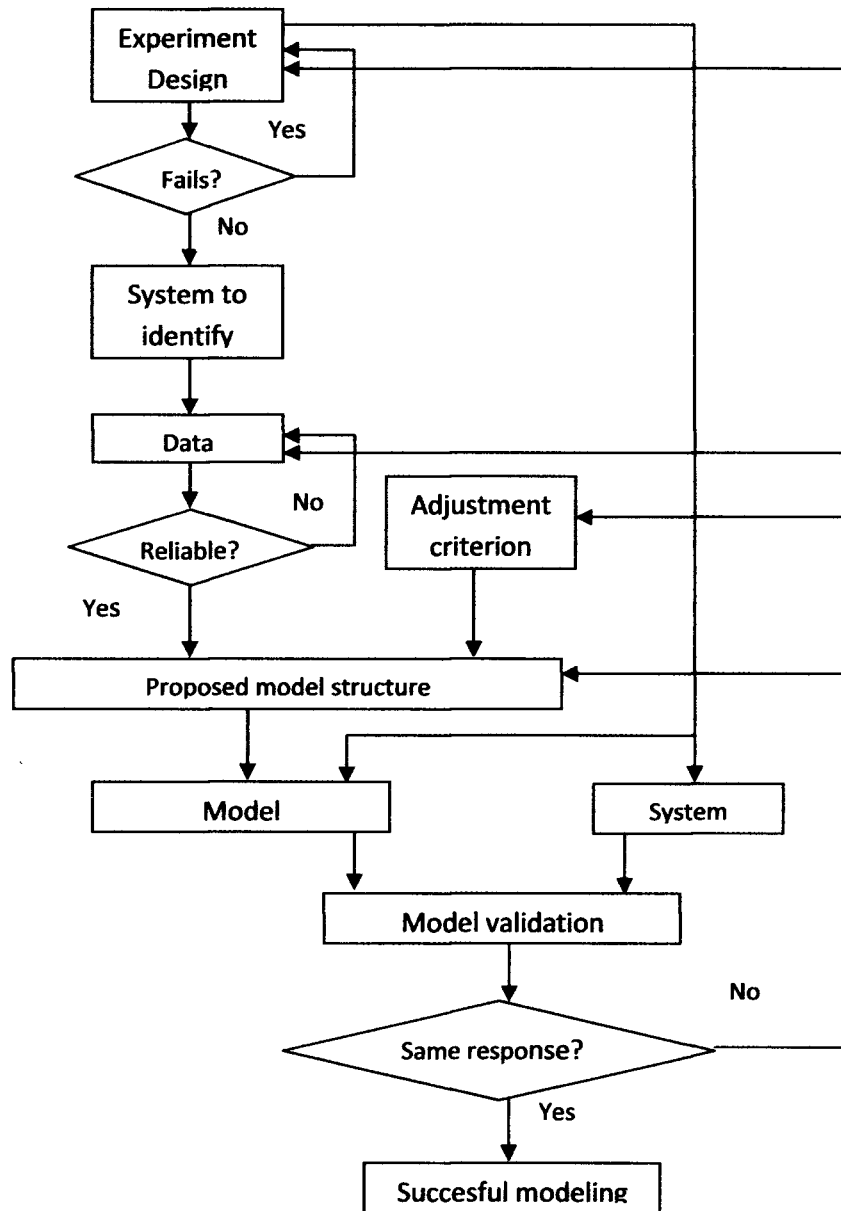


Figure 7. Block diagram of statistical modeling.

2.2.2. Control Theory

A model is a tool for the analysis of a process and a means to explore its interaction with other elements by simulation instead of experimentation (with the real process). So, a mathematical model must aim to give reliable information about the process dynamics and help to improve or deepen the understanding of the process as well.

Control theory can be used to modify the dynamics of the process response in order to get a specific behavior.

A control system consists of the following four basic elements:

1. **Process.** It is the physical element to be controlled.
2. **Sensor – Transmitter.** It is in charge of measuring the response of the system and traducing it to a signal the can be compared with the reference, commonly to an electric signal.
3. **Controller.** It is the brain of the system, because it is in charge of changing the systems dynamics to accomplish a desired behavior (Smith & Corripio, 2006).
4. **Final control element.** It is also known as the actuator, since it is the responsible of the physical action over the system, depending on the signal sent by the controller,

The main information flows among the above components constitute the variables of the system which are listed below:

1. **Process variable.** It is the response of the system.
2. **Set point.** It is the trajectory to follow by the response of the system, also known as the reference.
3. **Error.** The result of comparing the reference with the actual output of the system is known as error.
4. **Manipulated variable.** It is the signal sent by the controller to the actuator.
5. **Disturbances.** External signals that affect the control system, they usually can be found after and before the plant.
6. **Noise.** Alterations of the measurement of the process variable due to electromagnetical interferences with the sensor.

A control system can be operated in manual and automatic modes, which correspond to the open and closed loop configurations, respectively:

- **Open loop system.** In this system, the process variable has no influence on the control action. This means that the process variable is neither measured nor fed back for comparison with the set point.
- **Closed loop system.** In this system, the process variable and the reference are compared and using the difference is used by the controller to determine a corrective action.

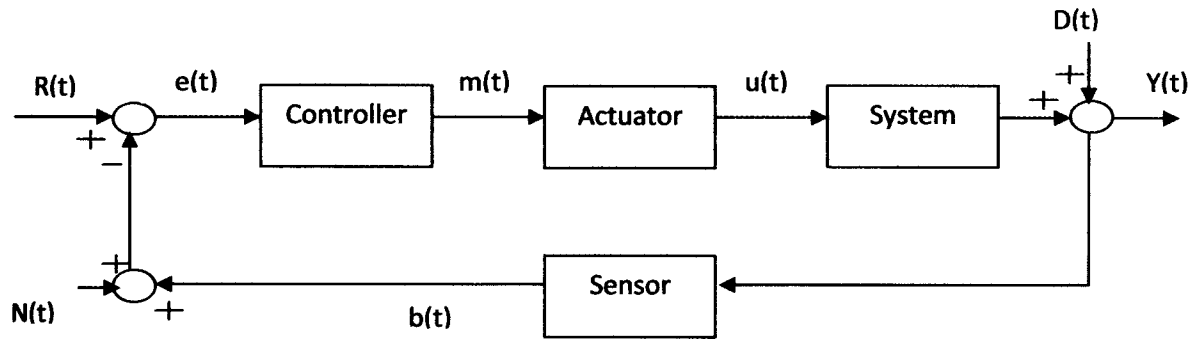


Figure 8. Control system block diagram. $R(t)$ is the reference signal, $e(t)$ is the error, $m(t)$ the manipulated variable, $u(t)$ the input to the system, $y(t)$ the output, $b(t)$ the measured output. $D(t)$ is the disturbance at the output, and $N(t)$ noise added to the sensor.

As mentioned above, the purpose of applying a control action is to force the output of the system to a desired reference, even if disturbances are being applied to the system. Nevertheless, according to Smith & Corripio (2006), there are two control objectives:

1. Regulatory control. When the controlled variable deviates from the set point because of disturbances, this control scheme will compensate the undesired effects in order to return the variable to a specific reference.
2. Servo control. This control scheme is used when it is desired that the output of the system follows a change in the reference.

Knowing the two basic schemes of control theory, several strategies have been developed in order to design the controller; those methods mostly depend on the complexity of the system. In the next chapter, some advanced control strategies will be explained.

Chapter 3

State of the art

This chapter contains the principal models that have been used to represent the plasma glucose level behavior, as well the control strategies that have been applied to the glucose-insulin system, and finally it will be pointed out the areas of opportunity that could increase the performance in this complex and nonlinear system.

3.1. Glucose model development

As stated in chapter 2, the plasma glucose level depends on several factors, such as insulin and glucagon hormones, exercise, meals, among other. So, in order to develop a model that quantifies the glucose in the blood, it is necessary to take in count most of those aspects or, if possible, all of them.

Since the human body could be harmed if experiments were done in an unpractical form, the analytical approach is often used to obtain a physiological model. In the next sections, these models are explained.

3.1.1. Ackerman's model

In 1965, Ackerman and colleagues developed one of the first known mathematical analysis of insulin-glucose interactions (Parker, 2000). Basically, it considers only one global compartment that represents the plasma glucose and insulin in the body (Sánchez, 2008). This model was developed, via an experiment that is known as glucose tolerance test. This test is used to observe how the blood glucose concentration behaves after a patient intake a high carbohydrates meal (Guyton & Hall, 2001).

The Ackerman model can be described by the next nonlinear equations:

$$\frac{dG}{dt} = f_1(G, H) + p(t) \quad (3.1)$$

$$\frac{dH}{dt} = f_2(G, H) + u(t) \quad (3.2)$$

The initial conditions are specified as: $G(t = 0) = G_0$, $H(t = 0) = H_0$, $p(t = 0) = 0$ and $u(t = 0) = 0$. The variable $G(t)$ is the glucose level in plasma, $H(t)$ is the hormone level (in this case, insulin concentration), $p(t)$ is the external intake of glucose and $u(t)$ is the insulin infusion rate (Sánchez, 2008).

Equations 3.1 and 3.2 are mass balances that represent the inputs and outputs of the compartment described by Ackerman. The factors involved are self-removal of glucose, reduction of glucose in response to insulin, self-removal of insulin, increase of insulin due to glucose increment, external glucose and insulin uptake. So this model can be converted into a linear one for a specific narrow range as

$$\frac{dG}{dt} = -\text{glucose self removal} - \text{glucose reduction due to insulin} + \text{glucose uptake} \quad (3.3)$$

$$\frac{dH}{dt} = -\text{insulin self removal} + \text{insulin production due to glucose increase} + \text{insulin uptake} \quad (3.4)$$

Using the constants obtained by Yipintso et al. (1975) for the Ackerman model in terms of deviation variables $g(t) = G(t) - G_0$ and $h(t) = H(t) - H_0$, the final equations are

$$\frac{dG}{dt} = -0.0009g(t) - 0.0031h(t) + p(t) \quad (3.5)$$

$$\frac{dH}{dt} = -0.0415h(t) + u(t) \quad (3.6)$$

It can be seen in equation 3.6, that insulin increment due to glucose increase is neglected since diabetic type I patients cannot produce this hormone (Sánchez, 2008). The constants are in min^{-1} .

3.1.2. Sorensen's model

3.1.2.1. Sorensen's base model

In 1985, Sorensen developed a nonlinear 19th order glucose-insulin model, based in the differential concentration balances in the main organs, such as, brain, heart, liver, kidney and periphery, which are involved in the glucose –insulin interaction. In figure 9, a schematic of the different compartments in the model is presented.

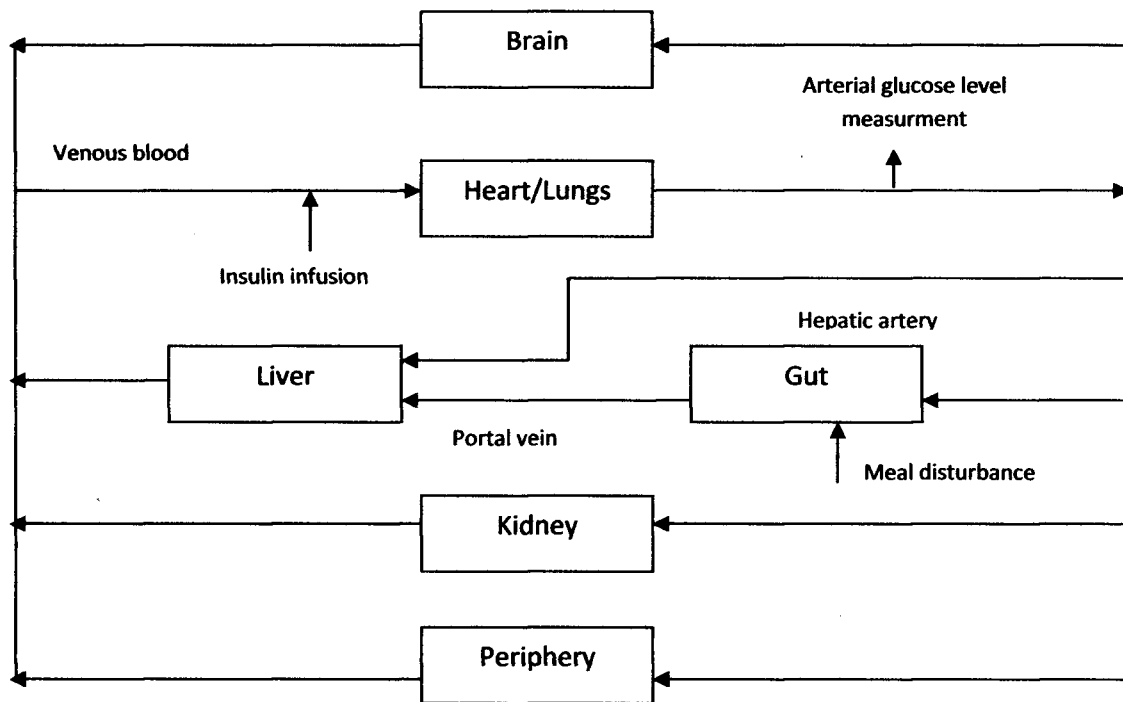


Figure 9. Compartments in Sorensen's model

The parameters of the Sorensen model were obtained using clinical data (Sorensen, 1985). The model considers metabolic sink and source rates, and convection and diffusion transport mechanisms for glucose and insulin. Later improvements have been proposed by different researches to include the effects of meal and exercise disturbances (Parker, 2000; Lenart & Parker, 2002).

It is important to state that this model includes the two hormones involved in arterial glucose regulation, insulin and glucagon and how they interact with the main organs. More detailed information can be found in Appendix 1 and in Sorensen (1985).

As an example of the balances of the model, the differential concentration balance of the brain is shown in equations 3.7, 3.8 and 3.9.

$$V_B \frac{dG_B(t)}{dt} = (G_H(t) - G_B(t))q_B - (G_B(t) - G_B^T(t)) \frac{V_B^T}{T_B} \quad (3.7)$$

$$V_B^T \frac{dG_B^T(t)}{dt} = (G_B(t) - G_B^T(t)) \frac{V_B^T}{T_B} - \Gamma_{BU} \quad (3.8)$$

$$V_B \frac{dI_B(t)}{dt} = (I_H(t) - I_B(t))Q_B \quad (3.9)$$

Where, V_B is the volume of the capillary space, G_B is the glucose concentration in the brain (mg/dL), G_H the total arterial blood glucose concentration, q_B vascular flow rate (dL/min), V_B^T is the volume in the interstitial space, T_B is the diffusion time constant (min), G_B^T is the glucose concentration in the interstitial space, Γ_{BU} is the metabolic sink rate in the brain, and the terms in equation 3.9 mean the same but with insulin hormone.

3.1.2.2. Sorensen's model with the addition of exercise as a disturbance

In chapter 2, glycolysis route and exercise effects in homeostasis were explained, and it could be inferred that exercise will produce several changes, like an increase of glycogenolysis and gluconeogenesis and oxygen consumption rate, and a decrease of glucose concentration along with other effects.

Knowing the clinical consequences is not enough, so it is necessary to compute them in a model, in order to represent their interaction with the plasma glucose and insulin dynamics. Lenart & Parker (2002) modified Sorensen's model with the intention of adding the exercise disturbance and the alterations that it produces in glucose and insulin levels.

The modified variables and new variables are

1. FAMM (active muscular mass fraction) [dimensionless]
2. PAMM (active muscular mass percentage) [%]
3. PVO_2^{\max} (percentage of maximum oxygen consumption rate) [%]
4. Blood flows. [dL/min for glucose compartments and L/min for insulin compartments]
5. PGU (glucose uptake by the periphery) [mg/min]
6. PGU_A (glucose uptake by the periphery due to exercise) [mg/min/kg]
7. HGP (hepatic glucose production) [mg/min]
8. HGP_A (hepatic glucose production due to exercise) [mg/min/kg]

9. KIU (insulin uptake by the kidneys) [mU/min]
10. PIU (insulin uptake by the periphery) [mU/min]

Firstly, PVO_2^{max} is quantified, using the clinical data reported in section 2.1.52., via the following equation:

$$\frac{dPVO_2^{max}}{dt} = -\frac{5}{3}PVO_2^{max} + \frac{5}{3}\overline{PVO_2^{max}} \quad (3.10)$$

where, $\overline{PVO_2^{max}}$ is the target exercise level of the patient at steady state.

In second place, PAMM was calculated as:

$$FAMM = \frac{x \text{ kg active muscle mass}}{28 \text{ kg total muscle mass}} \quad (3.11)$$

$$PAMM = FAMM \times 100 \quad (3.12)$$

According to Snyder (1975), the total volume of muscle mass in a 70 kg patient is 28 kg. X is the actual active muscle mass.

Equations 3.10 and 3.11 quantify the exercise done by a person. Equation 3.10 is necessary, since measuring PAMM is unlikely due to its difficulty (Lenart & Parker, 2002).

The next step is to introduce the glucose and insulin uptakes due to exercise, being the first one a direct function of PVO_2^{max} dynamics. Clinical data have been reproduced using Fick's law (Ahlborg & Felig, 1986). In figure 10, the reported clinical data are shown.

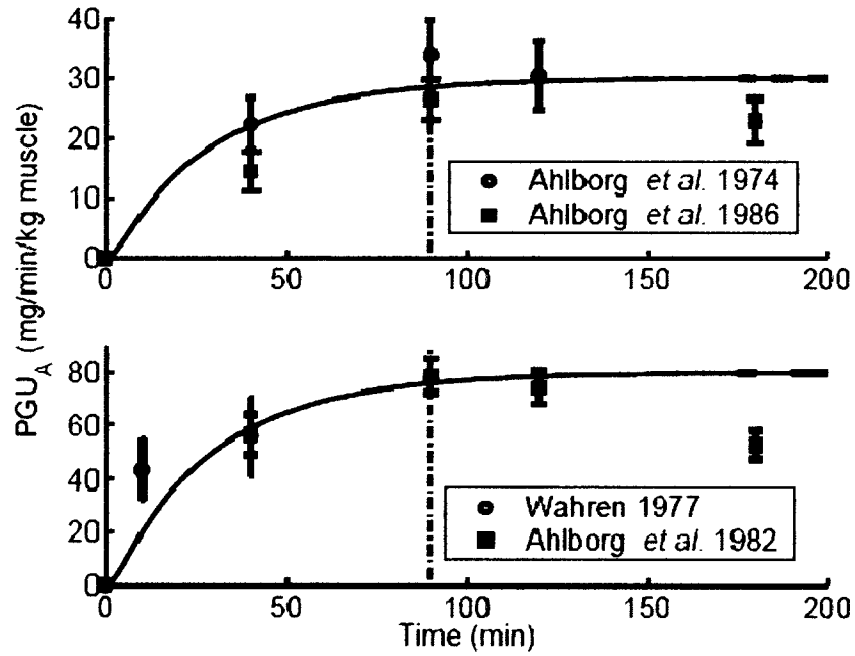


Figure 10. Peripheral glucose uptake by exercising muscle. Solid line is the prediction by the model proposed by Lenart and dash-dot is the clinical data. The upper figure corresponds to 30% PVO_2^{max} and the lower figure is for 60% PVO_2^{max} . Taken from Lenart & Parker, 2002.

From figure 8, the steady state value of \overline{PGU}_A is 28 mg/(min kg muscle) for 30% of PVO_2^{max} and 75 mg/(min kg muscle) for 60% of PVO_2^{max} . Lenart and Parker (2002) developed the following equation for PGU_A dynamics:

$$\frac{dPGU_A}{dt} = -\frac{1}{30}PGU_A + \frac{1}{30}\overline{PGU}_A \tag{3.13}$$

After getting the peripheral glucose uptake due to exercise, it is necessary consider it on the total peripheral glucose uptake, remarking that this is sensible to contributions from insulin and glucose, the new equation is

$$PGU = M^I M^G M^E \times 35 \tag{3.14}$$

In the equation, M is a dimensionless factor representing the effect of the corresponding hormone or disturbance, which are indicated by the superscript letters I , G and E for insulin, glucose and exercise, respectively. The constant 35 [mg/min] is the basal peripheral glucose uptake.

Clearly, the factor the M^E must be altered by PGU_A . Lenart & Parker (2002) propose

$$M^E = 1 + \frac{PGU_a F_{AMM} \times 28}{35} \quad (3.15)$$

Equation 3.15 is multiplied by the factor 28 kg and divided by the basal PGU value in order to obtain a dimensionless variable. The constant 1 is used because if no exercise is done, the peripheral glucose uptake must not be altered by this modification. Equations 3.14 and 3.15 were defined, so the peripheral glucose uptake increases up to 20 times the basal level, according to the clinical data reported.

Concerning to hepatic glucose production due to exercise, Lenart & Parker (2002) assumed that it is the same as its uptake. So the total hepatic glucose production was described as

$$HGP = M^I M^G M^E M^N \times 155 \quad (3.16)$$

In the equation, N stands for glucagon and the constant 155 [mg/min] is the basal hepatic glucose production. Once again, the factor M^E must be altered by HGP_A . Lenart & Parker (2022) propose

$$M^E = 1 + \frac{HGP_a F_{AMM} \times 28}{155} \quad (3.17)$$

As glucose decreases, according to section 2.1.5.4., insulin must do it too. Lenart & Parker (2002) represented the uptakes in the Kidney and Peripheral with the following functions:

$$KIU = F Q_K^I I_H \quad (3.18)$$

$$PIU = \frac{I_P (1 + 2.4 F_{AMM})}{\left(\frac{1 - F}{F \times Q_P^I} - \frac{\tau_I}{6.3} \right)} \quad (3.19)$$

In equation 3.15, F is a fractional extraction term representing a portion of insulin removal from the blood stream upon entering the kidney compartment, Q_K^I is the kidney blood flow rate (L/min), I_H is the insulin blood concentration (Lenart & Parker, 2002). Also, the author considered that PIU has a direct relationship with the exercise done where it is affirmed that maximum PIU due to exercise, is 3.4 times the basal level. In equation 3.19, τ_I is a diffusion time constant from vascular to tissue space in the muscles, I_P is the insulin concentration in the muscle, Q_P^I is the peripheral blood flow rate through the capillary space in the muscles. The values of the parameters can be found on Appendix 1.

The outcomes of the authors' simulation can be seen in figures 11 and 12.

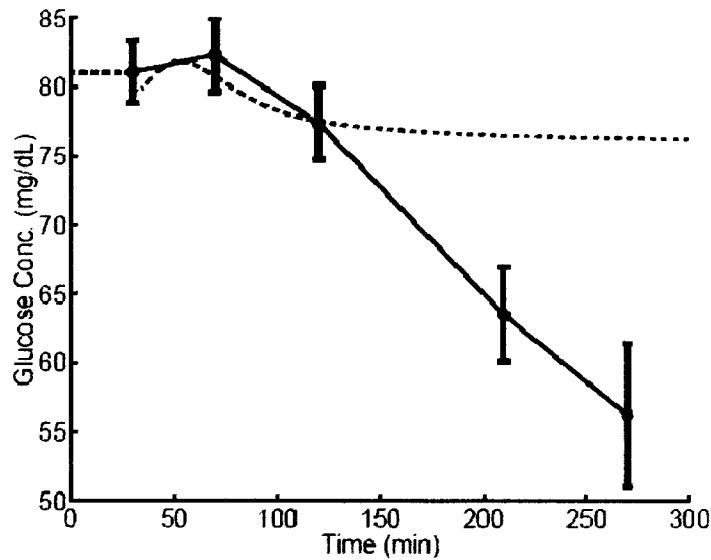


Figure 11. Glucose response to a 30% PVO_2^{max} step. Dotted line represents the output of the model. Taken from Lenart & Parker (2002).

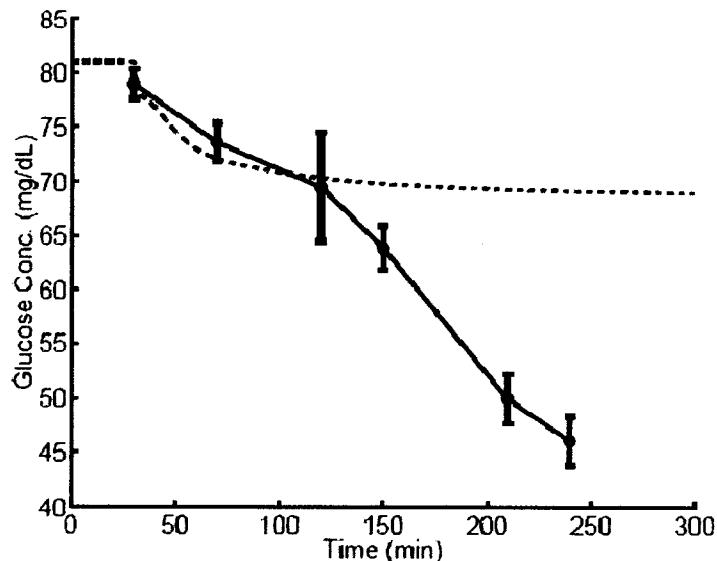


Figure 12. Glucose response to a 60% PVO_2^{max} step. Dotted line represents the output of the model. Taken from Lenart & Parker (2002).

As it was stated by the authors, this model is only valid for periods of exercise shorter than 90 minutes.

A diagram of the resulting model is expressed in figure 13.

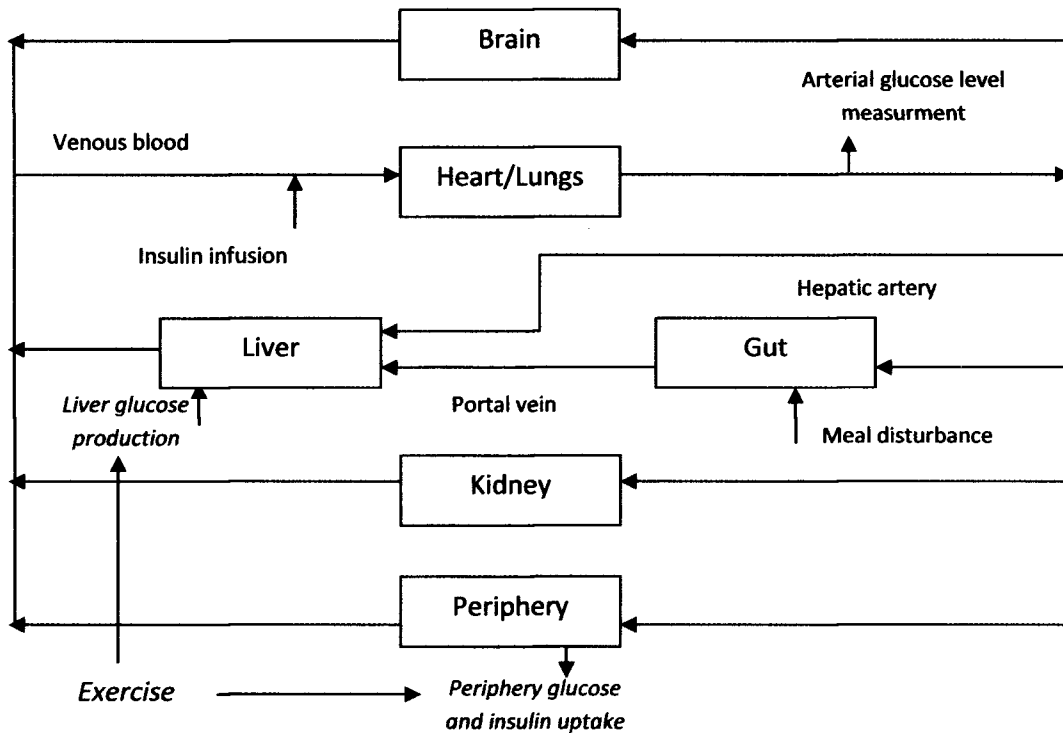


Figure 13. Sorensen's model adding the effect of exercise.

3.1.3. Bergman's model

3.1.3.1. Bergman's base model

In 1981, a glucose-insulin minimal model was developed by Bergman. It quantified the pancreatic responsiveness and the insulin sensitivity in a diabetic patient using a three-compartmental mathematical model (Roy & Parker, 2007). The compartments of plasma insulin (I , $\mu\text{U}/\text{mL}$), remote insulin (X , $\mu\text{U}/\text{mL}$) and glucose (G , mg/dL) are represented using differential concentration balances. Figure 14 depicts a schematic of the model.

The interaction among the compartments is the following: external insulin u_1 is infused into the body, so some of this exogenous hormone enters the remote insulin compartment in order to promote glucose uptake by the liver and the periphery. Glucose compartment can be altered if external glucose enters the system via u_2 . The initial plasma insulin concentration is represented as I_b and is achieved by a basal insulin supply u_{1B} .

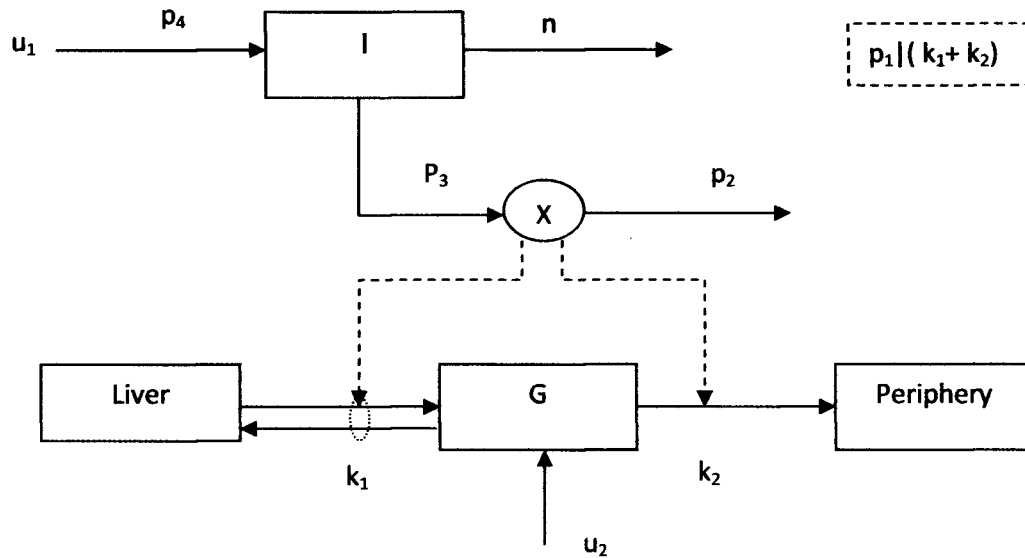


Figure 14. Bergman's minimal order model of glucose-insulin interaction.

The model is described by the following equations:

$$\frac{dI}{dt} = -nI(t) + p_4 u_1(t) \quad I(0) = I_B = \frac{p_4}{n} u_{1B} \quad (3.20)$$

$$\frac{dX}{dt} = -p_2 X(t) + p_3 (I(t) - I_B) \quad X(0) = 0 \quad (3.21)$$

$$\frac{dG}{dt} = -p_1 G(t) - X(t)G(t) + p_1 G_B(t) + \frac{u_2(t)}{Vol_G} \quad G(0) = G_B \quad (3.22)$$

The values of the parameters in equation 3.20-3.22 are shown in Table IV.

Table IV. Parameters values of Bergman's minimal order model.

Parameter	Value	Unit
p_1	0.035	$\frac{1}{min}$

p_2	0.05	$\frac{1}{min}$
p_3	0.000028	$\frac{mL}{\mu U min^2}$
p_4	0.098	$\frac{1}{mL}$
n	0.142	$\frac{1}{min}$
Vol_G	117.0	dL
G_B	80	$\frac{mg}{dL}$

3.1.3.2. Bergman's base model with the addition of exercise as a disturbance

As in section 3.1.3.1., the first step is the quantification of exercise intensity. Roy & Parker (2007) used the following equation:

$$\frac{dPVO_2^{max}}{dt} = -0.8PVO_2^{max} + 0.8u_3(t) \quad (3.23)$$

Remembering that PVO_2^{max} at a basal level is 8%, $u_3(t)$, representing the ultimate exercise intensity above the basal level, can only be in the range from 0 to 92%. The value of $\tau = 1.25$ (min), was chosen so the ultimate exercise intensity could be achieved at 5 minutes.

Roy added the principal effects of exercise, which Lenart also considered, but he also represented the effect of glycogenolysis, that is not figured in Sorensen's model, as well the result of insulin drop in the plasma. The new modified Bergman's minimal order model was adjusted to fit the data reported by Wolfe and colleagues (1986):

$$\frac{dI}{dt} = -nI(t) + p_4u_1(t) - I_e(t) \quad I(0) = I_B = \frac{p_4}{n}u_{1B} \quad (3.24)$$

$$\frac{dX}{dt} = -p_2X(t) + p_3(I(t) - I_B) \quad X(0) = 0 \quad (3.25)$$

$$\begin{aligned} \frac{dG}{dt} = & -p_1(G(t) - G_B) - X(t)G(t) \\ & + \frac{W}{Vol_G} (G_{Prod}(t) - G_{gly}(t)) - \frac{W}{Vol_G} G_{Up}(t) \\ & + \frac{u_2(t)}{Vol_G} \end{aligned} \quad G(0) = G_B \quad (3.26)$$

$$\frac{dG_{Prod}}{dt} = a_1 PVO_2^{max}(t) - a_2 G_{Prod} \quad G_{Prod}(0) = 0 \quad (3.27)$$

$$\frac{dG_{Up}}{dt} = a_3 PVO_2^{max}(t) - a_4 G_{Up} \quad G_{Up}(0) = 0 \quad (3.28)$$

$$\frac{dI_e}{dt} = a_5 PVO_2^{max}(t) - a_6 I_e \quad I_e(0) = 0 \quad (3.29)$$

where, $I_e(t)$ ($\mu\text{U/mL/min}$) represents the rate of insulin removal from plasma due to exercise, $\frac{W}{Vol_G} (G_{Prod}(t) - G_{gly}(t))$ is the total glucose production, $G_{Prod}(t)$ (mg/kg/min) is glucose production due to exercise and $G_{gly}(t)$ (mg/kg/min) is the decline rate of glycogenolysis during exercise. $G_{Up}(t)$ (mg/kg/min) is the uptake of glucose by the muscles, W (kg) is the total weight of the patient and Vol_G is the volume of the glucose compartment (capillary space). The values of the parameters are shown in Table V.

Table V. Parameters values of modified Bergman's minimal order model

Parameter	Value	Unit
a_1	0.00158	$\frac{\text{mg}}{\text{kg min}^2}$
a_2	0.055	$\frac{1}{\text{min}}$
a_3	0.00195	$\frac{\text{mg}}{\text{kg min}^2}$
a_4	0.0485	$\frac{1}{\text{min}}$
a_5	0.00125	$\frac{\mu\text{U}}{\text{mL min}}$
a_6	0.075	$\frac{1}{\text{min}}$
W	70	Kg

Vol_G	117.0	dL
---------	-------	----

In order to obtain the dynamics of how glycogenolysis rate decreases depending in exercise intensity and duration, Roy fitted a sub-model of it using clinical data reported by Pruett (1970). The submodel explains that glycogenolysis rate starts to decrease when the energy required for satisfying the demands due to exercise reaches a threshold, which is a function of exercise duration and intensity:

$$u_3(t) = PVO_2^{max}(t) - PVO_2^{max} basal \quad (3.30)$$

$$A_{TH} = u_3(t)t_{gly}(u_3(t)) \quad (3.31)$$

$$t_{gly} = -1.1521u_3(t) + 87.471 \quad (3.32)$$

where A_{TH} (%) is the threshold value, $u_3(t)$ (%) the exercise intensity, t_{gly} (min) is the duration of exercise that can be done at the desired intensity, before the glycogenolysis rate starts to decrease. Figure 15 shows how equation 3.32 was obtained.

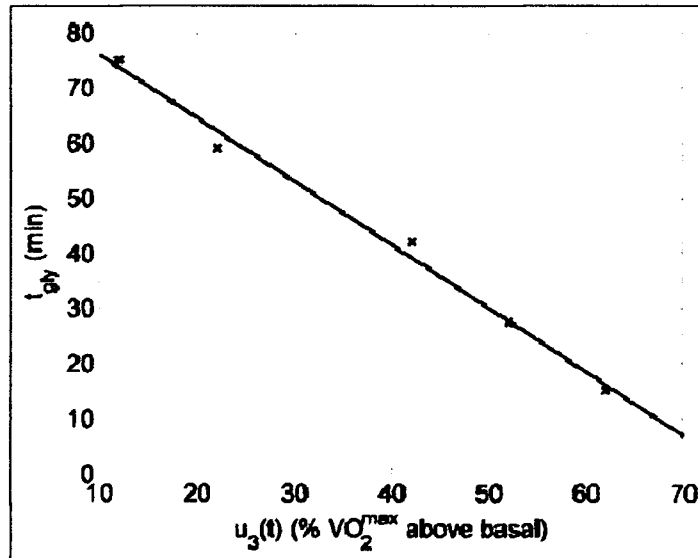


Figure 15. Dependence of glycogen depletion commencement time, t_{gly} on exercise intensity $u_3(t)$.
Taken from Roy & Parker (2007).

It is important to calculate the threshold value, A_{TH} as direct function of exercise intensity, so equation 3.32 is substituted in 3.31, to get

$$A_{TH} = -1.1521u_3(t)^2 + 87.471u_3(t) \quad (3.33)$$

With A_{TH} already computed, it is required to obtain the value of the total intensity of the exercise done $A(t)$, which is calculated as

$$\frac{dA}{dt} = \begin{cases} u_3(t) & u_3(t) > 0 \\ -\frac{A(t)}{0.001} & u_3(t) = 0 \end{cases} \quad (3.34)$$

The final step is to represent the glycogenolysis dynamics as a function of exercise intensity and the threshold value, which can be seen in equation 3.35:

$$\frac{dG_{gly}}{dt} = \begin{cases} 0 & A(t) < A_{TH} \\ k & A(t) \geq A_{TH} \\ -\frac{G_{gly}(t)}{T_1}, & u_3(t) = 0 \end{cases} \quad (3.35)$$

where k and T_1 are constant parameters that stand for glycogenolysis decline rate due to exercise and the time needed so glycogenolysis rate level returns to its basal value, respectively.

The effects modeled by equations 3.30 – 3.35 can be summarized as: when exercise at a desired intensity is done, the glucose demands are met until a threshold value is reached, at this point the glucose production will start to decrease because all glycogen stored in the liver and muscles will start to deplete, causing glucose level to decrease until exercise is stopped. Finally, in the recovery time, glycogenolysis rate starts to increase. Table VI, shows the value of k and T_1 . Figures 16 and 17 show the results obtained with this model.

Table VI. Parameters values of glycogenolysis depletion rate.

Parameter	Value	Unit
k	0.0108	$\frac{mg}{kg \min^2}$
T_1	6.0	min

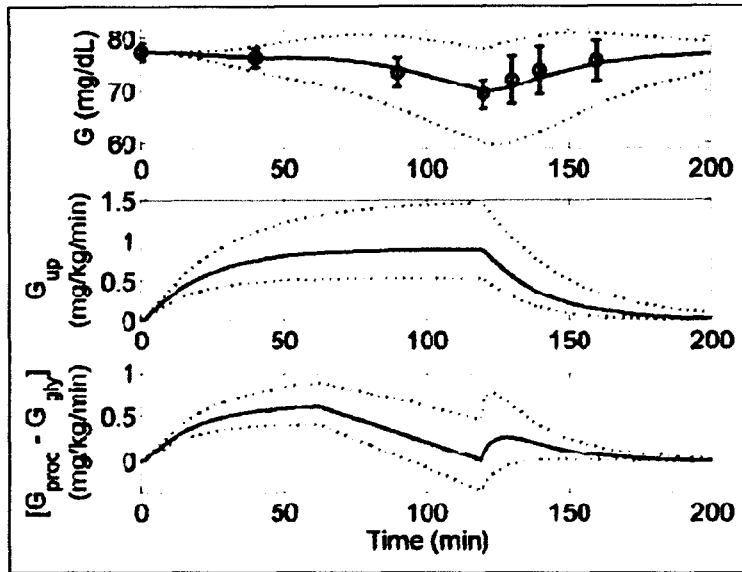


Figure 16. Glucose (Top) dynamics due to exercise at intensity of 30% PVO_2^{max} , lasting from $t=0$ to 120 minutes. Published data (circles) from Ahlborg. Model fit (solid line), and 95% confidence interval of fit (dotted lines). Glucose uptake (middle) and Glucose net liver production (Bottom) Taken from Roy & Parker (2007).

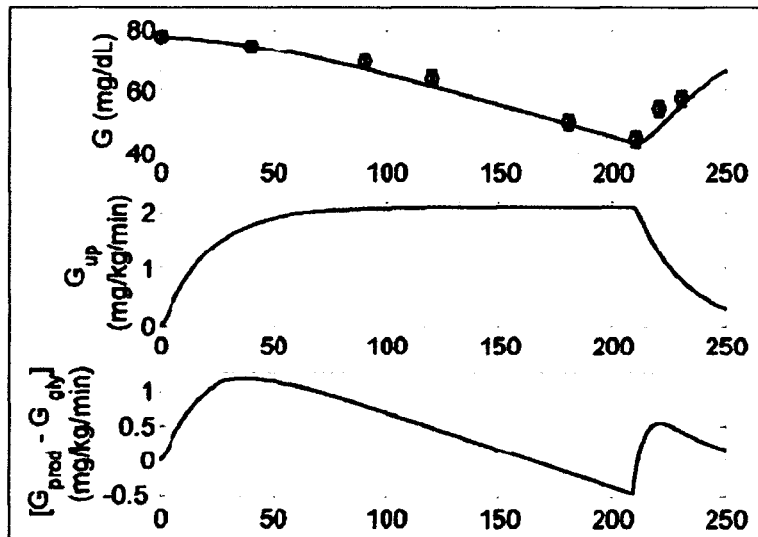


Figure 17. Glucose dynamics due to exercise at intensity of 60% PVO_2^{max} , lasting from $t=0$ to 210 minutes. Published data (circles) from Ahlborg. Model fit (solid line), and 95% confidence interval of fit (dotted lines). Glucose uptake (middle) and Glucose net liver production (Bottom). Taken from Roy & Parker (2007).

3.2. Glucose control strategies

Since 1960, scientists were encouraged to develop control strategies to regulate plasma glucose level by automation of insulin delivery devices (Doyle, Jovanic, & Seborg, 2007). It is important to notice the basic variables involved in this system:

1. System: glucose – Insulin interaction.
2. Actuator: insulin infusion pump or Insulin injection.
3. Sensor: glucose detector
4. Manipulated variable: external insulin or glucagon
5. Process variable: plasma glucose level
6. Disturbances: high carbohydrate meals, exercise, etc.
7. Noise: electromagnetic interferences with the sensor signal.

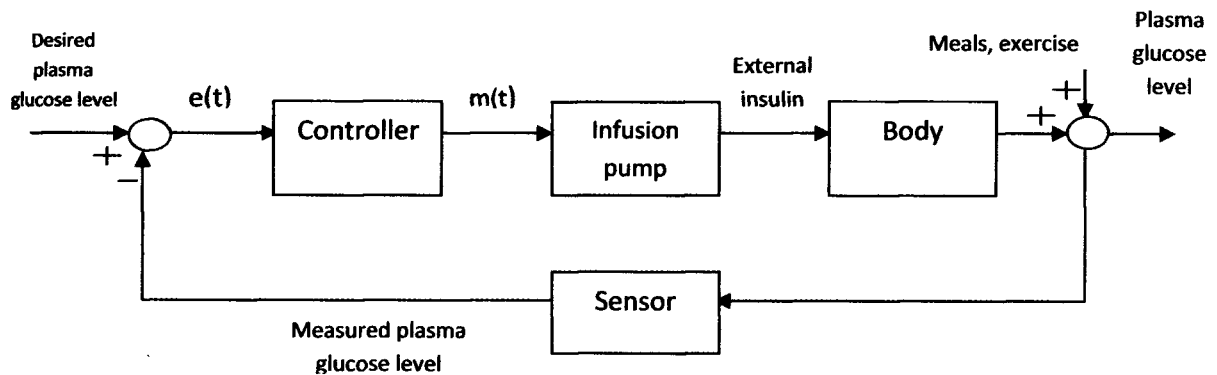


Figure 18. Block diagram of glucose – insulin control system.

Several control techniques have been applied in the last 30 years to this physiological system, from feedback to advanced strategies. The usage of more sophisticated techniques arose because simple methods lack of accuracy in glucose level regulation and often present hypoglycemic episodes due to an excess of insulin infusion. Some of the techniques that have been proposed in this issue are:

- Feedback control
- Adaptive control
- Robust control
- Optimal control

3.2.1. Feedback strategy

3.2.1.1. Definition

This strategy is based in the generation of an error signal, which is the subtraction of the desired reference and the response value. The manipulation signal that is calculated as a function of the error is sent to the system, in order to take the response variable to the reference point. There are several algorithms that can be implemented using this technique, such as on – off, PID control, etc.

3.2.1.2. Application to glucose-insulin system

According to Doyle (2007), the first feedback strategy applied to glucose-insulin system was on – off control. Basically its function is sending the top value of the calibrated manipulation (insulin supply), if the error is negative (glucose above normal level), and sending the lowest value if the error is positive. The PID and PD controller have also been used; detailed information of these algorithms can be found in Ogata (2002). Nevertheless, these strategies have some disadvantages such as the offset error in the case of the PD and hypoglycemic levels due to an excess of insulin infusion caused by the integral action, in the case of a PID (Doyle, Jovanic, & Seborg, 2007).

3.2.2. Feedforward strategy

3.2.2.1. Definition

The main goal of a feedforward strategy is the compensation of disturbances that affect the output variable in the closed loop system (Rollins et al., 2008). For designing a disturbance compensator, it is necessary to measure and model the disturbance that is impacting the system (Smith & Corripio, 2006). Figure 19 depicts a schematic of this technique. The major advantage of this strategy is that it maintains the output variable at a desired value, by rejecting the disturbance effect in the system.

3.2.2.2. Disturbance modeling applied to the glucose – insulin system

The most common perturbations in the glucose-insulin system model are meals and exercise, among other body variables (Rollins et al, 2008). In a study reported by Rollins and colleagues, a model of the response of glucose levels to different disturbances is approximated. The modeling technique employed was the Hammerstein – Wiener (H-W) strategy, which is explained in chapter 4 of this thesis. According to the authors, the strength of this method relies in that the response of glucose can be predicted with the use of different inputs, based on the dynamics of each of these inputs. The results presented by Rollins can be seen in figures 20. Rollins and coworkers have suggested the use of H-W modeling for

feedforward control, but they have not reported such application. This thesis designs a feedforward control based on H-W modeling.

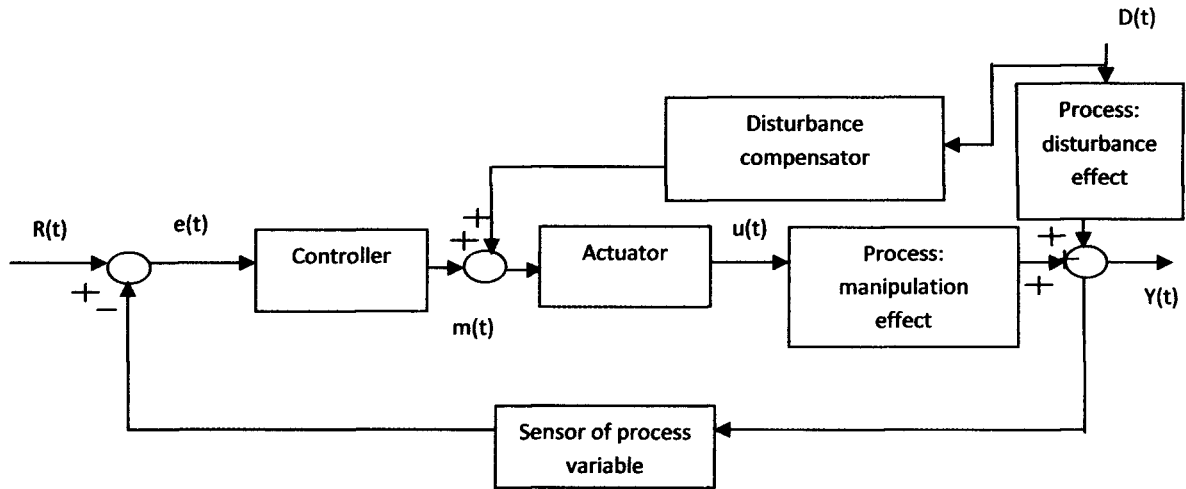


Figure 19. Block diagram of Feedforward strategy.

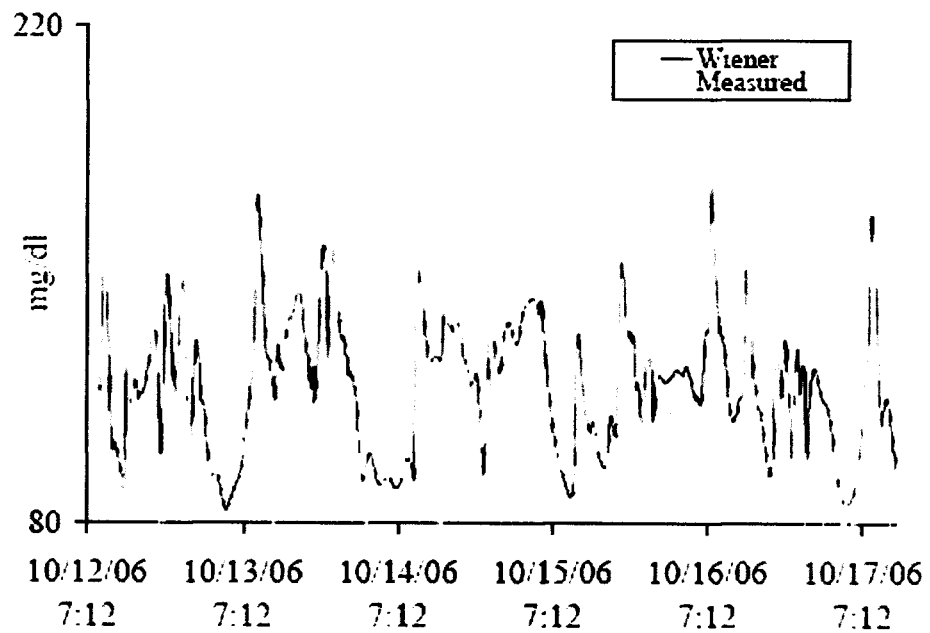


Figure 20. Glucose response prediction due to different inputs using H-W method in a five days trial. Taken from Rollins et al. (2008).

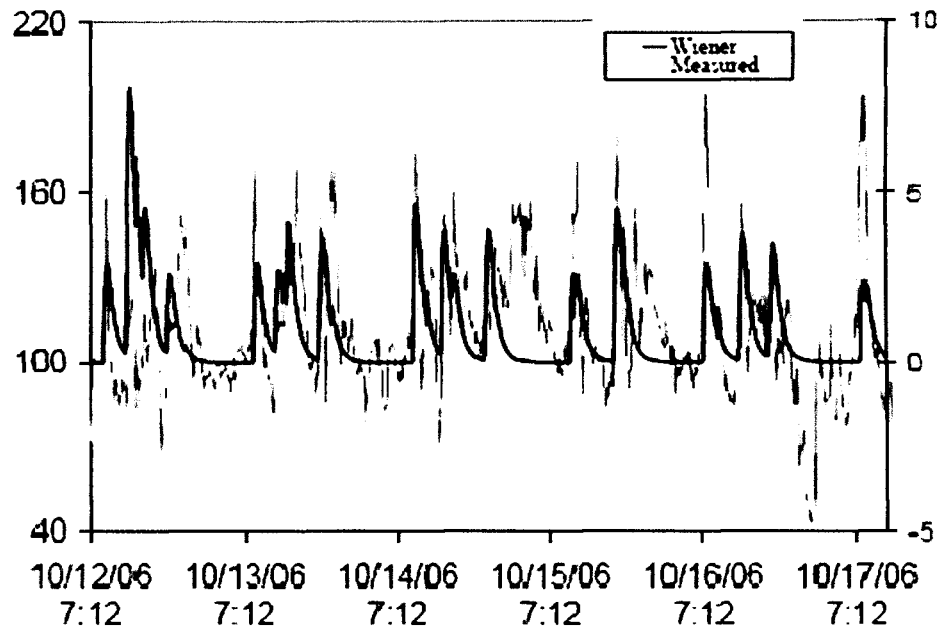


Figure 21. Glucose response prediction due to different inputs. Using H-W method on a five days trial. Scale on the right is for glucose(mg/dL) and left for the dynamic response of the input. Black line represents the output of the HW model. Gray line corresponds to experimental data. Taken from Rollins et al. (2008).

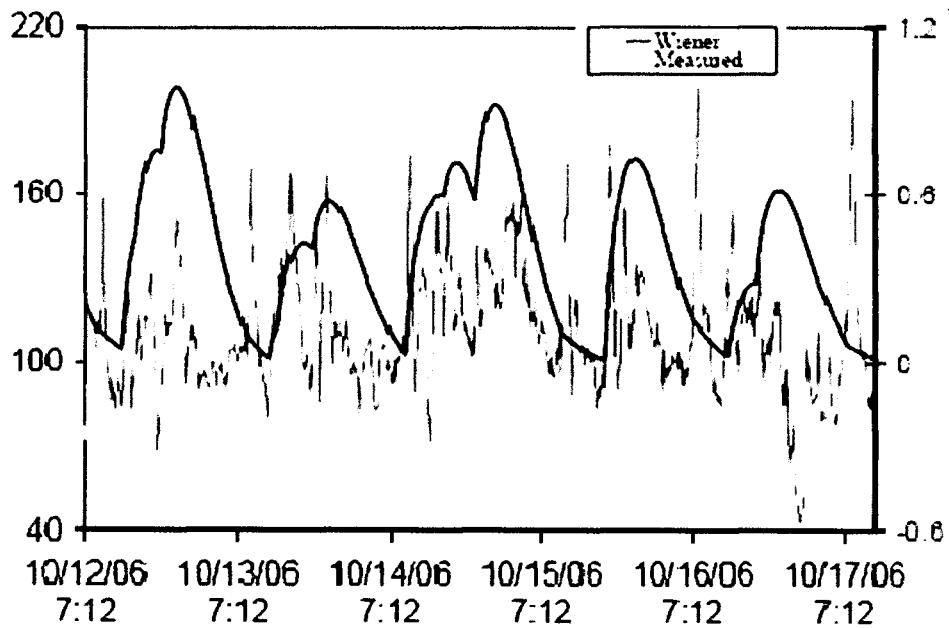


Figure 22. Glucose response prediction due to different inputs. Using H-W method on a five days trial. Scale on the left is for glucose (mg/dL) and right for the dynamic response of the input. Taken from from Rollins et al. (2008).

3.2.3. Adaptive control strategy

3.2.3.1. Definition

Adaptive control is a strategy that has the advantage of estimating the system's parameters online, using only its outputs and inputs. The updated parameters are used to adjust the controller continuously based on a reference model and a performance criterion (Slotine & Li, 1991).

This technique has the objective to reduce the parameter uncertainty in the model, as the operating point is changed. Figure 23 shows a scheme of the adaptive control strategy.

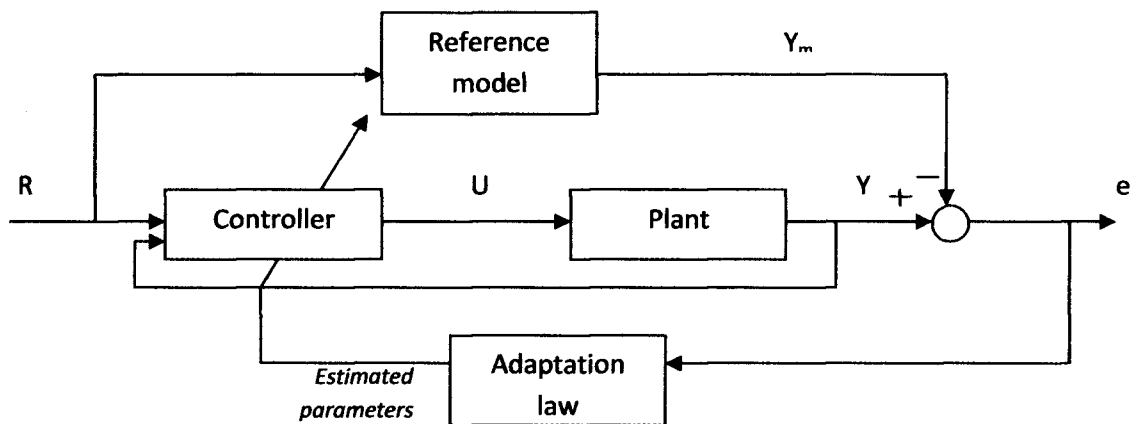


Figure 23. Block diagram of adaptive control strategy.

3.2.3.2. Application to glucose-insulin system

Variations of adaptive control, such as model-based predictive control (MPC) and run to run (R2R) techniques have had success in regulating glucose level (Doyle, Jovanic, & Seborg, 2007). MPC uses a reference model that is updated at a certain moment, depending on the outputs and inputs of the system. This strategy has the advantage that it does not need an error signal to control the plant and that it predicts the behavior of the output value before it happens.

On the other hand, the R2R strategy divides the day in five segments, and after the day ends, performance measurements of each segment are done in order to adjust the parameter values of the controller for the next day (Palerm, Zisser, Jovanovic, & Doyle, 2008). In the glucose-insulin system, the five segments are: before breakfast, sixty minutes after breakfast, sixty minutes after lunch, before dinner and finally sixty minutes after dinner (Campos-Delgado, 2008). With the glucose level measurements at each segment, the controller adjusts the insulin quantity that must be released in the next day at a specific segment. This technique has the advantage that the parameters do not have to be updated in a continuous form.

According to Palerm (2008), in order to have a successful regulation of glucose, the algorithm must iterate at least five times, this means that 40 measurements must be done before a fine result can be obtained with the strategy. Nevertheless, the disadvantage of this technique is that it considers that carbohydrates intake and insulin bolus are the same for a specific segment in all the days; in other words, the disturbances in the segments of one day can be different, but the following days must be the same as the first one. So this limits the application of the R2R strategy.

Figure 24 shows the results obtained by Palerm, 2008. As it can be seen, after five days of running this strategy, the regulation accuracy improves.

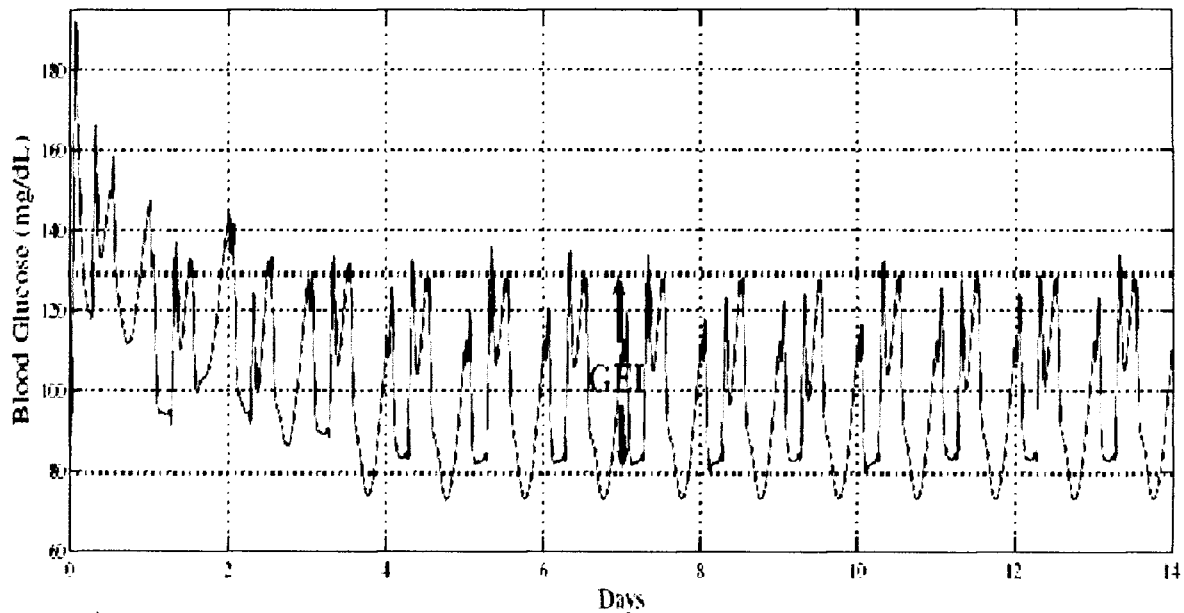


Figure 24. Results of glucose regulation using R2R strategy. The test was done for 14 days in a row. Taken from Palerm (2008).

3.2.4. Robust control strategy

3.2.4.1. Definition

Robust control theory considers that a controller can be synthesized in order to regulate a system, even if its parameters are not the exact ones that correspond to the real plant. It also allows the representation of the uncertainty of the parameters. This means, that the designed controller will be able to regulate different plant dynamics, near the desired operation point, in a satisfactory way. More information can be searched in Skogestad's book work (2005).

3.2.4.2. Application to glucose-insulin system

In 1993, Heinz Kienitz synthesized a H_∞ controller to regulate the plasma glucose level. He used a state space representation of the system and counted the effect of insulin, glucagon inputs and meal disturbances. The main goal of the author was to minimize the disturbance impact in the system and model parameter variations.

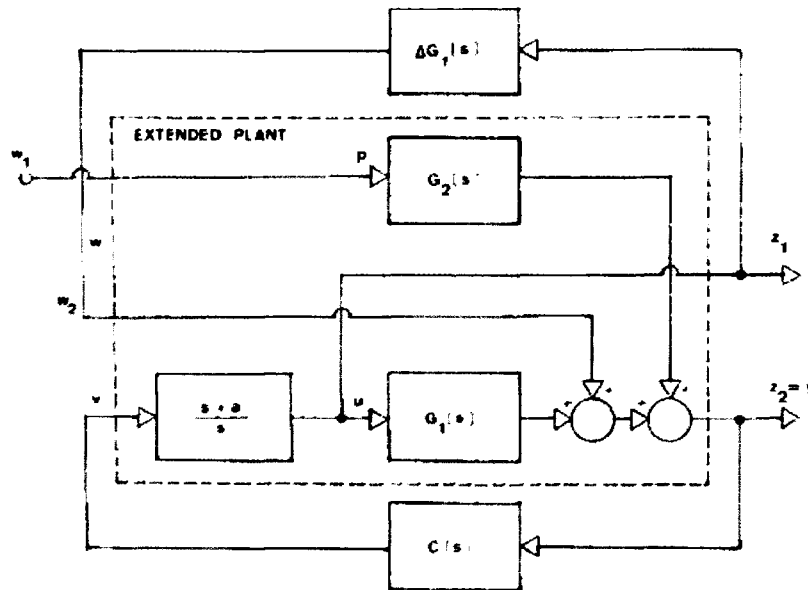


Figure 25. Schematic of a system's model, $G_1(s)$, with parameters uncertainty addition (ΔG_1) and a pre-compensator $(s+a)/s$ for "shaping of the plant". Also a disturbance entry (w_1) is included with its transfer function, $G_2(s)$, to the system's output. (w_1). $C(s)$ is the H_∞ controller. Taken from Heinz Keinitz (1993).

The results obtained from varying the parameters up to $\pm 50\%$ of their nominal value and adding a meal disturbance can be found in Keinitz, 1993..

3.2.5. Optimal control strategy

3.2.5.1. Definition

This strategy focus in determining a control law that minimizes a cost function given by:

$$J(u) = \frac{1}{2} e^T(t_f) S e(t_f) + \frac{1}{2} \int_{t_0}^{t_f} (e^T Q(t) e(t) + u^T R(t) u(t)) dt \quad (3.36)$$

Where $u(t)$ indicates the control law entering the state space model, $e(t)$ the error signal, S is a constant matrix; Q and R are time varying matrixes, S and Q must be positive semidefinite, and R is positive definite (Sánchez, et al., 2008).

3.2.5.2. Application to glucose-insulin system

Sánchez implemented in 2009, a glucose level regulator based on an optimal control strategy. The model used by the author was the one of Sorensen. A Kalman filter to estimate the insulin blood level and adaptive mechanisms to update the controller parameters were used.

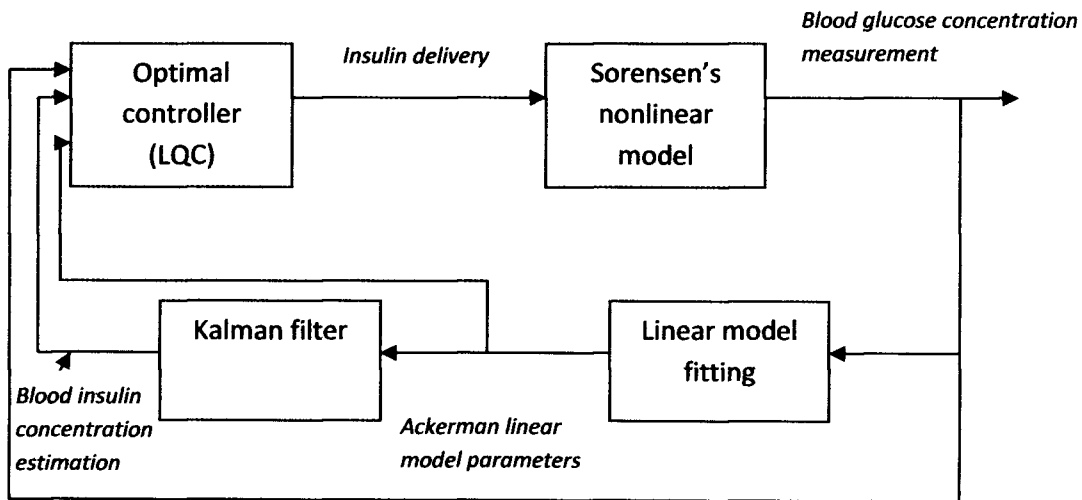


Figure 26. Block diagram of closed loop system for the regulation of Sorensen's glucose-insulin nonlinear model. Taken from Sánchez et al., 2009

The results, in figure 27, show a good meal disturbance rejection, with minimal insulin supply. This is an advantage because this technique impedes hypoglycemic levels, that carry negative symptoms to the patient.

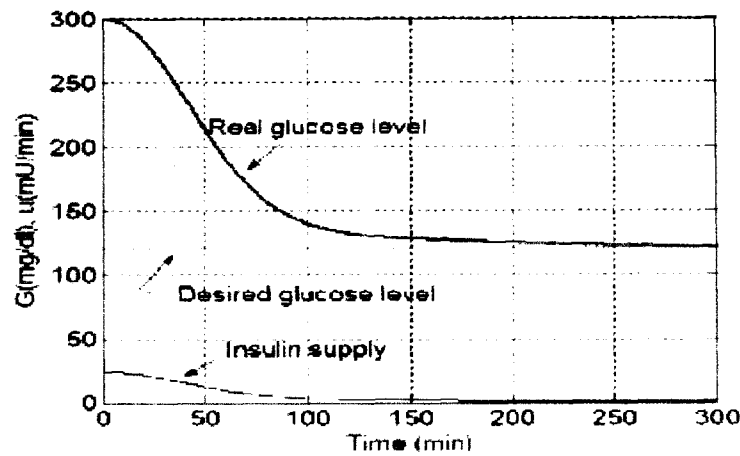


Figure 27. Glucose regulation using an optimal control strategy, with the block diagram shown in figure 25. Taken from Sánchez et al., 2009

3.2.6. Intelligent materials applied to glucose-insulin system

In 2008, Sánchez reported a glucose regulation system based on intelligent materials, specifically, an ionic hydrogel. The special characteristic of this material is that it swells to an extent that depends on the glucose concentration of the blood releasing a certain amount of preloaded insulin into the body.

Glucose responsiveness is achieved through pH changes in the microenvironment of the hydrogel system. The pH is altered by the transformation of glucose into gluconic acid catalyzed by the glucose oxidase enzyme contained in the hydrogel. This chemical response leads to a viscoelastic behavior described by

$$\tau \frac{dQ(t)}{dt} + Q(t) = KpH(t) \quad (3.37)$$

where Q is the ratio of the hydrated volume of the material with respect to its dry volume, the time constant τ is the relaxation time and the gain K is the mechanochemical compliance of the hydrogel material. Volume variations subsequently change insulin diffusivity and delivery. The results obtained are shown in figure 28. Insulin delivery rate has a constant decay, reaching its final value in the third day of operation. Nevertheless, during its active live cycle, the outcomes are even better than the ones obtained by using a controller. Nonetheless, undesired glucose concentration peaks in the post-prandial time are observed.

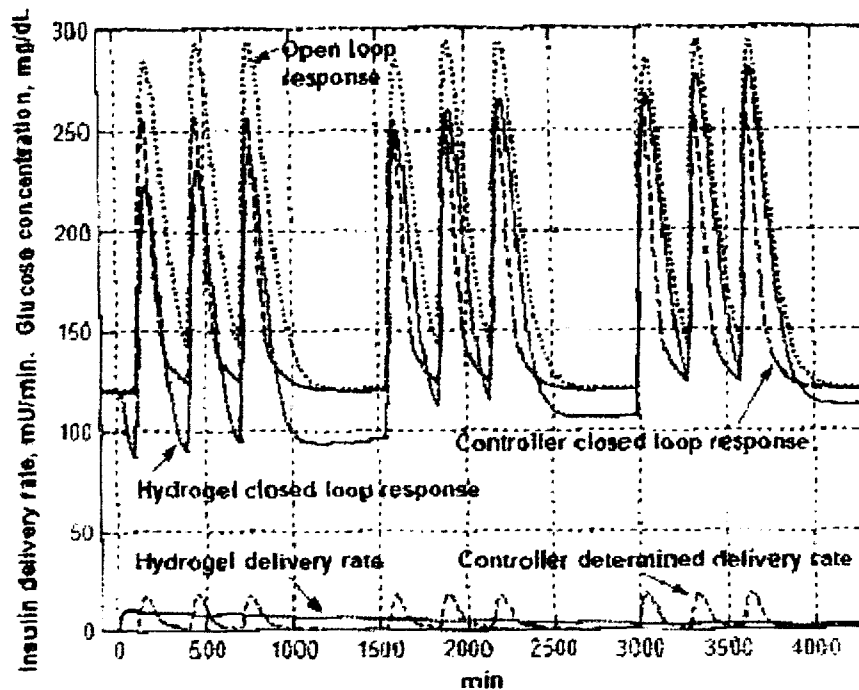


Figure 28. Plasma glucose and insulin responses, using an intelligent hydrogel, a controller and an open loop. Taken from Sánchez et al., 2008

3.3. Areas of opportunity

The major challenge in the analytical model is the addition of external glucagon infusion as an input in order to impede the decrement on insulin level.

As it was explained, there are many control strategies that have been applied to regulate the plasma glucose level. Some of them have had successful results in rejecting meal disturbances, but there has not been a technique used for controlling the glucose level when exercise is done, and it has been shown that this disturbance has a major impact on the glucose-insulin interaction, since it makes the system unstable; this means that glucose level will tend to decrease until exercise is stopped and will cause a hypoglycaemic episode in the diabetic patient.

Another challenge is the application of the feedforward control strategy to the glucose – insulin system, given that up to these days its implementation has not been reported in any investigation.

Chapter 4

Analytical modeling

According to the objective of this thesis, the metabolic process of glucose and insulin must be represented by a physiological model that considers exercise and glucagon input for counteracting the decrement of glucose levels, due to such disturbance.

Based on the reviewed literature (section 3.1), the Sorensen model has been augmented by exercise effects of increasing hepatic glucose production and peripheral insulin uptake, however the decay of glucogenolysis has only been incorporated in the Bergman model. Both models, by Sorensen and Bergman, only consider one drug input for exogenous insulin, when the compensation of exercise effects requires exogenous glucagon.

This chapter explains the changes made to the Sorensen and Bergman models in order to include the effects of exercise and external glucagon infusion. Another aspect that is covered is the combination of both analytical models.

4.1. Modeling exercise effects

4.1.1. Modification in Sorensen's model

The initial step is to quantify the exercise that is done by the patient. According to section 2.1.5. the relation of *PAMM* with PVO_2^{max} is essential because this function is the pioneer in all the effects of exercise in the glucose and insulin system. Equation 3.23 is modified using data reported by Lenart & Parker (2002). The resulting equation is

$$\frac{dPVO_2^{max}}{dt} = -0.8(PVO_2^{max} - \overline{PVO_2^{max}}) + .704 PAMM(t) \quad (4.1)$$

where the gain is calculated knowing that PVO_2^{max} is 8% in basal conditions ($PAMM = 0$) and that at 25% PAMM, PVO_2^{max} reaches a final steady state will of 30%. The time constant, τ , remains as in equation 3.23. $PAMM$ and PVO_2^{max} are dimensionless.

After quantifying the exercise, it is important to obtain the new dynamics of PGU_o and HGP_o . With the use of figure 8 and information from Lenart & Parker (2002), a new equation is obtained

$$\frac{dPGU_A}{dt} = -\frac{1}{30}(PGU_A - \overline{PGU_A}) + \frac{1.442}{30}(PVO_2^{max} - \overline{PVO_2^{max}}) \quad (4.2)$$

Because gains from graphs 8 are different, the step test from the basal state to 60% PVO_2^{max} is chosen to approximate a linear gain for PGU_A over a broader range. The time constant remains as reported in Lenart (2002), $\tau=30$ min. HGP_o dynamics is going to be the same as PGU_o , in order to be coherent with the information compiled by Lenart & Parker(2002). At a basal level $PGU_o(0)=HGP_o(0)=0$. Nevertheless, the final equations used are the ones developed by Roy (2008), 3.27 and 3.28, because their dynamics represent a more real interaction, where glucose uptake is greater than its production. While Lenart & Parker (2002) suppose that they are equal.

The equations 3.27 and 3.28 and the factors W (*weight of the subject*), $PAMM$, and a constant 28 (*maximum kg of muscle involved in exercise*) are used to calculate PGU_o , HGP_o (mg/min/kg active muscle) in Sorensen's model, since in Bergman's model the units are mg/min per kg of weight of the subject (mg/min/kg):

$$\frac{dHGP_o}{dt} = \frac{W}{FAMM \times 28} \left[\frac{dG_{prod}}{dt} \right] = \frac{W}{FAMM \times 28} [a_1 PVO_2^{max}(t) - a_2 G_{prod}] \quad (4.3)$$

$$\frac{dPGU_o}{dt} = \frac{W}{FAMM \times 28} \left[\frac{dG_{up}}{dt} \right] = \frac{W}{FAMM \times 28} [a_3 PVO_2^{max}(t) - a_4 G_{up}] \quad (4.4)$$

$$\frac{d \text{net } HGP_o}{dt} = \frac{d HGP_o}{dt} - \frac{dG_{Gly}}{dt} \frac{W}{FAMM \times 28} \quad (4.5)$$

After certain time of exercising, hepatic glucose production decreases due to the depletion of glycogen reserves. This decrease in glycogenolysis, $\frac{dG_{Gly}}{dt}$, has been modeled by Roy and Parker with equations 3.30 through 3.35 These equations can be used to quantify the net rate of change in hepatic glucose production due to physical activity.

With the calculation of net HGP_o , equation 3.17, the one that quantifies the glucose production due to exercise is modified as

$$M^E = 1 + \frac{\text{net } HGP_a \text{FAMM} \times 28}{155} \quad (4.6)$$

As new dynamic equations are formulated, it is necessary to introduce how blood flow rates change due to an increase in PVO_2^{max} demand. Using Table III, that indicates that blood flow depends on PVO_2^{max} , and knowing from Andersen (1985) that the relation is linear, two sets of equations are obtained; one set for blood flow for glucose concentration compartments or mass balances and a second set for blood flow for insulin concentration compartments. For glucose transport in the liver (l), brain (b), kidney (k), periphery (p) and hepatic artery (la), the blood flows (in dL/min) as functions of PVO_2^{max} are

$$q_l(PVO_2^{max}) = -0.1253 PVO_2^{max} + 13.6024 \quad (4.7)$$

$$q_b(PVO_2^{max}) = 5.9 \quad (4.8)$$

$$q_k(PVO_2^{max}) = -0.09252 PVO_2^{max} + 10.8402 \quad (4.9)$$

$$q_p(PVO_2^{max}) = 1.6145 PVO_2^{max} + 2.184 \quad (4.10)$$

$$q_{la}(PVO_2^{max}) = 0.198 q_l \quad (4.11)$$

For insulin transport, the blood flows (in L/min) change with PVO_2^{max} are

$$Q_l(PVO_2^{max}) = -0.00895 PVO_2^{max} + 0.9716 \quad (4.12)$$

$$Q_b(PVO_2^{max}) = 0.45 \quad (4.13)$$

$$Q_k(PVO_2^{max}) = -0.006595 PVO_2^{max} + 0.77276 \quad (4.14)$$

$$Q_p(PVO_2^{max}) = 0.112267 PVO_2^{max} + 0.15186 \quad (4.15)$$

$$Q_{la}(PVO_2^{max}) = 0.2 Q_l \quad (4.16)$$

4.1.2. Simulation of modified Sorensen model

After obtaining the new equations, the whole Sorensen model was implemented and simulated in Simulink®, in order to verify the response of each new variable. Figure 29 depicts the main model with external insulin and glucose (meal, and PAMM as inputs, and arterial blood glucose and insulin concentrations as outputs. The different compartments of the body used in this model, as well the effect of exercise are represented in figure 30. In figure 31, a more detailed schematic of exercise influence in the model is shown. The next step was is to experiment with the model implemented, in order to recognize if the responses are the same as in the clinical data.

The first test used the values shown in table VII.

Table VII. Values used in test I with Sorensen's model.

Parameter	Value	Unit
<i>External insulin</i>	9.3	<i>mU/min</i>
<i>Basal metabolic source of glucose</i>	155	<i>mg/min</i>
<i>PAMM</i>	25	%
<i>Basal glucose level</i>	120	<i>mg/dL</i>
<i>Exercise duration</i>	120	<i>min</i>

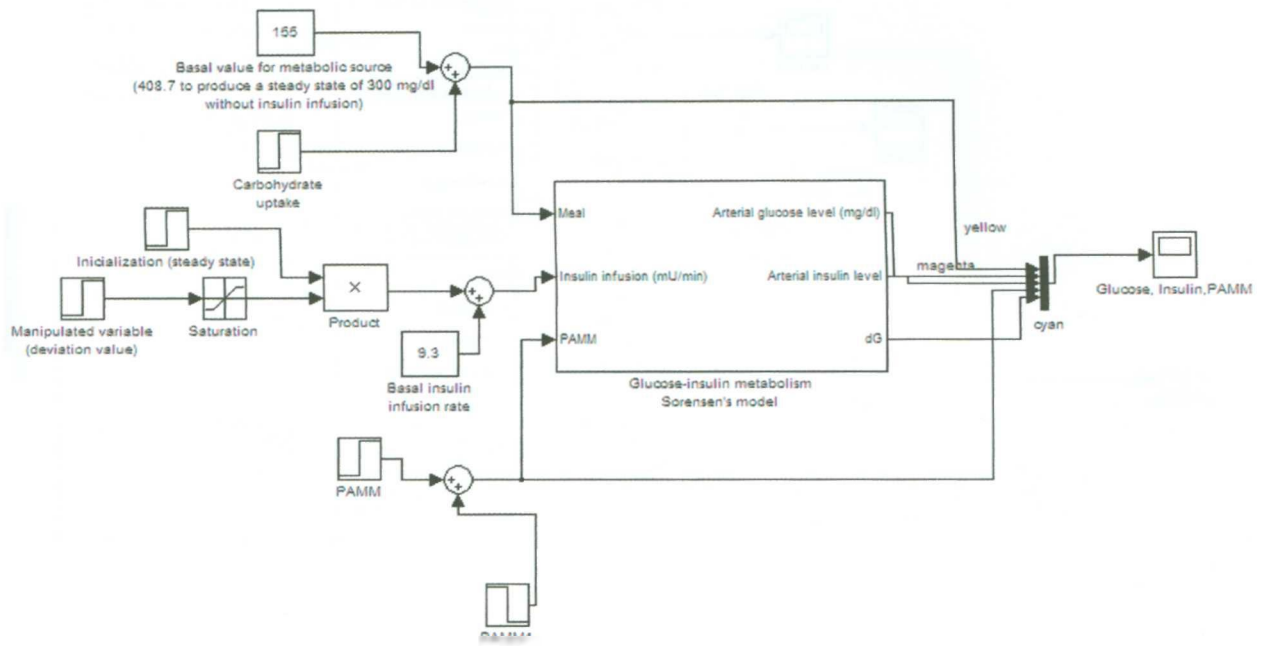


Figure 29. Schematic of the implementation of the global Sorensen's model.

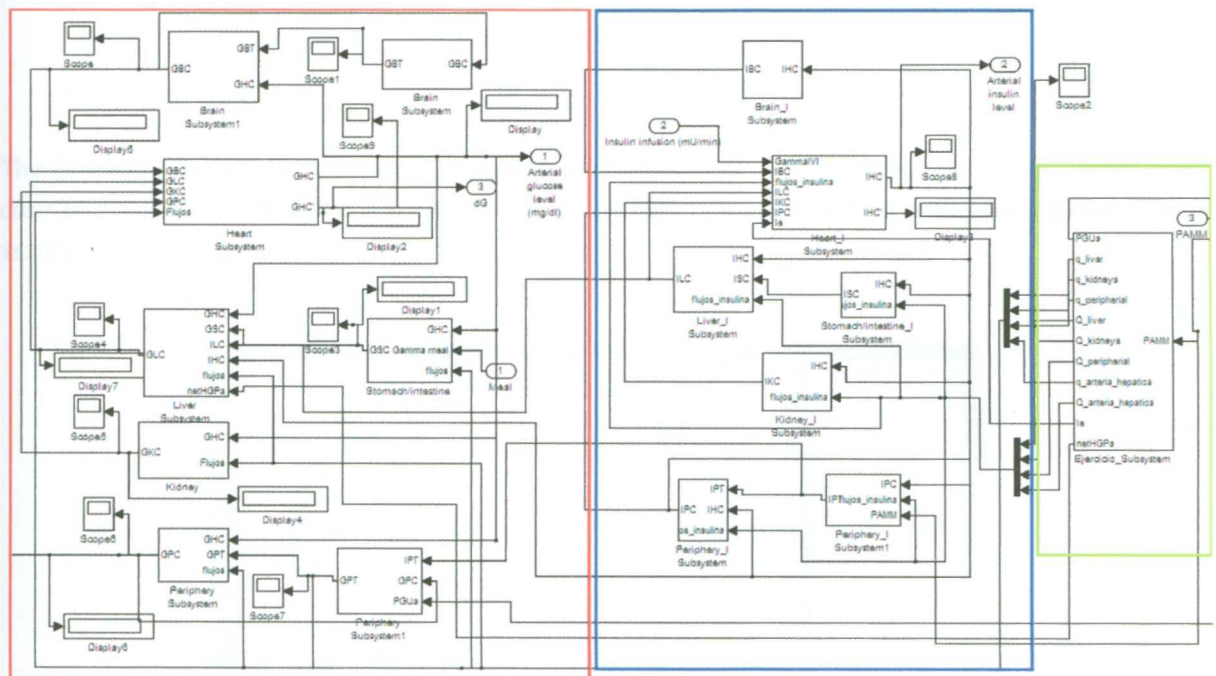


Figure 30. Schematic of the compartments in Sorensen's model. Red lines limit glucose compartments; blue lines limit insulin compartments; green lines limit compartments for the calculation of exercise effects on variables that affect glucose and insulin levels.

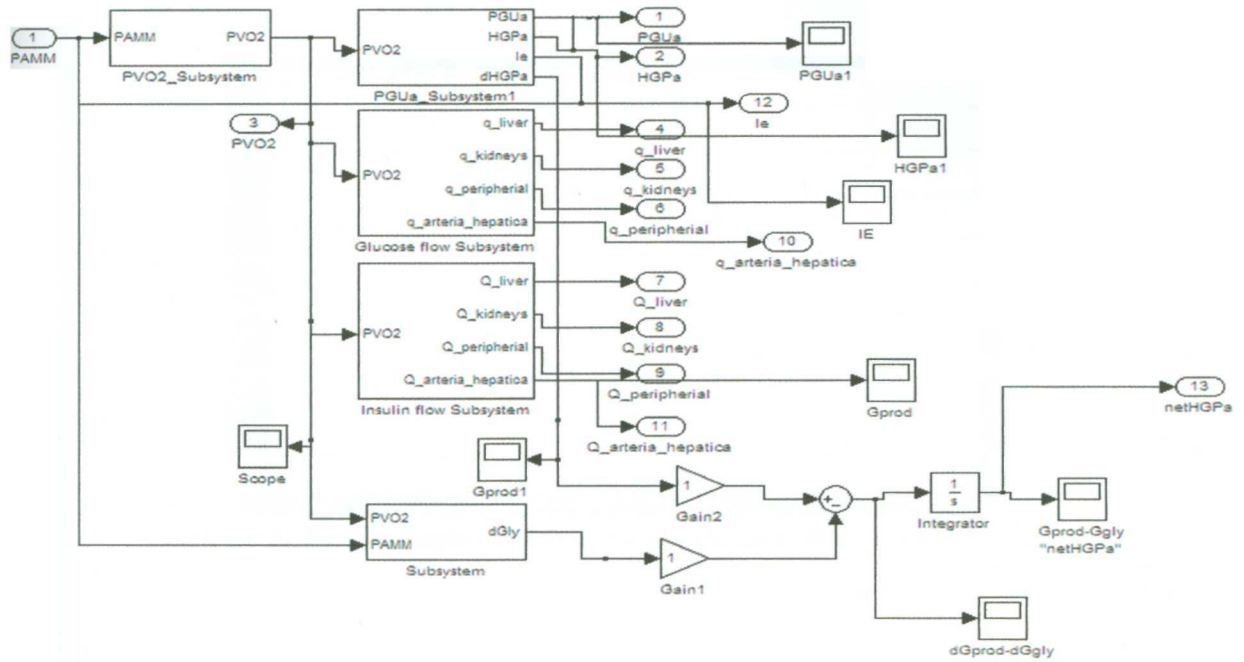


Figure 31. Schematic of exercise effects in Sorensen model: pancreatic glucose uptake and hepatic glucose production, insulin removal from the circulatory system, blood flows and glycogenolysis decay ratio.

The following figures (32 through 37) show the responses of PVO_2^{max} , PGU_a , net HGP_a , blood flows, glucose and insulin levels when a physical activity of 25% is maintained for two hours (time scale of horizontal axis is in minutes).

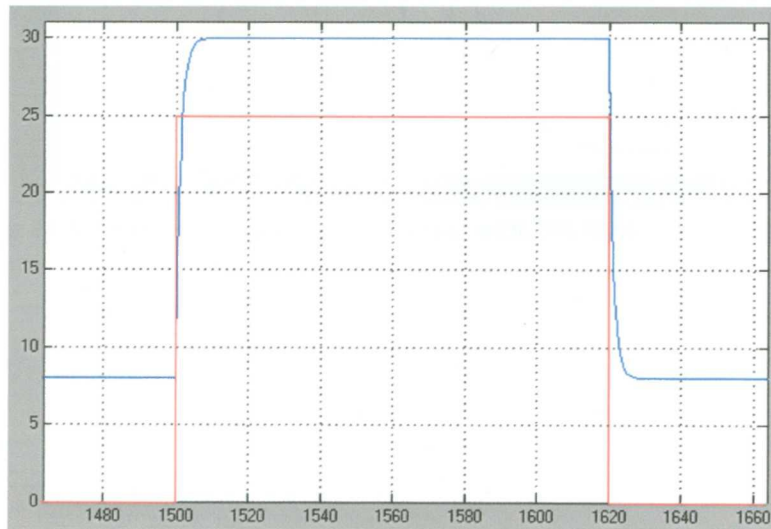


Figure 32. Dynamic response of $\%PVO_2^{max}$ (blue) and 25% PAMM input (red).

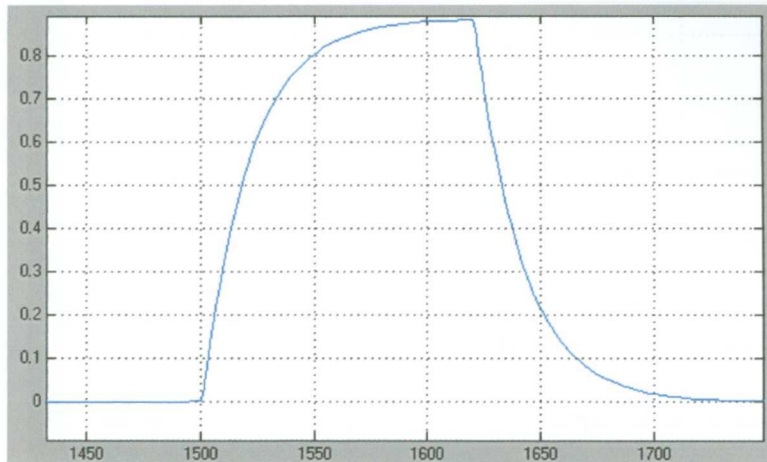


Figure 33. Dynamic response of PGU_a (blue) with 25% PAMM or 30% PVO_2^{max} .

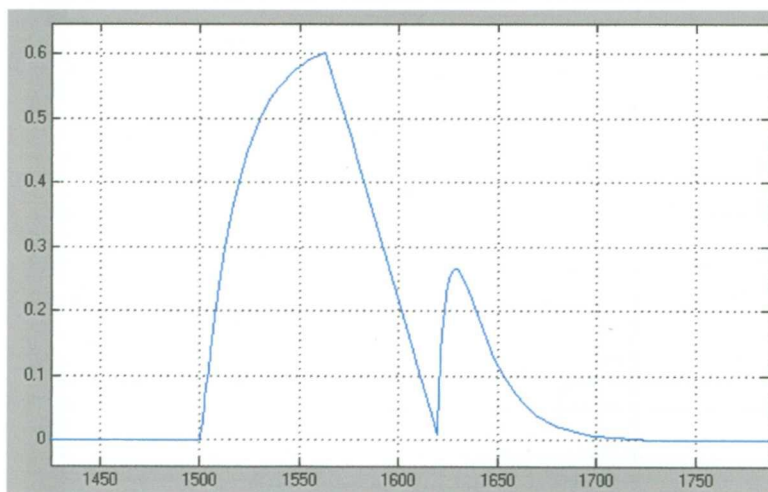


Figure 34. Dynamic response of net HGP_a (blue) with 25% PAMM or 30% PVO_2^{max} .

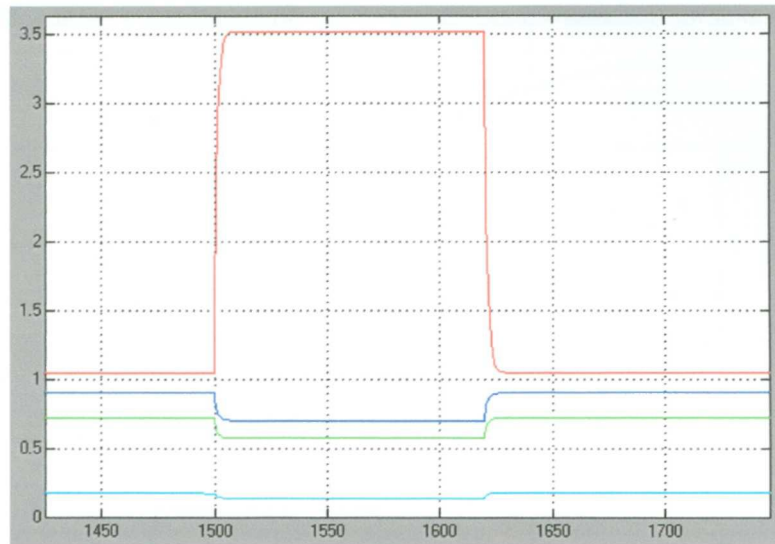


Figure 35. Dynamic responses of blood flows (L/min) for insulin transport in the periphery (red), liver (blue), kidneys (green) and hepatic artery (cyan) with 25% PAMM or 30% PVO_2^{max} .

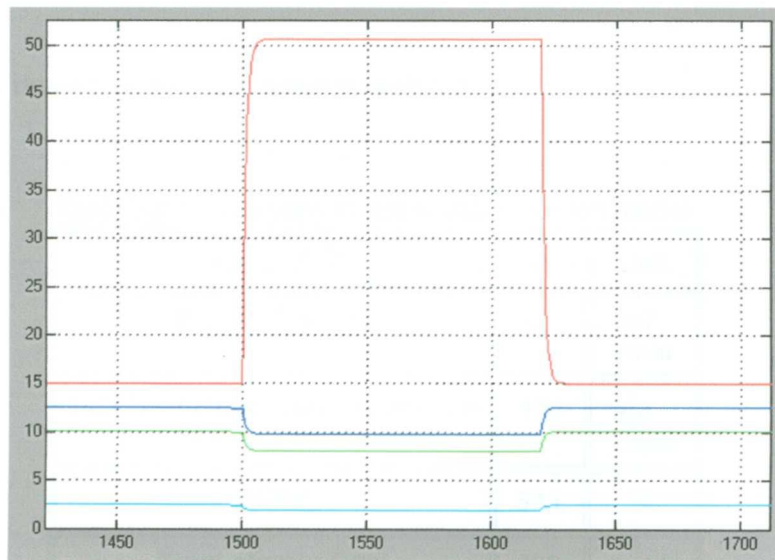


Figure 36. Dynamic responses of blood flows (dL/min) for glucose transport in the periphery (red), liver (blue), kidneys (green) and hepatic artery (cyan) with 25% PAMM or 30% PVO_2^{max} .

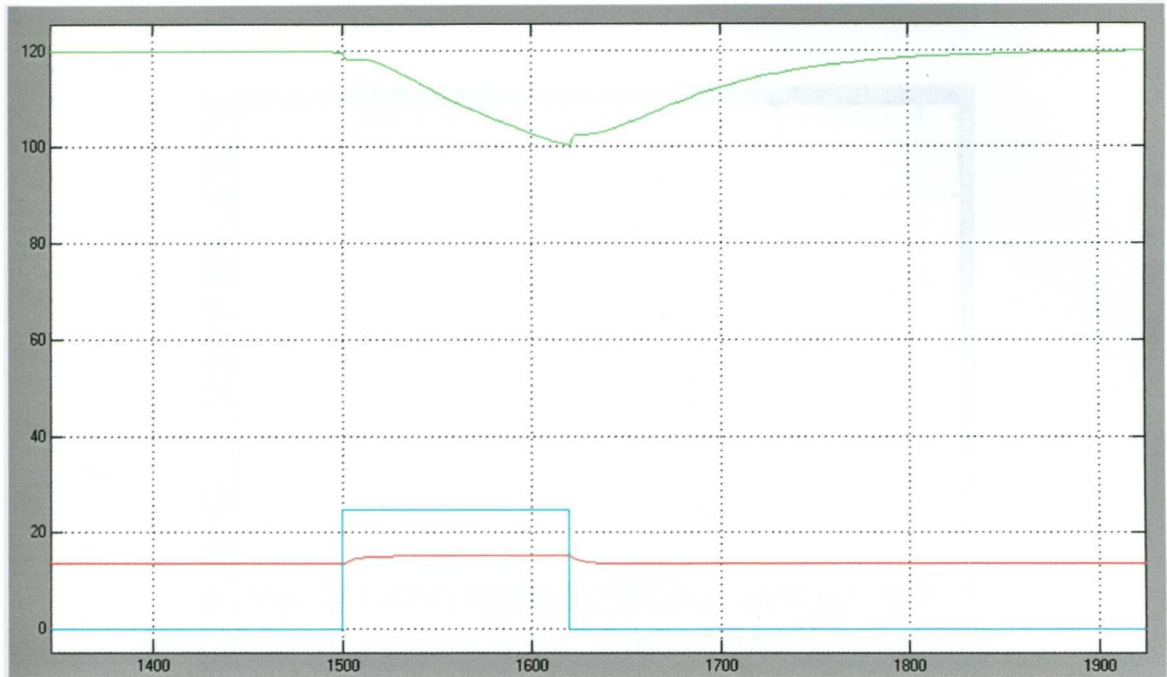


Figure 37. Dynamic responses of glucose (green) (mg/dL) and insulin (red) (mU/L) arterial concentrations with 25% PAMM or 30% PVO_2^{max} (cyan).

The conditions for the second test are shown in table VIII.

Table VIII. Values used in test II with Sorensen model.

Parameter	Value	Unit
<i>External insulin</i>	9.3	<i>mU /min</i>
<i>Basal metabolic source of glucose</i>	156	<i>mg /min</i>
<i>PAMM</i>	59.1	%
<i>Basal glucose level</i>	120	mg/dL
<i>Exercise duration</i>	120	min

Figures 38-43 show the results of test II, consisting of 2 hours of exercise with 59.1% of active muscular mass (time scale in minutes).

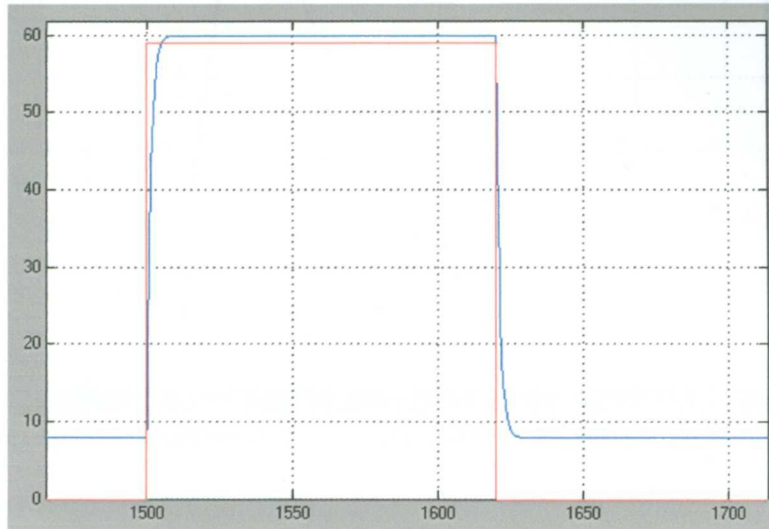


Figure 38. Dynamic response of %PVO₂^{max} (blue) and 59.1% PAMM input (red).

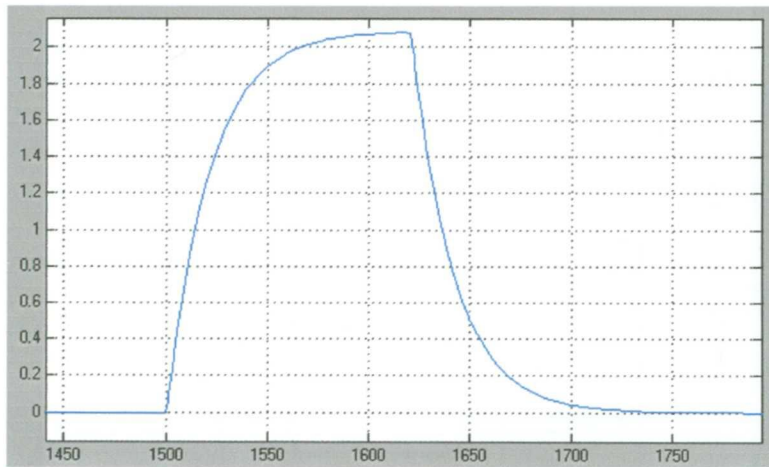


Figure 39. Dynamic response of PGU_o (blue) with 59.1% PAMM or 60% PVO₂^{max}.

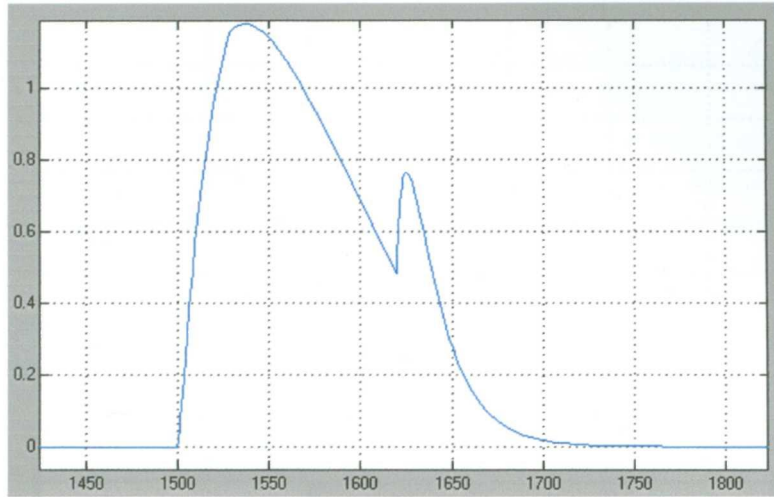


Figure 40. Dynamic response of net HGP_a (blue) with 59.1% PAMM or 60% PVO_2^{max} .

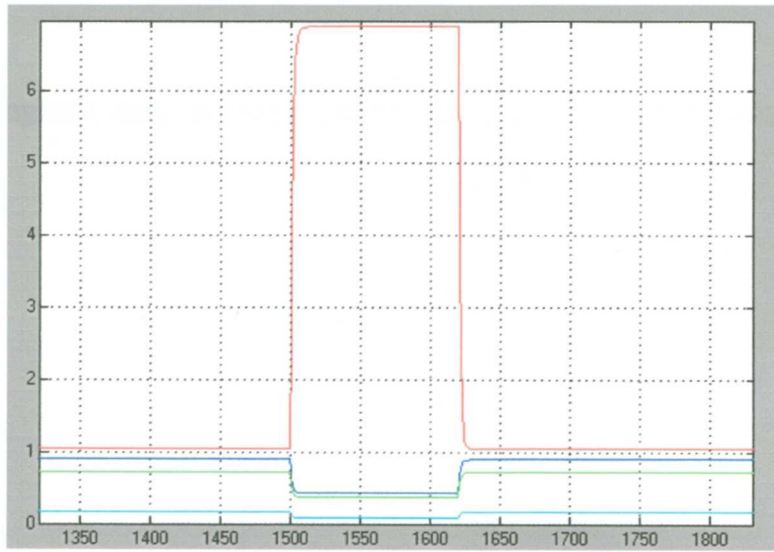


Figure 41. Dynamic responses of blood flows (L/min) for insulin convective transport. Periphery (red), Liver (blue), Kidneys (green), Hepatic artery (cyan) with 59.1% PAMM or 60% PVO_2^{max} .

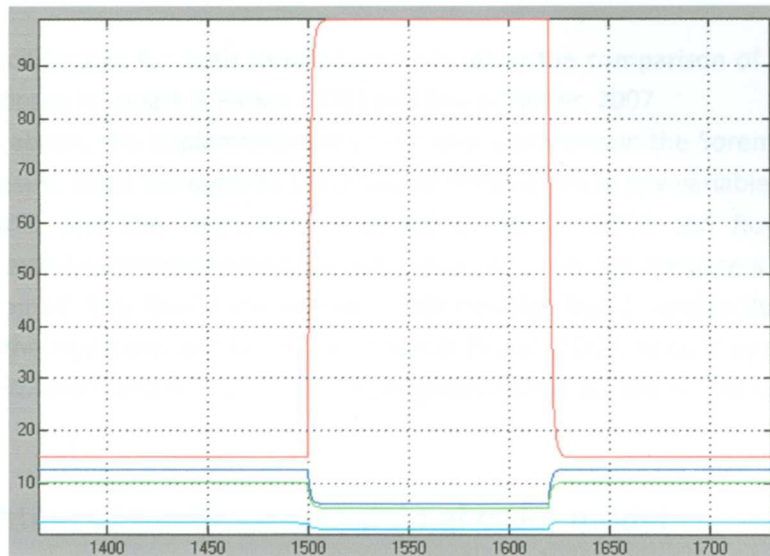


Figure 42. Dynamic responses of blood flows (dL/min) for glucose convective transport. Periphery (red), liver (blue), kidneys (green), hepatic artery (cyan) with 59.1% PAMM or 60% PVO_2^{max} .

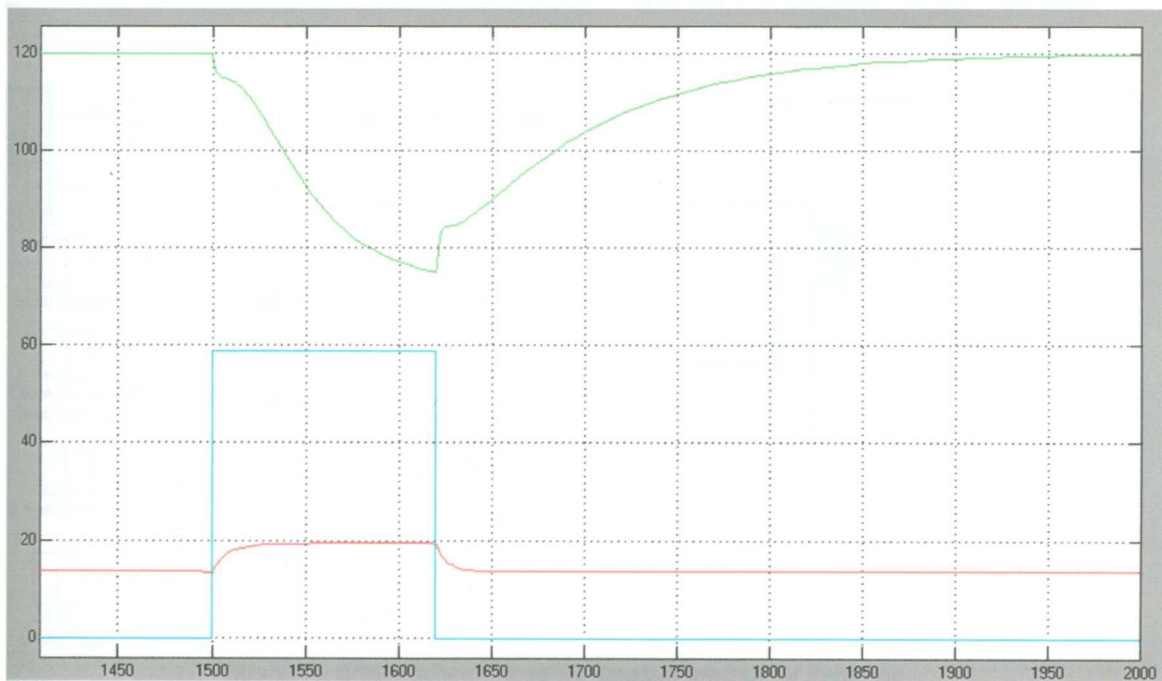


Figure 43. Dynamic responses of glucose (green (mg/dL)) and insulin (red) (mU/L) level with 59.1% PAMM or 60% PVO_2^{max} (cyan).

The proposed specifications for both simulations tests allow the comparison of the outcomes with clinical data and responses in Lenart & Parker, 2002 and Roy & Parker, 2007

As it can be seen above, the implementation of the new equations in the Sorensen model produce almost an excellent result, since the dynamics and steady state values of key variables, are similar to the reported medical data, and the responses in Lenart & Parker, 2002 and Roy & Parker, 2007. Nevertheless, insulin arterial concentration does not behave as expected, because a raising instead of a decaying trend is obtained. This flaw in the behavior indicates that insulin uptake due to exercise is not properly modeled in the equations established in Lenart & Parker, 2002, since they do not consider the effect of blood flow variations and diffusion time in periphery insulin uptake is held constant.

4.1.3. Simulation of the Bergman minimal order model

The Bergman model was also implemented in Simulink®. Once again, the purpose of simulating Bergman’s model with the addition of exercise effects is to compare its outcome with clinical data and responses of the Sorensen model modified in Lenart & Parker, 2002 and Roy & Parker, 2007. In figure 44, the global Bergman model is depicted, where its inputs and output are the ones in equations 3.24 - 3.29.

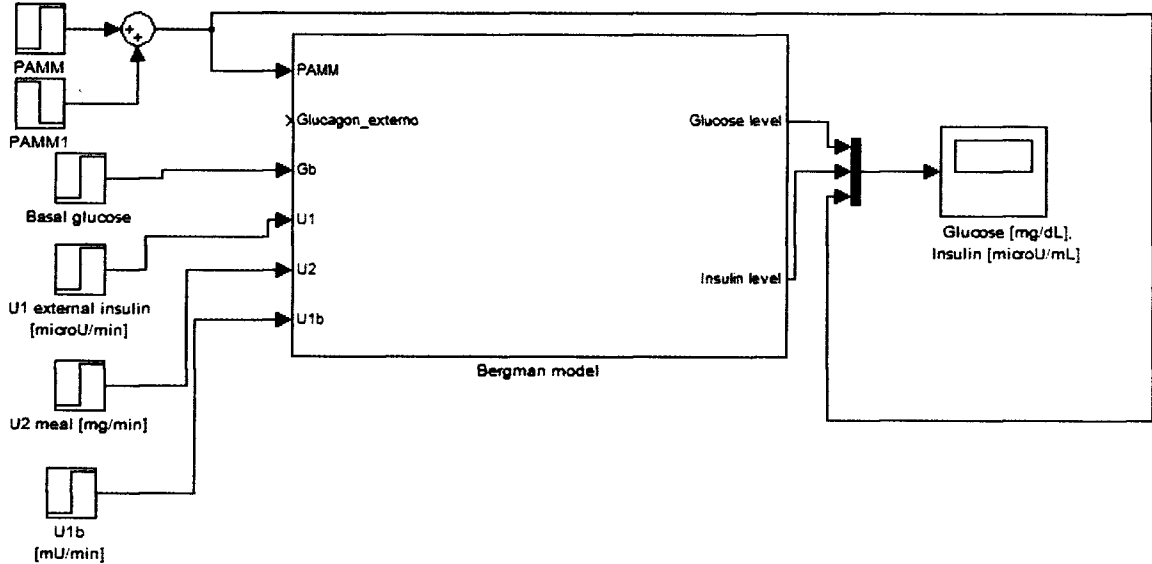


Figure 44. Global schematic of the implementation of Bergman model with addition of exercise effects.

The compartments considered in equations 3.24 – 3.26 can be seen in figure 45.

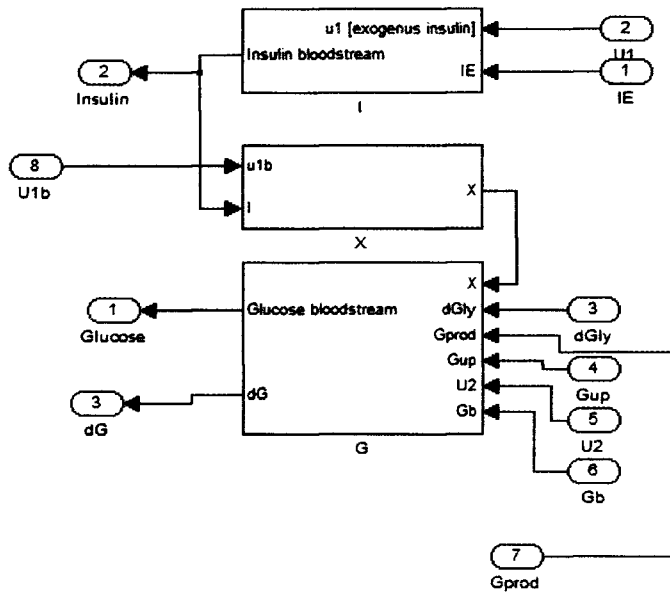


Figure 45. Compartments X (remote insulin), I (arterial insulin) and G (arterial glucose) of Bergman model.

The next figure illustrates the compartments where PVO_2^{max} , PGU_w and net HGP_a are calculated, in order to quantify the effects provoked by exercise.

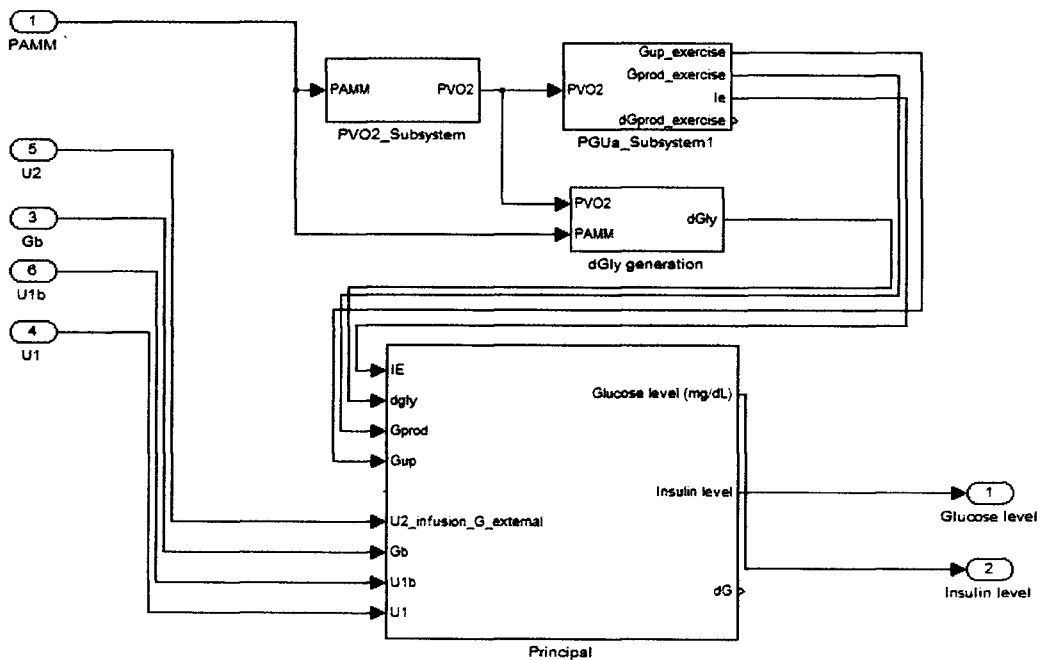


Figure 46. Schematic of the compartments where PVO_2^{max} , PGU_w and net HGP_a are calculated.

The same simulation conditions listed in tables VII and VIII are introduced in this model in order to make a consistent comparison. Because the equations used to calculate PVO_2^{max} , PGU_{av} and $net\ HGP_o$ are the same as in the modified Sorensen model, the responses of those variables are identical. However, because insulin removal due to exercise is computed with a different equation (3.29) than in the Sorensen model (that used equations 3.18 and 3.19), insulin arterial concentration behaves in a different and more realistic form. Figure 47 shows glucose and insulin concentrations dynamics for an input of 25% PAMM, and figure 48, for an input of 59.1% PAMM.

The responses in figures 47 and 48, show that the Bergman model behaves as the clinical data suggest (Wolfe, 1986) (figures 16 and 17), with a decrease in glucose and insulin concentration. Also the decline of glucose occurs according to physiological records, for more information check section 2.1.5.4. This is the reason why Bergman's model is selected for the rest of the work in this thesis, even though an external glucagon infusion input must be added to it.

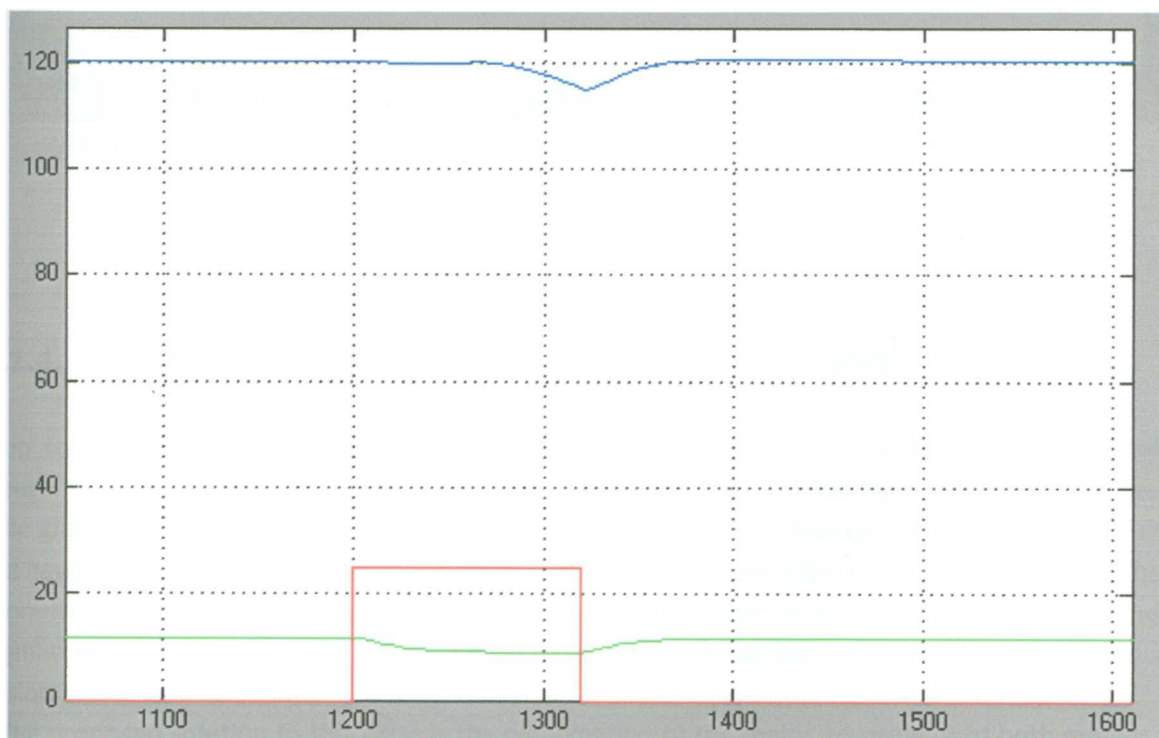


Figure 47. Response of glucose (blue)(mg/dL) and insulin (μ U/mL) arterial concentrations with an input of 25% PAMM or 30% PVO_2^{max} .

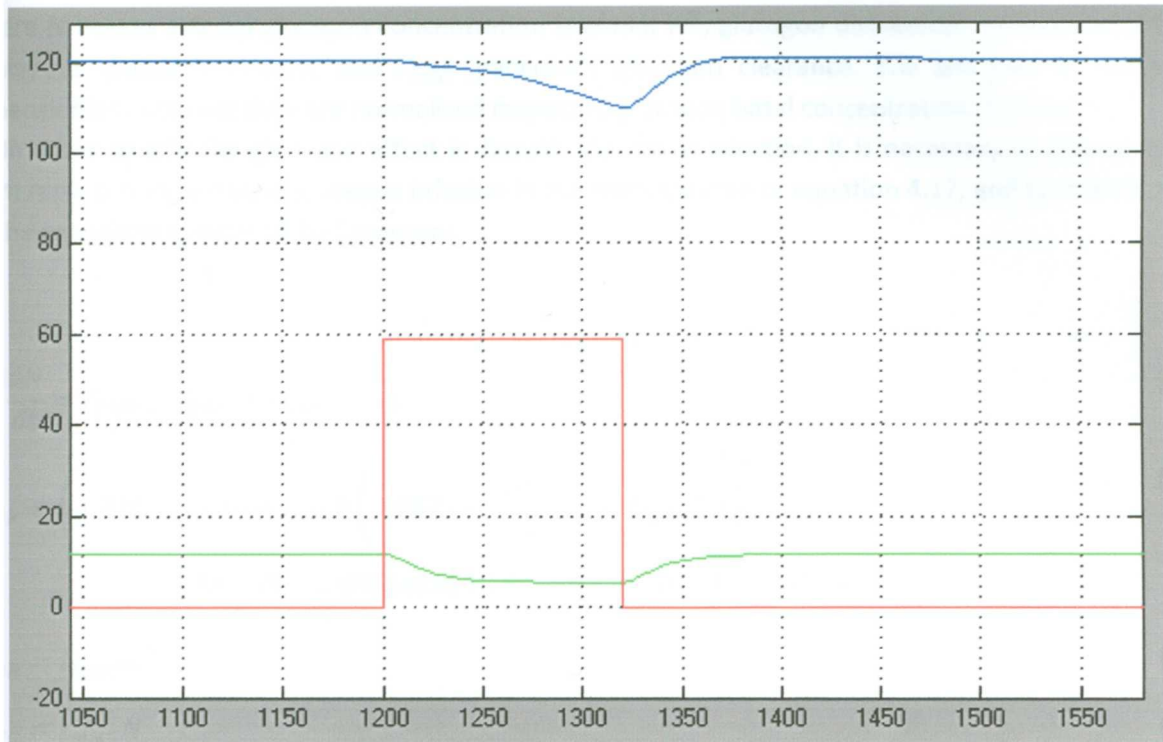


Figure 48. Response of glucose (blue)(mg/dL) and insulin ($\mu\text{U/mL}$) arterial concentrations with an input of 59.1% PAMM or 60%. PVO_2^{max} .

4.1.4. Combination of Bergman's and Sorensen's model

Up to this section, the principle advantages and disadvantages of the Bergman model and the Sorensen model have been established. Since the purpose of this thesis is the compensation of exercise in the glucose-insulin system in an automatic form with the use of glucagon, the mathematical model must have an input for this hormone. However, the model that quantifies the glucagon effects is the one of Sorensen one but the response of the insulin level does not react as expected. On the other hand, the Bergman model behaves according to clinical data, but does not have an input of external glucagon infusion.

The proposed solution to this issue is the combination of the major advantages of both models. This means that the Sorensen model's capability of quantifying glucagon effects is added to the Bergman's glucose –insulin interaction equations.

According to Sorensen's thesis (1985), the glucagon mass balance can be modeled by the following equation:

$$V^N \frac{dN}{dt} = \Gamma_{PNR} - \Gamma_{PNC} \quad (4.17)$$

where N means arterial glucagon concentration (pg/mL); V^N , glucagon distribution volume (mL); Γ_{PNR} , pancreatic glucagon release, and Γ_{PNC} , pancreatic glucagon clearance. The last two variables are dimensionless because they are normalized respect to glucagon basal concentration: 102 pg/mL.

In order to add the glucagon effect in hepatic glucose production, it is necessary to aggregate the term representing external glucagon infusion in the mass balance of equation 4.17, and to modify some of the equations developed by Sorensen:

$$V^N \frac{dN}{dt} = \Gamma_{PNR} - \Gamma_{PNC} + \Gamma_{EXT} \quad (4.18)$$

$$\Gamma_{PNR} = \left(1.3102 - 0.6101 \tanh \left(1.0571 \left(\frac{I_H^C(t)}{15.15} \right) - 0.46981 \right) \right) * \left(2.9285 - 2.095 \tanh(4.18(G_H(t) - 0.6191)) \right) * \Gamma_{PNR}^B \quad (4.19)$$

$$\Gamma_{PNR}^B = \Gamma_{MNC} N^B \quad (4.20)$$

$$\Gamma_{PNC} = \Gamma_{MNC} N \quad (4.21)$$

With $\Gamma_{MNC}=0.0091$ L/min and $V^N=9.1$ L, where Γ_{MNC} is the glucagon metabolic sink rate and is dimensionless, N^B is the glucagon basal level, Γ_{EXT} is the external glucagon infusion rate (pg/min). After deriving equations 4.18 – 4.21, N must be normalized with respect to its basal value.

$$\bar{N} = \frac{N}{N^B} \quad (4.22)$$

The next step is to include the normalized glucagon in the Sorensen's equation for hepatic glucose production:

$$\Gamma_{HGP} = 155 M_{INSULIN} * M_{GLUCOSE} * M_{GLUCAGON} \quad (4.23)$$

where $M_{INSULIN}$, $M_{GLUCOSE}$, $M_{GLUCAGON}$ (dimensionless) Indicate the contribution of glucose, insulin and glucagon in hepatic glucose production (Γ_{HGP} in mg/min), respectively.

Nevertheless, this quantity cannot be introduced in this form to Bergman's model equation 3.27, it is necessary to divide it by the patient's weight in order to have consistent units (mg/min/kg):

$$\frac{dG_{Prod}}{dt} = a_1 PVO_2^{max}(t) - a_2 G_{Prod} + \frac{\Gamma_{HGP}}{W} \quad G_{Prod}(0) = 0 \quad (4.24)$$

Figures 49 and 50, illustrate the schematics of this implementation.

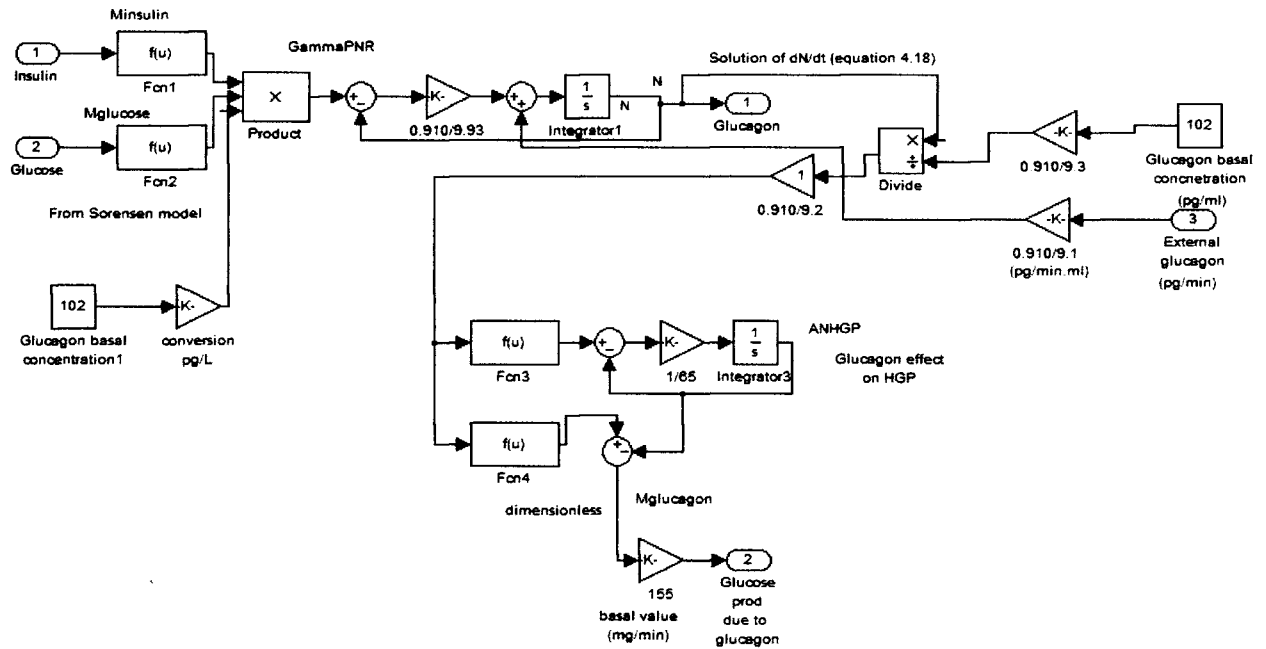


Figure 49. Schematic of the implementation of hepatic glucose production rate due to external glucagon infusion in Sorensen's model.

Figure 50 is described as follow: The hepatic glucose production due to glucagon administration is calculated by the subtraction of the production without exogenous glucagon from the production with glucagon infusion. This procedure is necessary since a direct estimation of glucose production from glucagon input is not possible due to the multiplicative effects of insulin, glucose and glucagon concentrations.

The response of glucose level of the two models due to an external infusion of glucagon is in the data range reported by Sorensen. Figure 51 shows the resulting dynamics of glucose.

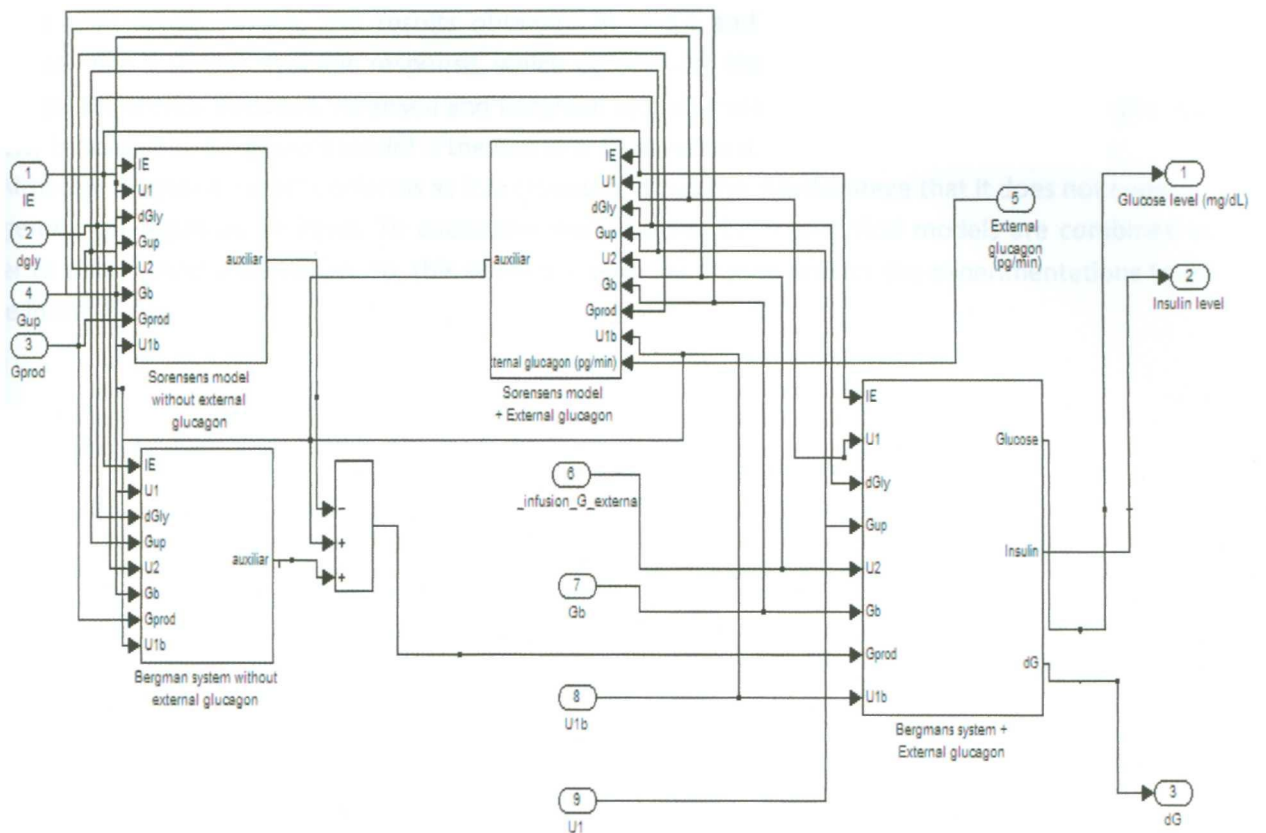


Figure 50. Schematic of the combination of Sorensen's and Bergman's models.

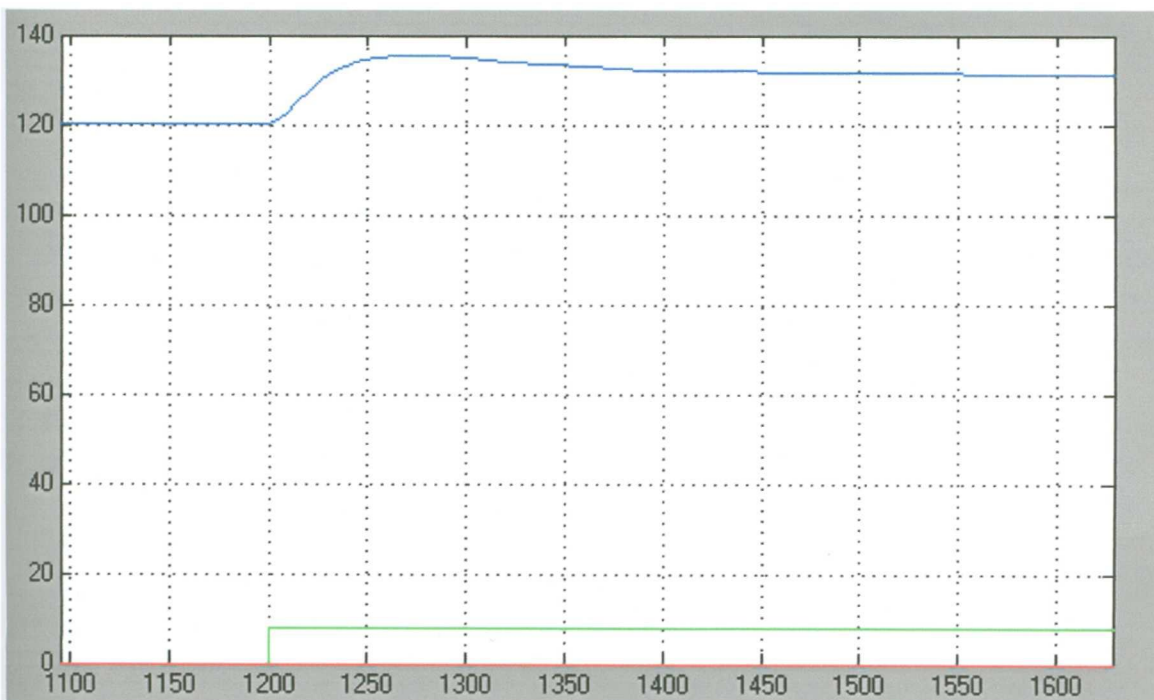


Figure 51. Response of glucose level (blue) (mg/dL) to external glucagon infusion rate step (green) (10^4 pg/min).

As a concluding remark, the results obtained in test I and II show that glucose concentration response have a similar dynamic response, which agrees with the clinical data reported. Nevertheless, the major difference between Sorensen and Bergman models rises in the insulin behavior when physical activity is done. The Bergman's model is the one that behaves as it is stated in medical literature.

Although Bergman model performs as it is expected, it has the disadvantage that it does not consider exogenous glucagon as an input. To overcome this problem, both analytical models are combined in order to obtain their advantages. So, this combination is the chosen one for the experimentations to be done in this thesis.

Chapter 5

Experiment design for statistical modeling

The previous chapter presents the development of a descriptive model of the glucose – insulin metabolism considering exercise effects. A statistical model is commonly used to design feedback and feedforward controllers because of practicality: eliminated analytical complexity; simple structures; discrete form.

The derivation of a statistical model is based on input – output data of the real process. In this case, the process is represented by the physiological model and the experimentation to produce input – output data refers to the simulation of the model before specific conditions.

This chapter describes the experiment design criterion followed to obtain a reliable statistical model that relates PAMM, glucagon and insulin administration with glucose level and its rate of change.

5.1. Criterion of the statistical experiment design

According to Rollins et. al. (2008), successful results for identifying the dynamics of several perturbations in glucose –insulin system had been obtained using Hammerstein – Wiener modeling technique. This method will be explained more detailed in the next chapter, but it basically consists in the representation of multiple inputs – outputs process by a combination of linear and nonlinear equations, whose coefficients must be determined.

An experiment design that fulfills Hammerstein-Wiener requirements is the Box-Behnken design (BBD), which has the following advantages (Rollins, 2004):

- Reduced experimentation time
- Production of accurate data for adjustment of the parameters in Hammerstein –Wiener model.
- Restriction less on static behavior of the system.
- Successful estimation when identifying quadratic behavior.
- Restriction less on the number of inputs and outputs.

- A priori assumptions can be used.

Montgomery establishes that when dealing with a BBD experiment with three inputs, the next norm must be followed:

Table IX. BBD experiment design input values.

Run	Input 1	Input 2	Input 3
1	-1	-1	0
2	-1	1	0
3	1	-1	0
4	1	1	0
5	-1	0	-1
6	-1	0	1
7	1	0	-1
8	1	0	1
9	0	-1	-1
10	0	-1	1
11	0	1	-1
12	0	1	1
13	0	0	0
14	0	0	0
15	0	0	0

Where -1, 0, 1 indicate minimum, mean and maximum value of each input. All inputs must be in deviation value form.

It can be inferred from Table IX that in the sequence followed in the experiment one input is hold at its mean value and the other inputs are changed.

5.2. Data used in glucose system experiment

As stated in chapter 4, the input to be managed to increase the blood glucose level is the infusion of external glucagon, so definitely this variable must be considered in the experiment.

The statistical model should only include the variables necessary for the purpose of controlling glucose levels under variations of physical activity. The model is defined as a system of three inputs and one output, meaning that a MI-SO (multiple inputs and single output) system is going to be identified. The output of the model is the glucose rate of change (mg/dL/min) and the inputs are

1. PAMM (%)
2. External glucagon infusion (pg/min)
3. External insulin infusion (mU/min)

Glucose rate of change is chosen as the output variable, because in order to use Hammerstein – Wiener technique, a steady state has to be achieved when the system is excited by the inputs. As it is seen in figure 48 and from physiological information, glucose level would tend to zero if exercise is not stopped, which means that no steady state can be reached. Therefore, the glucose level cannot be considered as an output. However, the first time derivative of glucose can reach a constant value after certain exercise duration. Figure 52 illustrates the response of glucose rate of change when exercise is done.

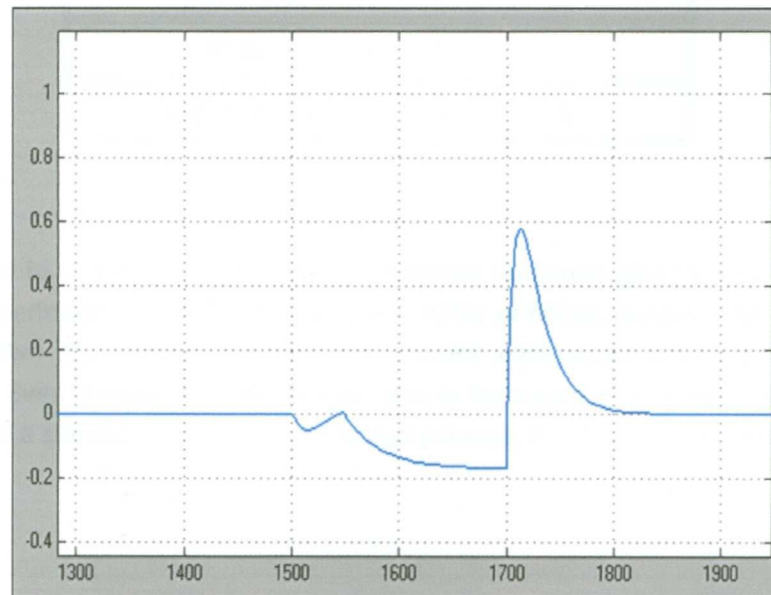


Figure 52. Glucose rate of change (mg/dL/min) response to a pulse input of 30 PAMM(%) from time 1500 to time 1700 min.

The range of the inputs for the experiment is chosen in such a form that the glucose levels stay around the desired or target value, to be maintained by a control system. Table X shows the ranges of the inputs and Table XI, the initial conditions considered in the experiment:

Table X. Range of the inputs in the experiment design. (Deviation values).

Input	Minimum value	Mean value	Maximum value
PAMM (%)	0	30	60
Glucagon (pg/min)	0	10000	20000
Insulin (mU/min)	0	10.45	20.9

Table XI. Initial conditions of the system prior to the experiment.

Variable	Initial condition
Glucose (mg/dL)	105
Glucose rate (mg/dL/min)	0
External Insulin (mU/min)	15.1
Glucagon (pg/min)	0
PAMM (%)	0
Sample time (min)	5

The data obtained in this experiment had an undesired outcome: glucose level dropping below 0 mg/dL. So a new experiment was designed using the BBD's principle, holding one input constant and changing the other two. But keeping in mind that glucose level would not drop to an unacceptable hypoglycemic value. Even though, the number of runs is increased, this is not a drawback since the experiment is done in a simulator and not in a physical process. In table XII, the new experiment design is shown:

Table XII. New experiment design input values.

Run	Time	Input 1	Input 2	Input 3
1	1500	0	-1	-1
2	1700	0	-1	0
3	1900	-1	-1	-1
4	2100	1	-1	-1
5	2300	1	-1	0
6	2500	-1	-1	0
7	2700	0	-1	1
8	2900	0	0	-1
9	3100	-1	-1	1
10	3300	1	-1	1
11	3500	1	0	-1
12	3700	-1	0	-1
13	3900	0	0	0
14	4100	0	0	1
15	4300	-1	0	0
16	4500	1	0	0
17	4700	1	0	1
18	4900	-1	0	1
19	5100	0	1	-1
20	5300	0	1	0
21	5500	-1	1	1
22	5700	1	1	0
23	5900	-1	1	0
24	6100	1	1	-1
25	6300	-1	1	-1

26	6500	0	1	1
27	6700	1	1	1

A time interval between runs or changes in input conditions is set in 200 minutes, because that is the time the glucose rate takes to get to its steady state.

With this new experiment design glucose level is kept above 40 mg/dL.

5.3. Data obtained in the experiment

The new experiment design produced the necessary transitory and steady state values. Moreover, the glucose level stayed in an acceptable range. Figures 53 and 54 show the output and inputs of the experiment.

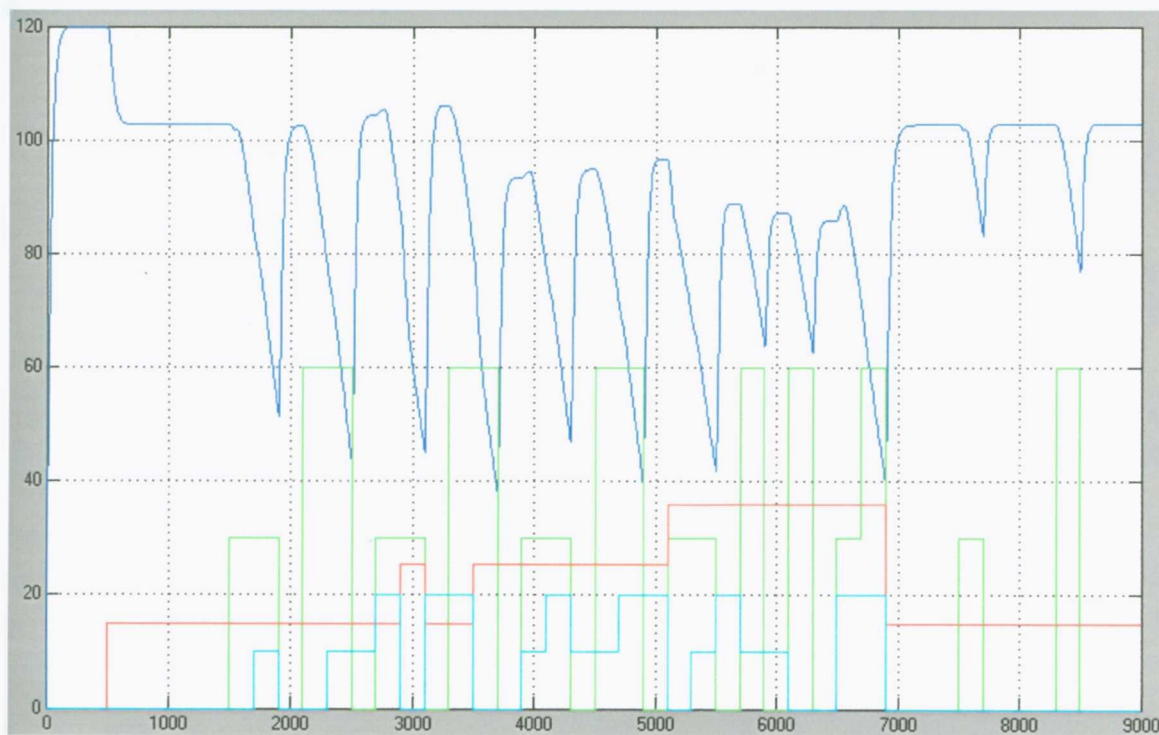


Figure 53. Data obtained in the experiment: Glucose concentration (blue) (mg/dL) response to PAMM (%) (green), External glucagon (cyan) (10^4) and External Insulin (red) (mU/min).

The data obtained in the experiment can be found in Appendix 2.

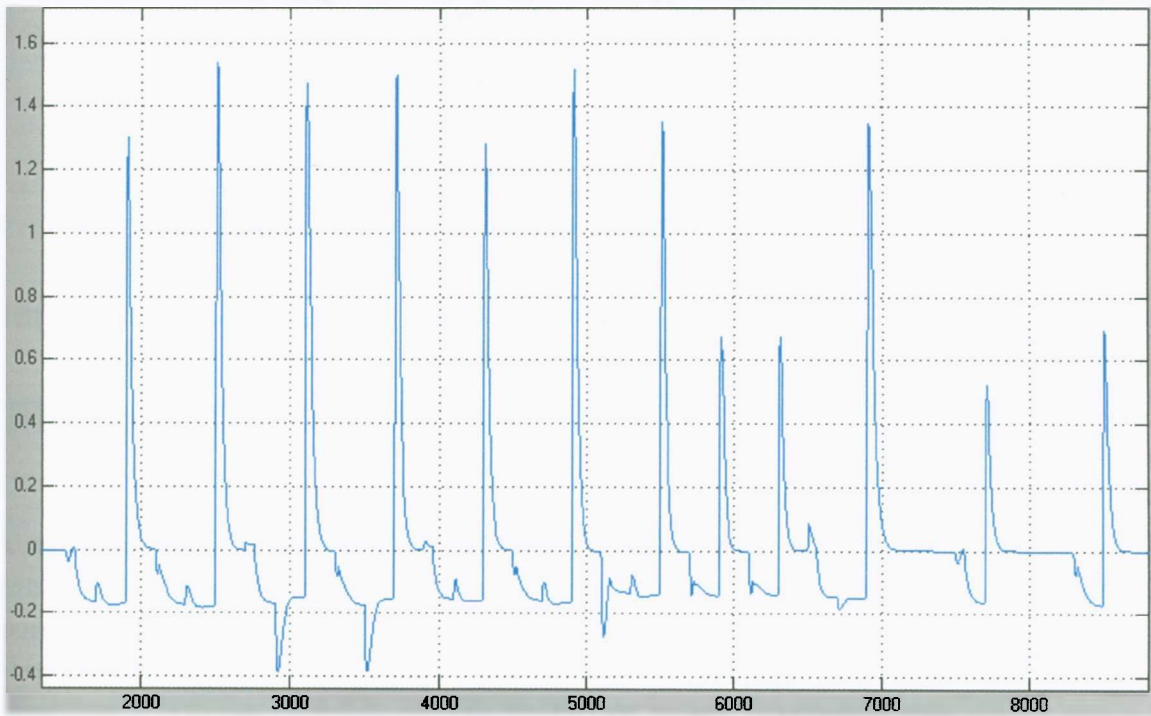


Figure 54. Data obtained in the experiment: Glucose rate of change (blue) (mg/dL/min).

Chapter 6

Statistical modeling

A statistical model is necessary for the characterization of glucose level response before exercise disturbance from physiological data; in this case, the data are generated from the physiological model proposed in chapter four.

This chapter focuses on statistical modeling and is divided in two parts: an introduction to Hammerstein – Wiener modeling and its application to the problem of this thesis. Also a brief explanation of the mathematical optimization methods used to adjust the parameters to the model is discussed.

6.1. Hammerstein – Wiener modeling technique

6.1.1. Definition

Dynamic predictive models that address nonlinear behavior are essential for optimal operation and control of many processes (Eskinat, 1991). A black – box modeling technique discussed in recent publications for non-linear processes is the Hammerstein – Wiener modeling (Rollins, Constrained MIMO dynamic discrete-time modeling exploiting optimal experimental design, 2004).

The Hammerstein and Wiener systems divide the plant to be identified in two parts: a group of linear dynamic blocks and a second group of blocks of nonlinear static gain, if Wiener technique is applied, but if Hammerstein method is used the order of the blocks is reversed. Figure 55 illustrates the Wiener system representation.

The major advantages of a Wiener system over a Hammerstein one rely on the fact that the former allows the inputs to have different dynamics and is able to treat nonlinear systems through non-differential equations (polynomials) in terms of outputs of the linear dynamics (Rollins, Bhandari, & Kotz, Critical modeling issues for succesful feedforward control of blood glucose in insulin dependent diabetics, 2008).

As it can be seen in figure 51, this modeling technique permits the development of a model with multiple inputs for the prediction of multiple outputs.

Basically, the functioning of a Wiener system is

- Each input (u_i) enters a linear block (G_{ij}), which represents a model of the input's dynamic impact over an output η_j of the nonlinear system.
- The output of each linear block will be called auxiliary variable, denoted as v_i .
- Afterwards, the auxiliary variables (v_i 's) are joint in a final block, which represents the static nonlinear gain ($f_j(v_i)$)of the output η_j of the system.
- The output of a nonlinear block is an output of the system.

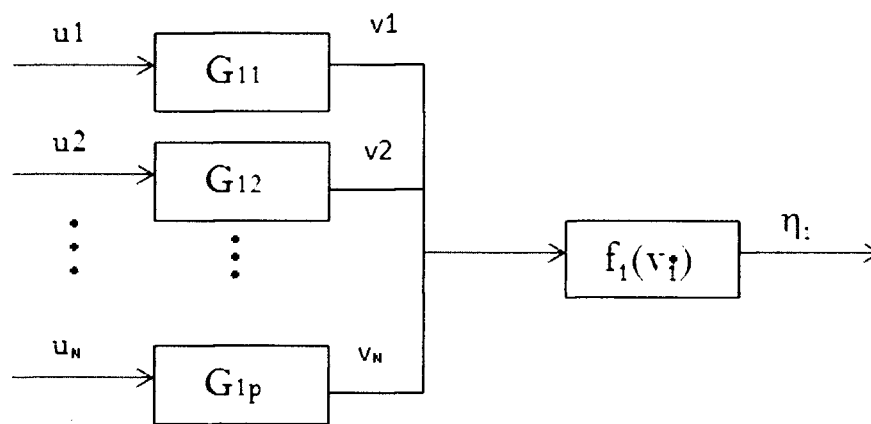


Figure 55. Block diagram of Wiener system for one output η_i .

For the purpose of this thesis, a multiple input – single output (MI-SO) system is considered. Another restriction, not imposed by a particular application but for the Wiener modeling technique itself, is that the process response must be stable. Moreover, a priori knowledge of the settling time of the process response is necessary.

6.1.2. System identification via Wiener technique

For modeling a system with the Wiener technique, there are several steps to follow, being the principal ones:

1. Selection of the experimental design. The following parameters and information must be specified:
 - Sample time

- Operating range for each input (u_1, u_2, \dots, u_n)
- Stabilization times of the process outputs
- Model structure of the steady state behavior
- Experimental test (BBD). BBD has advantages over PRBS (Bhandari, 2003)
- Randomization of the trials

2. Obtaining a fitted model for the ultimate response function (the nonlinear model)

In this step, the modeler uses the data obtained at the end of each trial, the corresponding inputs and a multiple regression technique to get a model (Rollins, Constrained MIMO dynamic discrete-time modeling exploiting optimal experimental design, 2004).

An example of this nonlinear model is:

$$\hat{\eta}(t) = \beta_1 v_1(t) + \beta_2 v_2(t) + \dots + (\beta_n v_n(t))^2 \quad 6.1.$$

where $\hat{\eta}$ is the estimated output of the system, v_1, v_2, \dots, v_n are the dynamic auxiliary variables of the system and $\beta_1, \beta_2, \dots, \beta_n$ are the parameters to be estimated.

To obtain the β parameters, the modeler can use the inputs (u_i) instead of auxiliary variables (v_i), with the steady output (η) because in the steady state response the values of u_i and v_i are the same. This is only valid at the final of each trial:

$$\hat{\eta}^\infty = \beta_1 u_1^\infty + \beta_2 u_2^\infty + \dots + (\beta_n u_n^\infty)^2 \quad 6.2.$$

Where the supraindex ∞ indicates a stable operation point.

If the modeler identifies that a β_i parameter is very small compared with the other β_j 's, the whole term that includes β_i can be eliminated.

3. Finding the dynamic models

After obtaining the nonlinear model parameters, it is necessary to adjust discrete time models that represent the dynamics of the n-inputs (u_i) with the n-auxiliary variables (v_i). It is seen in figure 51 that the number of linear discrete models depends on the number of inputs.

The models, due to its discrete nature, must be of an autoregressive with exogenous inputs kind (ARX). The number of autoregressive terms and exogenous terms can be initially set to two and one, respectively (Rollins, 2004). Later on, this assumption could be modified depending on the minimization criteria used for the difference between the estimated output of the model and the output of the real system.

The structure of the model can be seen in equation 6.3.

$$v_{j,t} = \sum_{k=1}^n \delta_{j,k} v_{j,t-k} + \sum_{l=1}^m \omega_{j,l} u_{j,t-l} + \left(1 - \sum_{k=1}^n \delta_{j,k} - \sum_{l=1}^m \omega_{j,l} \right) u_{j,t-(m+1)} \quad 6.3.$$

where j refers to the input with $j=1..n$; k denotes the current sampling time; δ and ω are the parameters of the autoregressive and exogenous terms, respectively; η is the order of autoregression and m is the number of exogenous inputs terms. The last term of the equation calculates the last coefficient as a sum of the other parameters.

For obtaining the parameters δ 's and ω 's of each model, the approach of constraining the parameters β of the nonlinear model to the values calculated by equation 6.2 is followed.

In this way the dynamic parameters of each linear model are calculated with the criteria of finding the minimum difference between the estimated output and the real output. Because the nonlinear parameters are constrained, generalized reduced gradient technique (GRG) is used. This method is a mathematical algorithm that adjusts the parameters so that the active constraints continue to be satisfied as the optimization moves from one point to another, until the optimal solution is found. Information about the mathematical background of this technique can be found in reference (LSU).

6.1.3. Wiener modeling advantages over other modeling methods

When dealing with nonlinear systems, models like nonlinear autoregressive moving average models with exogenous variables (NARMAX) and artificial neural networks (ANN) can be used for representing cause - effect relations in a system. Nevertheless, these two modeling options have significant drawbacks.

NARMAX drawbacks (Rollins, 2008) :

1. Because the model form is linear in parameters, the values of the fitted model coefficients are tied to the correlation structure of the model. Thus any change in the input correlation structure can produce large prediction errors. The model can produce highly incorrect results for independent changes in the inputs.
2. The strong natural correlation of common lag input variables causes ill conditioning and inflates estimation errors.

ANN drawbacks (Rollins, 2008):

1. The major disadvantage is the lack of phenomenological structure which is crucial when fitting nonlinear behavior.

- When the inputs combinations that were used in the training phase are change, extremely large prediction errors can occur due to the highly nonlinear transfer functions of the ANN.

After reviewing the disadvantages of the NARMAX and ANN techniques, it is important to specify what makes the Wiener method more efficient: the parameters in the nonlinear functions are independent from the ones of the linear dynamic functions and the terms in the static nonlinear functions depend on the variables from the dynamic blocks which are not strongly correlated (an auxiliary variable does not depend on other auxiliary variables) (Rollins, 2004). So it does not matter if the inputs are correlated or not, the predicted output will not be affected due to the Wiener modeling nature. In figure 56, the performances of the three proposed methods are illustrated in a graph, where it can be seen that Wiener modeling has the best accuracy in the testing phase.

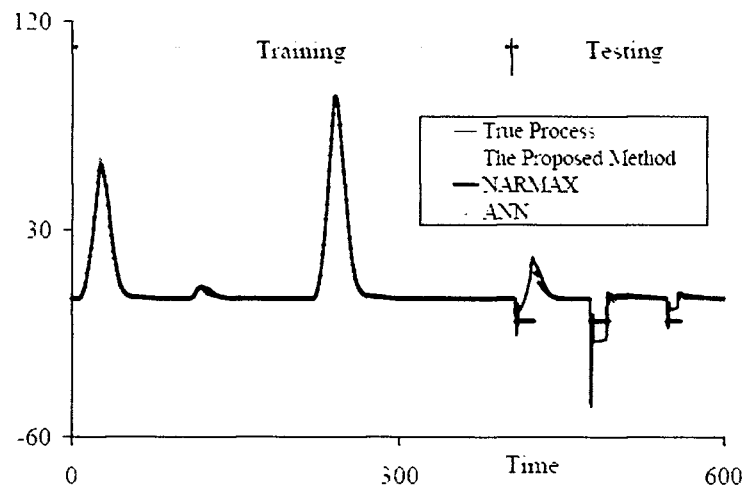


Figure 56. Performance of the system in the training and testing phases for different modeling techniques (Wiener, NARMAX and ANN). Inputs in testing phase are uncorrelated. Taken from Rollins (2008).

6.1.4. Wiener modeling applied to glucose regulation

In chapter five, the output and inputs to use in Wiener modeling were declared, being PAMM (%), external insulin infusion (mU/min) and external glucagon infusion (pg/min) the inputs and glucose rate of change (mg/dL/min) as the output.

Following the algorithm depicted in the last section, the proposed nonlinear model is:

$$\eta = \beta_1 v_1 + \beta_2 v_2 + \beta_3 v_3 + \beta_4 v_1 v_2 + \beta_5 v_1 v_3 + \beta_6 v_2 v_3 + \beta_7 v_1^2 + \beta_8 v_2^2 + \beta_9 v_3^2 \quad 6.4.$$

where v_1 is the auxiliary variable for PAMM, v_2 is the auxiliary variable for external insulin infusion, v_3 is the auxiliary variable for external glucagon infusion and η is the glucose rate of change. It can be seen that there is not a constant term in equation 6.4, this is done because the method indicates that deviation values must be used and in order to get a null response of the system when there is not a change in the inputs, the constant parameter must be eliminated.

The adjustment of the parameters of equation 6.4 is achieved using the data obtained at the end of each trial of the experiment described in chapter five. This procedure is done using MS-Office Excel's Regression Toolbox®, through introducing the inputs and the output of the trials and applying the multiple nonlinear least squares regression.

After adjusting the nonlinear model, the next goal is to select the order of the linear ARX models and find the parameters that will make an accurate prediction of the estimated output. Because the objective in this step is finding the dynamic response of each input, this procedure uses all the data from the experiment, not only the data at the end of each trial.

Three linear ARX models are developed, using the structure in equation 6.3, because three inputs are taken into consideration. Firstly, a model with 2 autoregressive terms and one exogenous term is specified for each input, if the estimated output is not accurate, the order of the model has to be increased.

With the usage of MS-Office Excel's Solver Toolbox®, which inherently applies the GRG optimization method, the linear ARX models parameters were obtained.

Previous data conditioning may be considered, due to a significant difference between the magnitudes of the inputs. The data was normalized with the following criteria and different models were developed:

- Row deviation data
- Normalization of the data in the theoretical form, using the mean and standard deviation, so that the data could have mean 0 and variance 1
- Scaling of each input data respect to (dividing by) its maximum deviation value, using different sample times (5 and 10 minutes)

6.1.4.1. Development of the Wiener model without normalization of data

The first model developed was without normalizing the data. Table XIII shows the best calculated nonlinear parameters in a Wiener model. The comparison between the predicted ultimate nonlinear gains and the ones obtained in the experiment is illustrated in figure 57.

Table XIII. Parameters of the nonlinear model.

Parameter	Value	Input variables affected by the parameter
β_1	-0.00774435	PAMM
β_2	0.00039288	Insulin infusion
β_3	-1.7083×10^{-7}	Glucagon infusion
β_4	2.488×10^{-5}	PAMM x Insulin infusion
β_5	-2.9722×10^{-9}	PAMM x Glucagon infusion
β_6	-8.7719×10^{-9}	Glucagon infusion x Insulin infusion
β_7	8.1296×10^{-5}	PAMM ²
β_8	-6.1049×10^{-6}	Insulin infusion ²
β_9	4.5×10^{-12}	Glucagon infusion ²

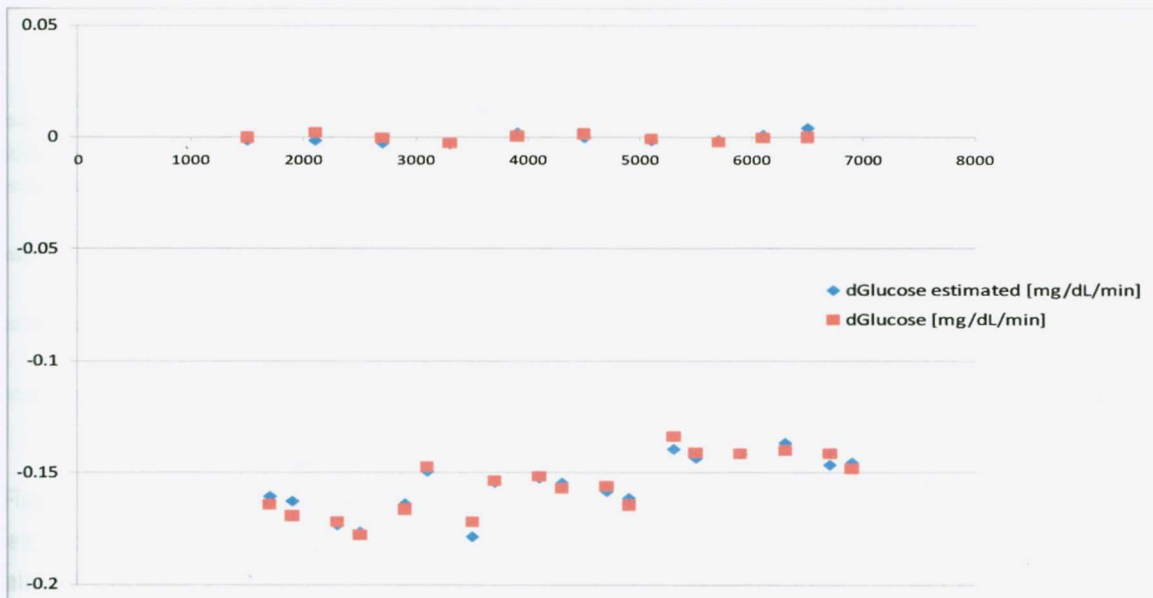


Figure 57. Comparison between the predicted nonlinear steady state glucose concentration rates and the obtained in the experiment without normalizing the data.

As it is shown, the obtained nonlinear model has an excellent accuracy in the prediction of nonlinear gains; this was verified with the coefficient of determination R^2 , which gave a value of 0.9972 and its multiple correlation coefficient was 0.9990. Both performance indexes describe the correlation between the constructed predictor and the response variable. Also, from the values of the parameters it appears that external glucagon infusion is the input with less impact in the nonlinear gain; however, this misunderstanding happens because the data is not normalized.

Respect to the linear ARX models, the best obtained models were of second order with two exogenous input terms, equations 6.5 – 6.7 show them:

$$v_{1,k} = \delta_{11}v_{1,k-1} + \delta_{12}v_{1,k-2} + \omega_{11}u_{1,k-1} + \omega_{12}u_{1,k-2} \quad 6.5.$$

$$v_{2,k} = \delta_{21}v_{2,k-1} + \delta_{22}v_{2,k-2} + \omega_{21}u_{2,k-1} + \omega_{22}u_{2,k-2} \quad 6.6.$$

$$v_{3,k} = \delta_{31}v_{3,k-1} + \delta_{32}v_{3,k-2} + \omega_{31}u_{3,k-1} + \omega_{32}u_{3,k-2} \quad 6.7.$$

where u_1 denotes PAMM, u_2 refers to external insulin infusion and u_3 is external glucagon infusion. The parameters for each model can be seen in table XIV.

Table XIV. Parameters obtained for the linear ARX models without normalizing the data.

Auxiliary variable (i)	Model	δ_{i1}	δ_{i2}	ω_{i1}	ω_{i2}
1	v_1	0.81077399	9.9678×10^{-6}	2.32248331	-2.13326727
2	v_2	0.99874311	0.00380755	0.00506445	-0.0076151
3	v_3	0.00019595	1.1448×10^{-14}	11.1466346	-10.1468306

Figure 58 shows the predicted and the real glucose rate of change, where it can be inferred that the developed model can be improved. Nonetheless, comparing the prediction performance with the ones obtained by Rollins, a significant enhancement has been achieved. Another aspect that can be noticed is that the model obtained has a drawback in representing the effect of external insulin infusion; this can be seen when the predicted glucose rate does not follow the same pattern as the real data in the time interval between 2940 and 3580 min; which corresponds to an input combination of PAMM and external insulin infusion at their mean value and without external glucagon infusion, according to the experiment design reported in table XII.

It is important to remark that the sample time was 10 min. The sample time was selected to be greater or equal than 5 minutes, because nowadays this is the fastest time interval that glucose sensors can make measurements.

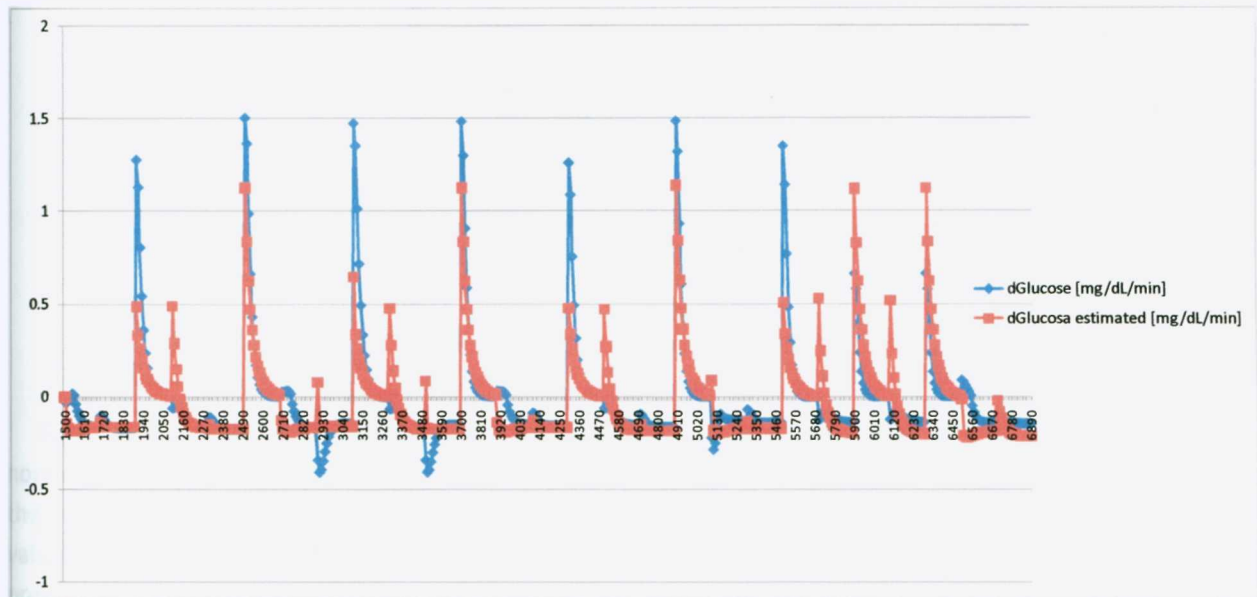


Figure 58. Predicted glucose rate of change and its real value obtained in the experiment, without normalizing the data.

Nevertheless, the quadratic sum of errors was 15.3712.

6.1.4.2. Development of the Wiener model with normalized data ($N(\mu=0, \sigma^2=1)$)

Due to a major difference in the inputs magnitudes, especially with external glucagon infusion, it was decided to normalize the data, so the numerical range of the inputs would not hide or distort the functional relation with the glucose rate of change. This data conditioning uses the basic principle of normalization, which is subtracting the mean and dividing by the standard deviation of the variable. This normalization criterion was done to the steady state inputs and output data.

The parameters for the nonlinear model that were obtained after normalizing the data are shown in table XV.

Table XV. Parameters of the nonlinear model with $N(\mu=0, \sigma^2=1)$.

Parameter	Value
β_0	2.2481×10^{-17}

β_1	-2.56624899
β_2	0.04534865
β_3	-0.0188697
β_4	0.14069266
β_5	-0.01608346
β_6	-0.01653439
β_7	1.68235165
β_8	-0.01532894
β_9	0.01034704

Figure 59 illustrates a comparison between the predicted and real steady state glucose rate normalized values. As it is shown, the new obtained nonlinear model has also an excellent accuracy in the prediction of glucose rate; this was verified with the coefficient of determination R^2 , which gave a value of 0.9972 and its multiple correlation coefficient was 0.9990. These values were the same as in the previous section, however the parameters have are similar in magnitude.

The best obtained linear ARX models were of 14th order with 15 exogenous inputs terms, equations 6.8 – 6.10 show them:

$$v_{1,k} = \delta_{1,1}v_{1,k-1} + \dots + \delta_{1,14}v_{1,k-14} + \omega_{1,1}u_{1,k-1} + \dots + \omega_{1,15}u_{1,k-15} \quad 6.8.$$

$$v_{2,k} = \delta_{2,1}v_{2,k-1} + \dots + \delta_{2,14}v_{2,k-14} + \omega_{2,1}u_{2,k-1} + \dots + \omega_{2,15}u_{2,k-15} \quad 6.9.$$

$$v_{3,k} = \delta_{3,1}v_{3,k-1} + \dots + \delta_{3,14}v_{3,k-14} + \omega_{3,1}u_{3,k-1} + \dots + \omega_{3,15}u_{3,k-15} \quad 6.10.$$

The parameters for each model are shown in table XVI.

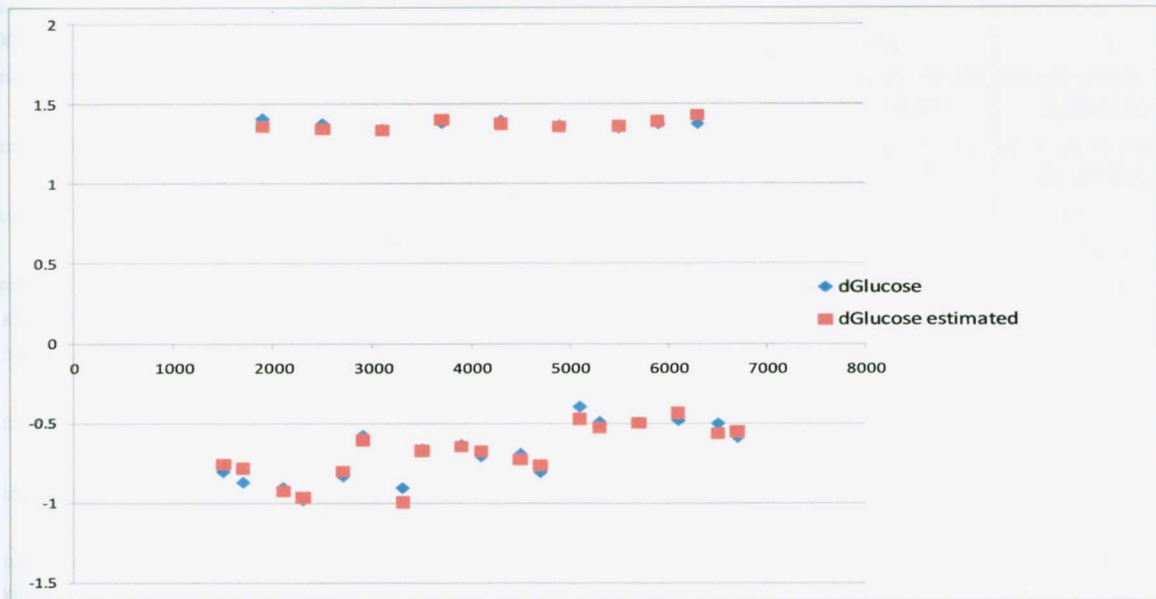


Figure 59. Comparison between the predicted nonlinear steady state glucose concentration rates and the obtained in the experiment with $N(\mu=0, \sigma=1)$.

Table XVI. Parameters obtained for the linear ARX models with $N(\mu=0, \sigma^2=1)$.

Auxiliary variable (i)	Model	δ_{i1}	δ_{i2}	δ_{i3}	δ_{i4}
1	v_1	2.23779676	0.39839314	-4.06639412	1.61775119
2	v_2	1.14124487	1.93935156	-2.74771556	-0.84663718
3	v_3	-0.15276258	2.55284005	0.33385339	-2.18270553
Auxiliary variable (i)	Model	δ_{i5}	δ_{i6}	δ_{i7}	δ_{i8}
1	v_1	1.94932475	-0.35869673	-0.6835537	-1.02529882
2	v_2	2.31201442	-0.51476923	-0.64443705	0.43464338
3	v_3	-0.2331662	0.63916385	-0.01975735	-0.03200659
Auxiliary variable (i)	Model	δ_{i9}	δ_{i10}	δ_{i11}	δ_{i12}
1	v_1	0.86906773	0.49159962	-0.51222695	-0.04383545
2	v_2	-0.12614824	0.15495844	-0.13748321	-0.09862844
3	v_3	0.12027379	-0.09913646	-0.12508818	0.14680067

Auxiliary variable (<i>i</i>)	Model	δ_{i13}	δ_{i14}	ω_{i1}	ω_{i2}
1	v_1	0.21387603	-0.0898321	1.47655307	-3.38814936
2	v_2	0.20857552	-0.07821921	-19.829199	28.4940679
3	v_3	0.07068713	-0.03831418	-9.60510083	24.7371935
Auxiliary variable (<i>i</i>)	Model	ω_{i3}	ω_{i4}	ω_{i5}	ω_{i6}
1	v_1	-0.57182711	6.19445156	-2.26848334	-3.21222792
2	v_2	27.4118984	-54.1368556	2.0098094	24.4575906
3	v_3	4.06848532	-47.0696161	18.8450326	21.7081983
Auxiliary variable (<i>i</i>)	Model	ω_{i7}	ω_{i8}	ω_{i9}	ω_{i10}
1	v_1	0.3276319	1.27901309	1.6677651	-1.3553616
2	v_2	-8.74670334	-0.05448204	0.23832341	0.2253957
3	v_3	-13.5370976	0.64292432	0.4692566	0.89190582
Auxiliary variable (<i>i</i>)	Model	ω_{i11}	ω_{i12}	ω_{i13}	ω_{i14}
1	v_1	-0.63702854	0.48889382	0.05064537	-0.06352662
2	v_2	0.20004774	-0.26908198	0	0
3	v_3	-0.67229433	-0.49127327	0	0
Auxiliary variable (<i>i</i>)	Model	ω_{i15}			
1	v_1	0.01367924			
2	v_2	0.00243882			
3	v_3	0.03170381			

After obtaining the linear parameters a comparison of the predicted and real glucose rate was made. The result can be seen in figure 60. The reported quadratic sum of errors was 32.2949; nonetheless this indicator is bigger than in the other criterion, it can be seen that the predicted output follows in a closer way the real data, even for drastic changes and when external insulin is infused. So, it can be inferred that the goal of giving the inputs a same weight has been achieved. The reason why the quadratic sum of errors is greater, is due to the normalization of the data. The maximum magnitude with this

normalization is 5.25 while without normalization is 1.5; hence, any difference between the model and the real output will have a greater error.

The sample time for developing this model was 10 min.

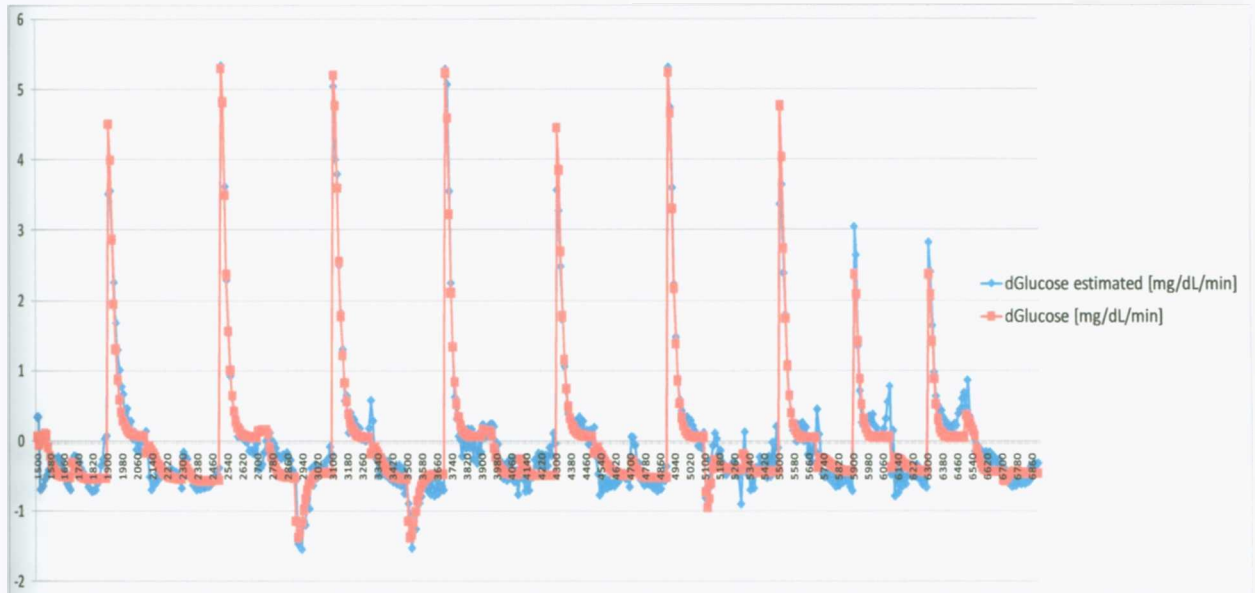


Figure 60. Predicted glucose concentration rate of change and its real value obtained in the experiment, with $N(\mu=0, \sigma^2=1)$.

6.1.4.3. Development of the Wiener model with scaling of each input with respect to its maximum value and a sample time of 10 minutes

The scaling of data by dividing by the maximum was used, because the purpose of developing an accurate predictive model is for the realization of an online controller. Therefore, if the theoretical normalization criterion were chosen it would take a minimum of a hundred samples before getting a reliable result. This drawback can be overcome by “normalizing” each input data respect to its maximum value, which is known. The output was not “normalized” by this criterion.

The nonlinear parameters that were obtained are shown in table XVII.

Table XVII. Parameters of the nonlinear model dividing each input by to its maximum value.

Parameter	Value
β_0	-0.00130833
β_1	-0.46466111

β_2	0.00821111
β_3	-0.00341667
β_4	0.0312
β_5	-0.00356667
β_6	-0.00366667
β_7	0.29266667
β_8	-0.00266667
β_9	0.0018

Figure 61 illustrates a comparison between the predicted and real steady state glucose concentration rates with the inputs scaled by its maximum value. The results were the same as in the other two cases, and as it was expected the values of the parameters have a similar order of magnitude.

The best obtained linear ARX models were of 15th order with 16 exogenous inputs terms, equations 6.11 – 6.13 show them:

$$v_{1,k} = \delta_{1,1}v_{1,k-1} + \dots + \delta_{1,15}v_{1,k-15} + \omega_{1,1}u_{1,k-1} + \dots + \omega_{1,16}u_{1,k-16} \quad 6.11.$$

$$v_{2,k} = \delta_{2,1}v_{2,k-1} + \dots + \delta_{2,15}v_{2,k-15} + \omega_{2,1}u_{2,k-1} + \dots + \omega_{2,16}u_{2,k-16} \quad 6.12.$$

$$v_{3,k} = \delta_{3,1}v_{3,k-1} + \dots + \delta_{3,15}v_{3,k-15} + \omega_{3,1}u_{3,k-1} + \dots + \omega_{3,16}u_{3,k-16} \quad 6.13.$$

The parameters for each model are shown in table XVIII.

A comparison between the predicted and real glucose rate with data conditioning procedure is illustrated in figure 62. It can be seen, that so far, this is the best predictive model calculated with a quadratic sum of errors is 3.6098.

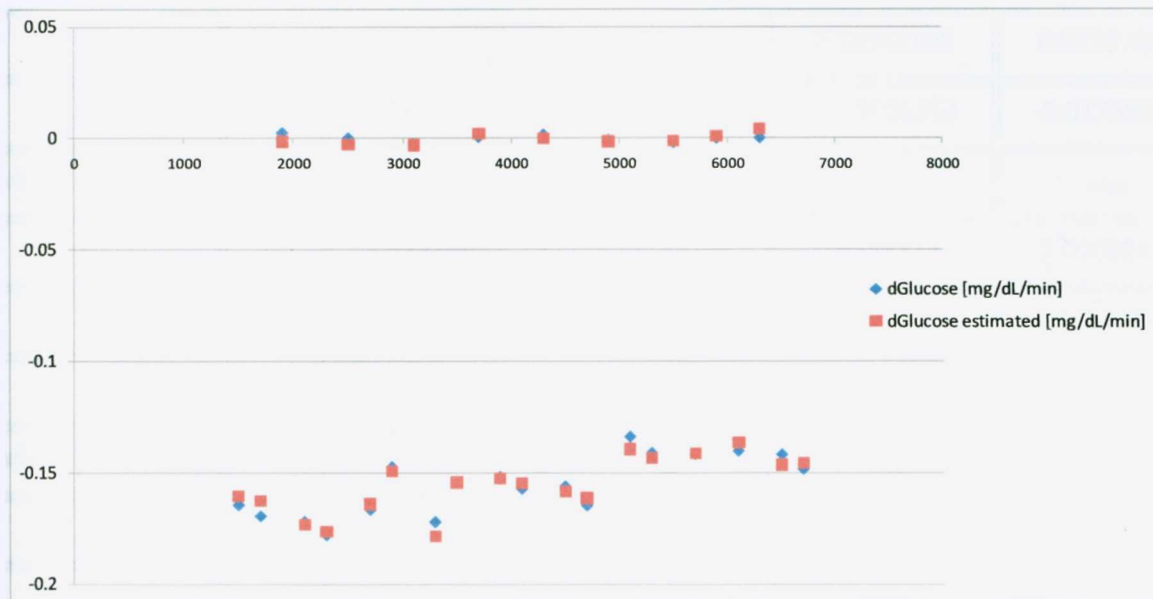


Figure 61. Comparison between the predicted nonlinear steady state glucose concentration rates and the obtained in the experiment with the inputs divided by its maximum value with a sample time of 10 minutes.

Table XVIII. Parameters obtained for the linear ARX models normalizing each input respect to its maximum value.

Auxiliary variable (i)	Model	δ_{i1}	δ_{i2}	δ_{i3}	δ_{i4}
1	v_1	2.19597365	-1.57084583	-0.34381103	0.87622164
2	v_2	1.95435617	-1.72308085	0.56874273	-0.13683583
3	v_3	0.81271076	0.88768425	-0.71424498	-0.04459945
Auxiliary variable (i)	Model	δ_{i5}	δ_{i6}	δ_{i7}	δ_{i8}
1	v_1	0.4802319	-1.41400914	1.27600785	-1.29635569
2	v_2	0.13032491	-0.0776995	0.14135655	0.06440516
3	v_3	0.08135725	0.12817232	-0.4145987	-0.02885872
Auxiliary variable (i)	Model	δ_{i9}	δ_{i10}	δ_{i11}	δ_{i12}
1	v_1	1.3971722	-0.32488428	-0.95752056	0.21217765

2	v_2	0.09118942	-0.20689813	0.18392105	0.07897269
3	v_3	0.16421721	-0.02614071	-0.19696253	-0.01755639
Auxiliary variable (i)	Model	δ_{i13}	δ_{i14}	δ_{i15}	ω_{i1}
1	v_1	1.67219572	-2.12148196	0.85352123	2.01081431
2	v_2	-0.01185795	0.00603049	-0.06328246	-50.3896566
3	v_3	0.41446875	0.09435009	-0.29744658	-16.4521489
Auxiliary variable (i)	Model	ω_{i2}	ω_{i3}	ω_{i4}	ω_{i5}
1	v_1	-4.38335621	2.92559372	0.92569752	-1.65154672
2	v_2	98.5577036	-80.5098868	26.5589322	-2.94020932
3	v_3	13.8057239	15.675809	-10.6717858	-0.83464296
Auxiliary variable (i)	Model	ω_{i6}	ω_{i7}	ω_{i8}	ω_{i9}
1	v_1	-1.33822487	2.92632482	-2.2107883	2.16637054
2	v_2	1.32842655	4.88963797	6.89715417	4.6742625
3	v_3	-0.61062278	1.03772485	-6.47427813	-0.59260142
Auxiliary variable (i)	Model	ω_{i10}	ω_{i11}	ω_{i12}	ω_{i13}
1	v_1	-2.89742113	1.15553586	1.81454262	-1.01144765
2	v_2	-0.97448276	-3.70129127	-0.03908991	3.50730037
3	v_3	1.49761885	5.21153998	-0.40592774	-3.40919145
Auxiliary variable (i)	Model	ω_{i14}	ω_{i15}	ω_{i16}	
1	v_1	-2.30643474	3.52236857	-1.58262171	
2	v_2	1.86648352	-1.06489899	-8.6600297	
3	v_3	2.60201512	0.34101412	-0.56279919	

The sample time used for the development of this model was 10 min.

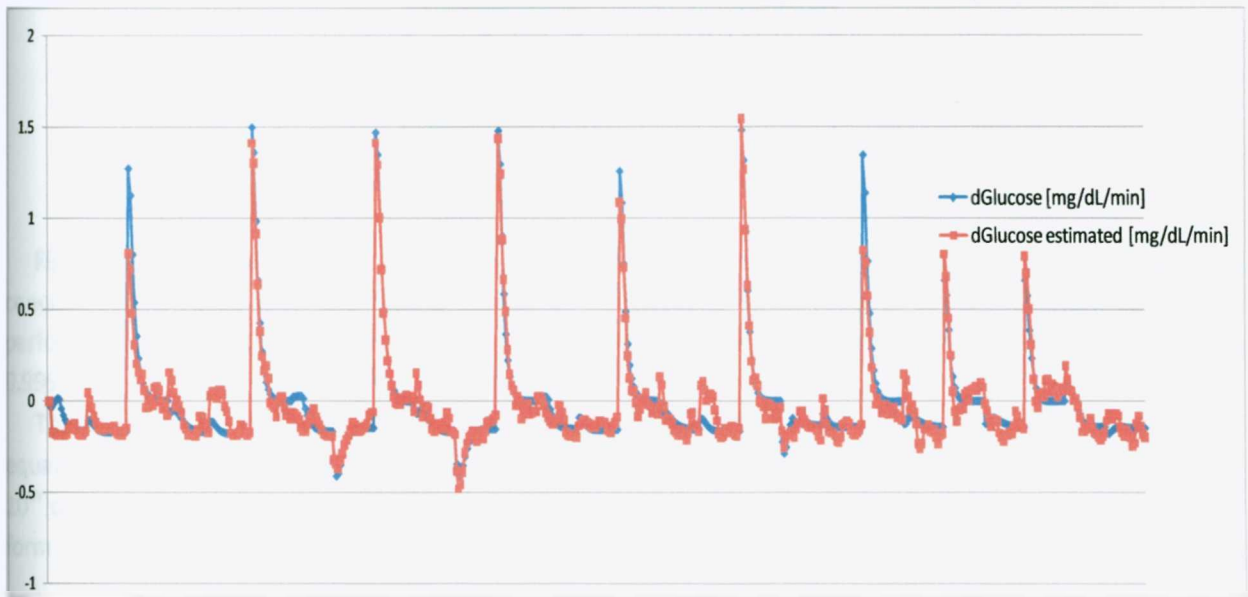


Figure 62. Predicted glucose rate of change and its real value obtained in the experiment, scaling each input respect to its maximum value with a sample time of 10 minutes.

6.1.4.4. Development of the Wiener model with scaling of each input by dividing by its maximum value and a sample time of 5 minutes

Basically, this data conditioning method was the same as in the previous section, but with the difference of using a smaller sample time.

The nonlinear parameters that were obtained are shown in table XIX.

Table XIX. Parameters of the nonlinear model dividing each input by its maximum value.

Parameter	Value
β_0	0
β_1	-0.54261364
β_2	0.00741414
β_3	-0.00399141
β_4	0.04341515
β_5	-0.00461818
β_6	-0.00451818
β_7	0.33778788

β_8	-0.00201212
β_9	0.00225455

Figure 63 illustrates a comparison between the predicted and real steady state glucose concentrations rates with the inputs scaled or “normalized” with respect to its maximum value. The performances indicators had a small change, R^2 was 0.9432 and its multiple correlation coefficient, 0.9995.

The most efficient obtained linear ARX models were of 5th order with 5 exogenous inputs terms, equations 6.14 – 6.16 show them. It is important to remark that when the model was increased up to a 10th order with 10 exogenous inputs terms the sum of quadratic errors did not change in a significant form.

$$v_{1,k} = \delta_{1,1}v_{1,k-1} + \dots + \delta_{1,5}v_{1,k-5} + \omega_{1,1}u_{1,k-1} + \dots + \omega_{1,5}u_{1,k-5} \quad 6.14.$$

$$v_{2,k} = \delta_{2,1}v_{2,k-1} + \dots + \delta_{2,5}v_{2,k-5} + \omega_{2,1}u_{2,k-1} + \dots + \omega_{2,5}u_{2,k-5} \quad 6.15.$$

$$v_{3,k} = \delta_{3,1}v_{3,k-1} + \dots + \delta_{3,5}v_{3,k-5} + \omega_{3,1}u_{3,k-1} + \dots + \omega_{3,5}u_{3,k-5} \quad 6.16.$$

The linear ARX models parameters are shown in table XX.

A comparison between the predicted and real glucose rate with this criterion is illustrated in figure 64. The quadratic sum of errors was 13.3455, which results in the second best obtained model.

The sample time used for the development of this model was 5 min.

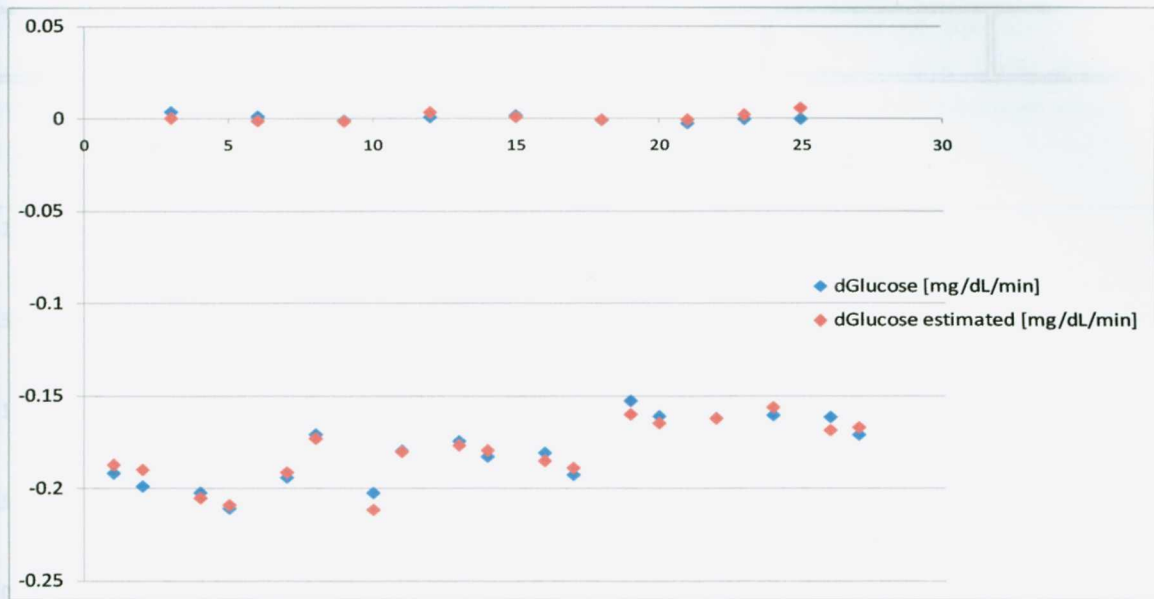


Figure 63. Comparison between the predicted nonlinear steady state glucose concentration rates and the obtained in the experiment with the inputs divided by its maximum value with a sample time of 5 minutes.

Table XX. Parameters obtained for the linear ARX models dividing each input by its maximum value with a sample time of 5 minutes.

Auxiliary variable (<i>i</i>)	Model	δ_{i1}	δ_{i2}	δ_{i3}	δ_{i4}
1	v_1	2.43539719	-1.33194562	-0.76278787	0.76003929
2	v_2	1.78868561	-0.35080926	-0.74946231	0.28509997
3	v_3	2.49698677	-1.73083123	-0.26530096	0.71645415
Auxiliary variable (<i>i</i>)	Model	δ_{i5}	ω_{i1}	ω_{i2}	ω_{i3}
1	v_1	-0.10155083	1.92158433	-4.45804033	2.02235454
2	v_2	0.02649845	-33.1754844	57.0461805	-19.6443092
3	v_3	-0.2179112	-9.25356113	20.9469872	-12.2029933
Auxiliary variable (<i>i</i>)	Model	ω_{i4}	ω_{i5}		
1	v_1	1.6766308	-1.16168151		
2	v_2	0.73260928	-4.95900863		

3	v_3	-1.3304141	1.84058376		
---	-------	------------	------------	--	--

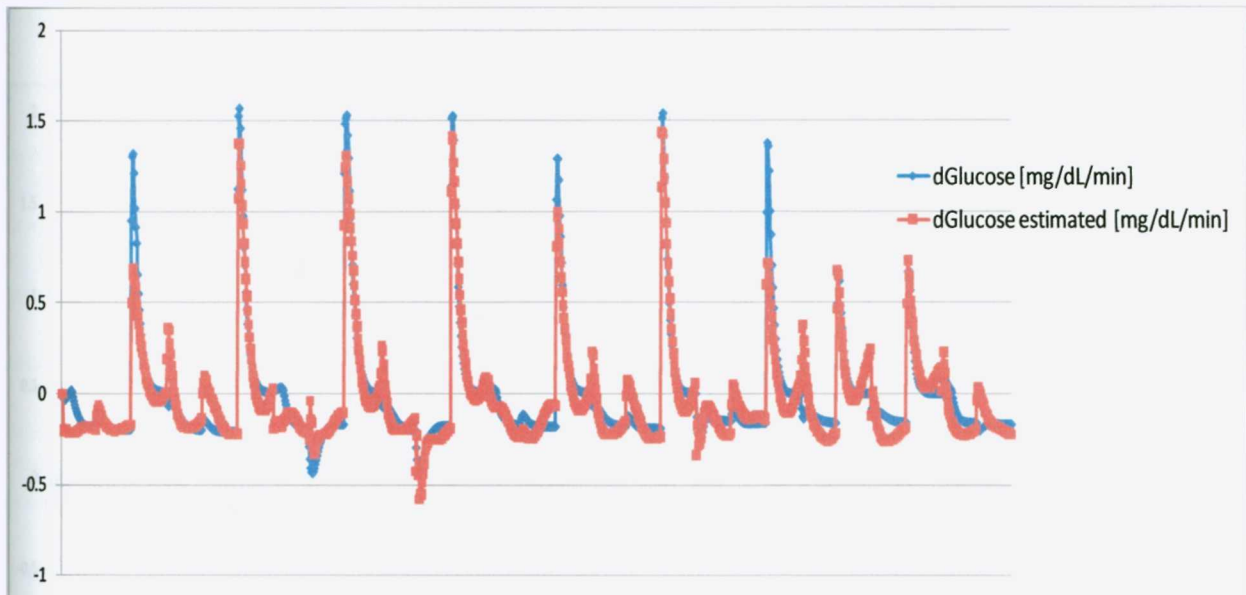


Figure 64. Predicted glucose concentration rate of change and its real value obtained in the experiment, scaling each input with respect to its maximum value with a sample time of 5 minutes.

All the data used in the adjustment of the models parameters are found on appendix 2.

6.1.4.5. Modifications in the chosen predictive model

The selected model for glucose rate prediction is the one that uses a sample time of 10 minutes and having each of its inputs data scaled by its maximum value. However, there is a noteworthy drawback; the linear ARX model for external glucagon infusion has a one iteration delay. In the next chapter, this disadvantage will be explained in detail. In order to have an immediate impact of external glucagon infusion on glucose rate, the structure of equation 6.13 had a small modification, deriving in the next equation:

$$v_{3,k} = \delta_{3,1}v_{3,k-1} + \dots + \delta_{3,15}v_{3,k-15} + \omega_{3,1}u_{3,k} + \dots + \omega_{3,16}u_{3,k-15} \quad 6.17.$$

Since the linear ARX parameters are calculated with the constraint of the nonlinear model coefficients, the second ones will not suffer any changes. However, the new linear ARX models parameters are shown in table XXI and its response in figure 65. The reported minimum square error was 3.1.



Figure 65. Predicted glucose concentration rate of change and its real value obtained in the experiment, scaling each input with respect to its maximum value with a sample time of 10 minutes and with equation 6.17.

Table XXI. Parameters obtained for the linear ARX models scaling each input with respect to its maximum value and using equation 6.17.

Auxiliary variable (<i>i</i>)	Model	δ_{i1}	δ_{i2}	δ_{i3}	δ_{i4}
1	v_1	2.12216226	-1.45141476	-0.33851334	0.79242162
2	v_2	2.28288382	-2.5373466	1.57808859	-0.90934023
3	v_3	1.68933604	-0.09229609	-1.19489255	0.6835463
Auxiliary variable (<i>i</i>)	Model	δ_{i5}	δ_{i6}	δ_{i7}	δ_{i8}
1	v_1	0.42283155	-1.29140525	1.27727133	-1.28739329
2	v_2	0.52342501	-0.10839356	-0.03072891	0.23134826

3	v_3	-0.026635	0.22846514	-0.67989825	0.44738501
Auxiliary variable (i)	Model	δ_{i9}	δ_{i10}	δ_{i11}	δ_{i12}
1	v_1	1.28301637	-0.30629255	-0.85354712	0.20758478
2	v_2	-0.17253125	0.10484072	-0.05470616	0.16179867
3	v_3	-0.02698684	0.34097845	-1.34648417	0.75246141
Auxiliary variable (i)	Model	δ_{i13}	δ_{i14}	δ_{i15}	ω_{i1}
1	v_1	1.55845562	-2.05213891	0.8446799	1.90982253
2	v_2	0.04494333	-0.1512706	0.03694595	-43.8399912
3	v_3	1.21616755	-1.32070544	0.32155674	-4.24610847
Auxiliary variable (i)	Model	ω_{i2}	ω_{i3}	ω_{i4}	ω_{i5}
1	v_1	-3.96954878	2.5654936	0.65478079	-1.31578261
2	v_2	92.4780388	-81.6353866	27.7415146	-1.01179887
3	v_3	-1.82608994	13.0334502	-1.09433009	-8.64154646
Auxiliary variable (i)	Model	ω_{i6}	ω_{i7}	ω_{i8}	ω_{i9}
1	v_1	-0.88913562	2.27235293	-2.08205223	1.98869884
2	v_2	1.6334355	3.34771023	4.57377878	3.07761047
3	v_3	2.24629062	4.29948877	-3.62515142	-4.76157529
Auxiliary variable (i)	Model	ω_{i10}	ω_{i11}	ω_{i12}	ω_{i13}
1	v_1	-2.55922401	1.43356379	1.33123207	-1.39502802
2	v_2	-0.95026533	-1.91709341	1.22926685	2.48663453
3	v_3	5.09875716	0.52734603	2.16581087	-13.9652491
Auxiliary variable (i)	Model	ω_{i14}	ω_{i15}	ω_{i16}	
1	v_1	-1.35846898	2.97054107	-1.48496359	
2	v_2	0.05749465	-1.197899	-6.07300711	

3	v_3	8.01160594	13.9035949	-11.1182921	
---	-------	------------	------------	-------------	--

6.1.4.6. Testing phase of the predictive model

According to Rollins, after the training stage is completed, it is necessary to test the models with different combinations of inputs to see if they predict the output in an accurate form.

Even though external insulin infusion was considered as an input in the system's model, it was discarded in the testing phase because when a person is doing exercise, the less desired situation is that glucose concentration drops below a healthy level, therefore automatic insulin supply would be cut off.

The testing trials are shown in table XXII, which represent possible situations for the patient. In each trial, a physical activity level (of up to 45% PAMM) is maintained for about 3.5 hours (200 min) with a recovery of normoglycaemia in approximately 1.5 hours, with a possible constant glucagon supply during the exercise period.

The results of the tests can be seen in figures 66 to 71, the time axis is in minutes.

Table XXII. Testing trials of the selected models.

Trial	% PAMM	Glucagon (pg/min)
1	40	10,000
2	45	20,000
3	30	10,000
4	10	7,500
5	45	0
6	20	0

From the shown graphs, it can be observed that the results of the trials 2,4,6 give the worst approximation to the real response. From this information, the proposed statistical models is valid in the range of PAMM from 0 to 40 %.

Since the quadratic sum of errors was a bit high, the model fails in its predictions above 40% PAMM, so for getting a precise response the model was limited to function up to this quantity. Nevertheless, due to the complexity and highly nonlinear behavior of the system, in the range of operation from 0 to 40% the model is considered to produce a good approach, remarking that 60% PAMM represents high exercise intensity (Lenart, 2002).

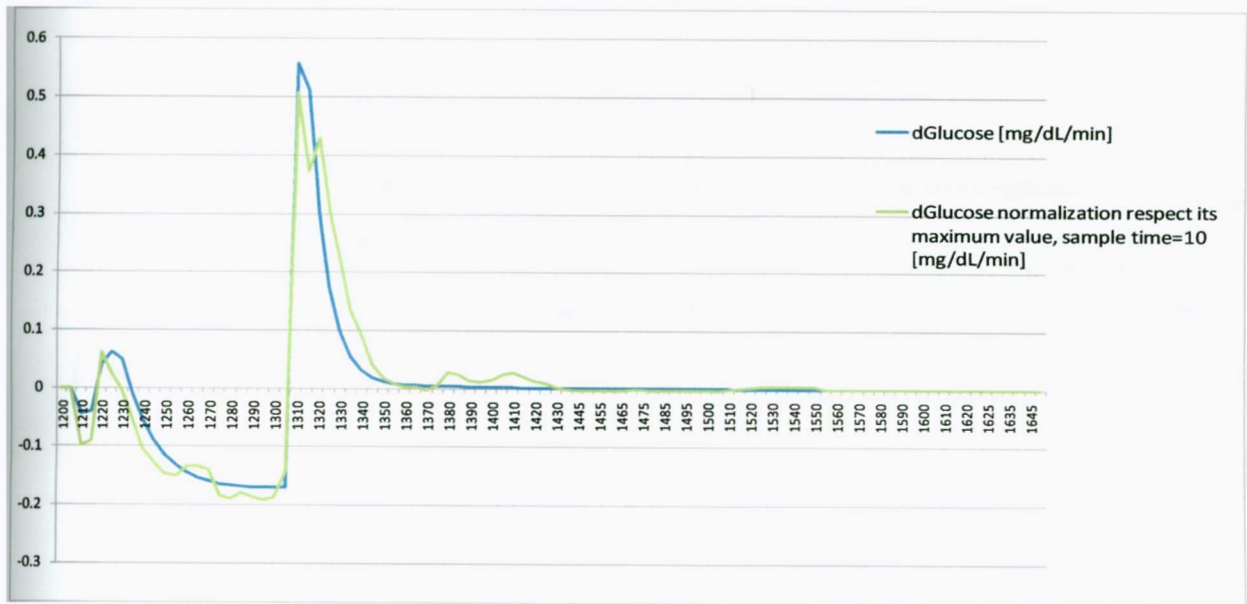


Figure 66. Comparison between the predicted and real glucose concentration rate in trial #1.

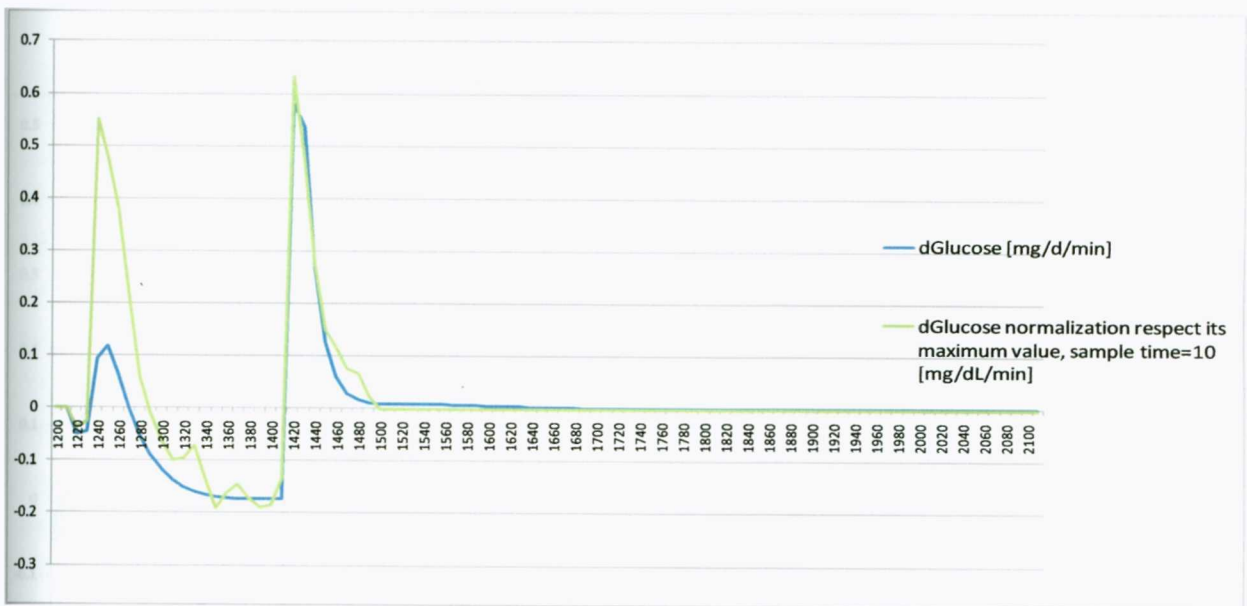


Figure 67. Comparison between the predicted and real glucose concentration rate in trial #2.

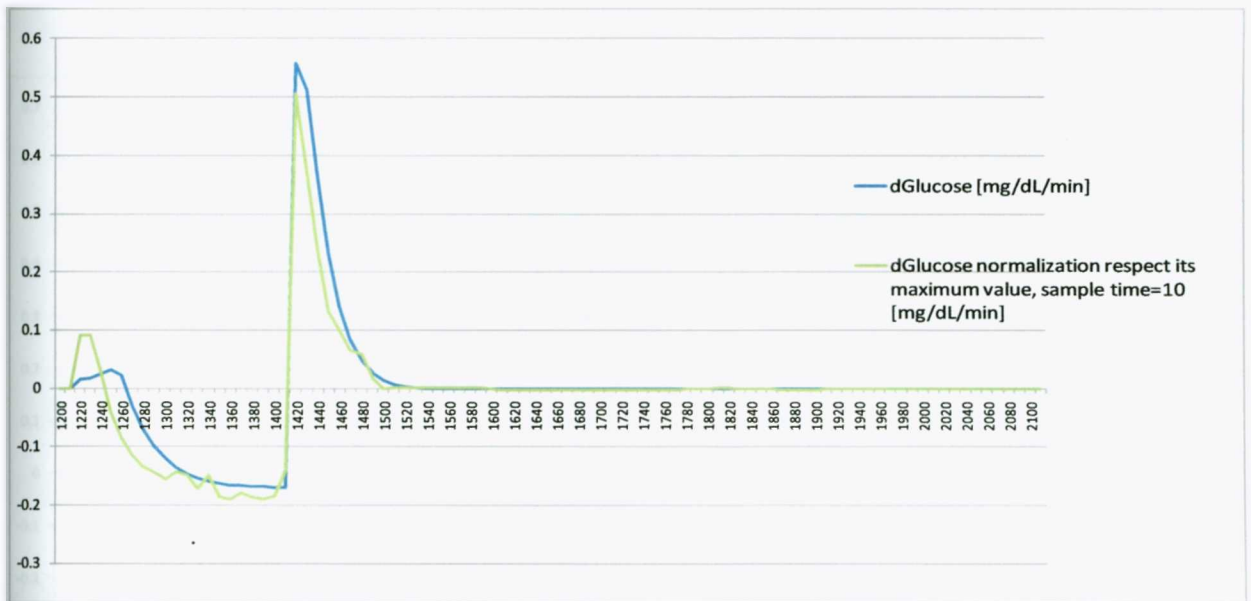


Figure 68. Comparison between the predicted and real glucose concentration rate rate in trial #3

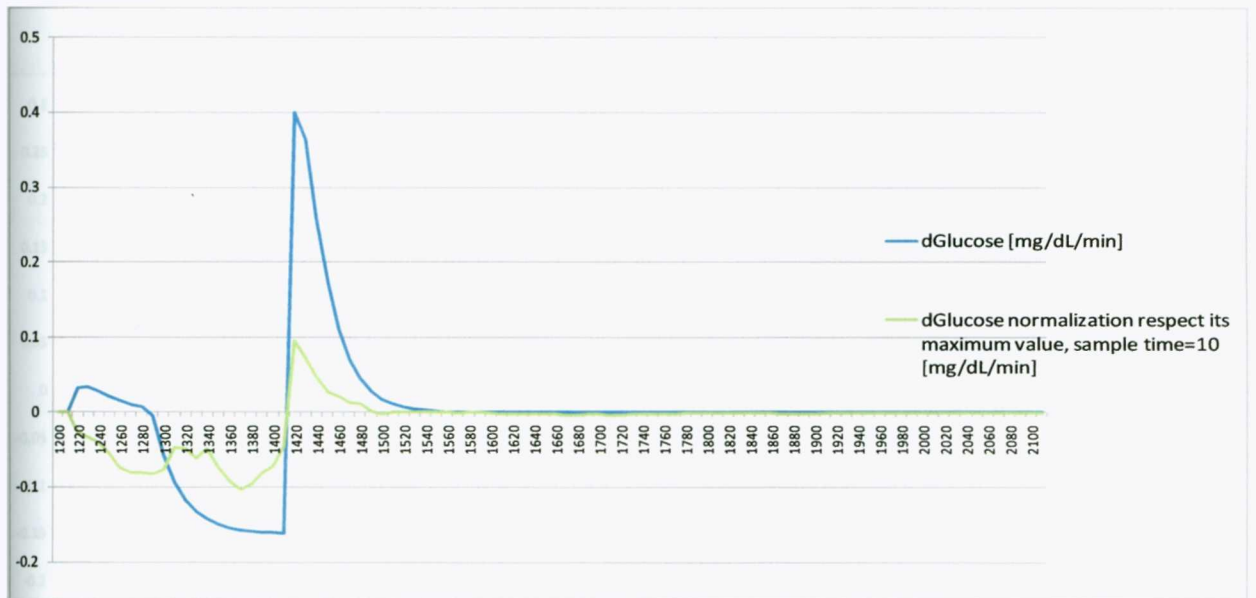


Figure 69. Comparison between the predicted and real glucose concentration rate in trial #4.

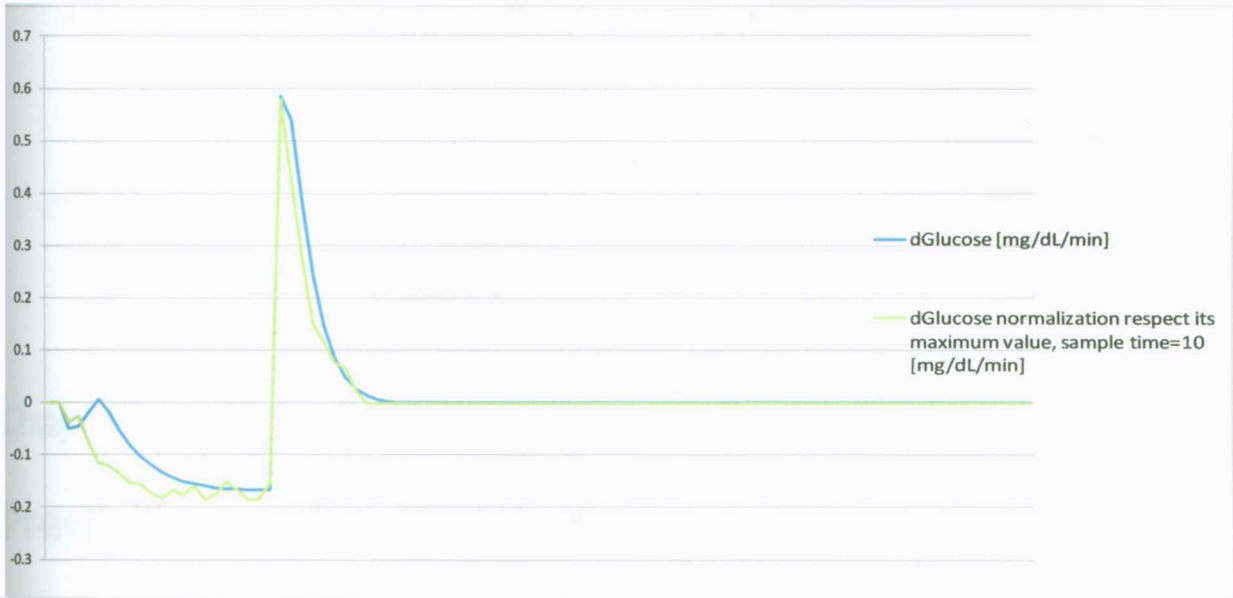


Figure 70. Comparison between the predicted and real glucose concentration rate in trial #5.

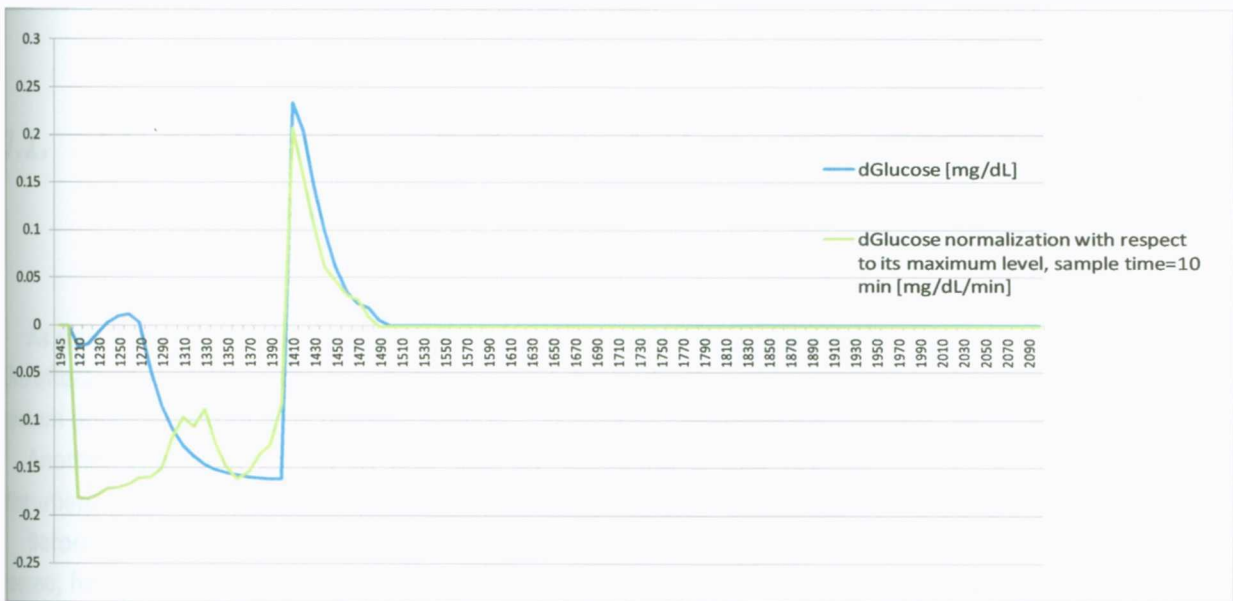


Figure 71. Comparison between the predicted and real glucose concentration rate in trial #6.

Chapter 7

Predictive controller design

After obtaining the statistical discrete model that suits the best behavior of the physiological system, the next step is to develop a model based predictive controller that will impede the decreasing of glucose.

This chapter explains the method applied for the issue described above, as well as the different tests that were involved, in order to evaluate its performance.

7.1. Model based predictive control strategy applied to glucose level regulation

As stated above, one of the goals of this thesis is to design a regulation strategy that will compensate the effects of exercise in the blood glucose level. Basically, the major problem is that exercise makes the system unstable and that its dynamics when it starts and when it is ended is different.

Another important aspect to take into consideration is that exercise is considered as an output disturbance, because it is not related with the manipulation of the feedback controller.

Before developing a predictive control strategy, a discrete PID with conservative parameters was tested, but its performance lacked in accuracy. The three reasons why it failed to prevent hypoglycemic episodes before exercise are

- It was synthesized based on a servocontrol or set point tracking specified performance, assuming a stable glucose level response, which becomes unstable during exercise.

- Its manipulated variable is external insulin infusion, which does not have the ability of increasing the blood glucose level.
- Its tuning parameters and structure are linear, while the process dynamics is nonlinear specially due to the exercise effects.

Its response to a 40 %PAMM pulse change is seen in figure 72, where the reasons stated above can be corroborated. Table XXIII shows the initial conditions in the test.

Table XXIII. Initial conditions for PID controller test with exercise as output disturbance.

Parameter	Value	Unit
<i>Basal insulin level</i>	15.1	<i>mU /min</i>
<i>PAMM</i>	40	%
<i>Basal glucose level</i>	80	mg/dL
<i>Exercise duration</i>	120	min

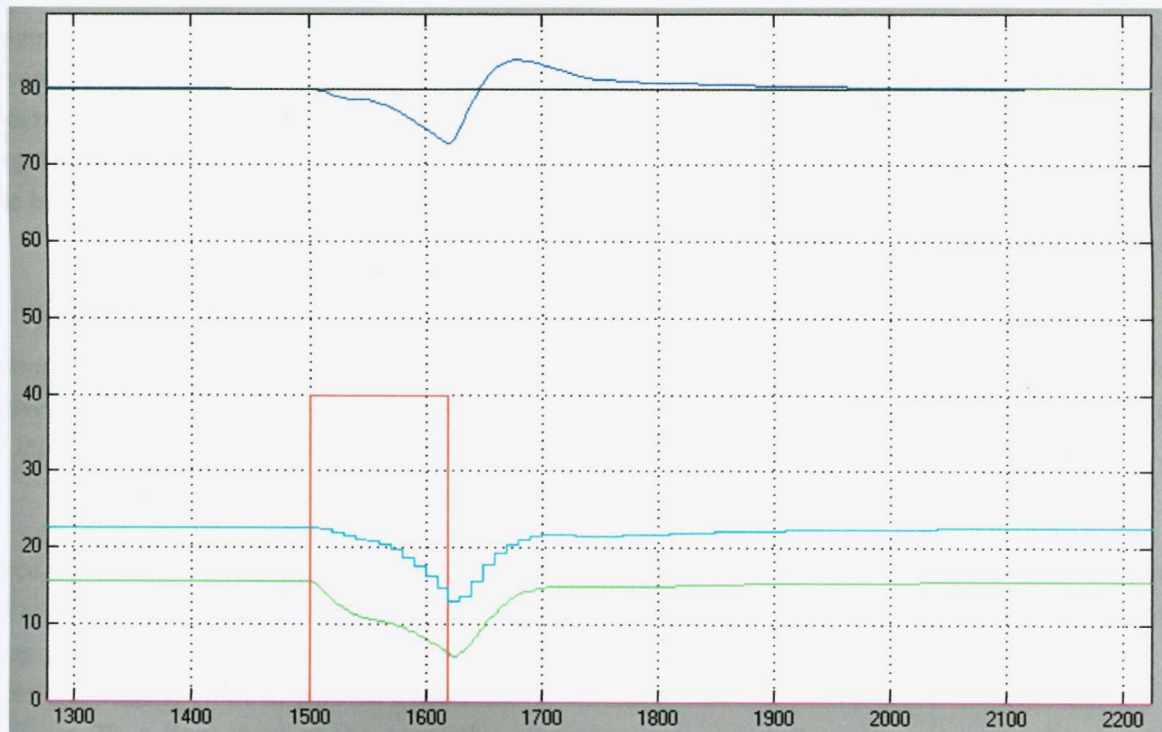


Figure 72. Response of glucose level (mg/dL) (blue) in close loop, with a discrete PID controller in the presence of a 40 %PAMM (red) pulse change. External insulin infusion (mU/min)(cyan), arterial insulin level (mU/min) (green), Basal glucose level (mg/dL)(black); time scale in minutes.

Equation 7.1 shows the discrete implementation of the PID controller used to close the glucose control loops and the tuning parameters and sample time are presented in table XXIV:

$$u = u_{k-1} + K_c \left((e_k - e_{k-1}) + \left(\frac{T}{\tau_i} \right) \left(\frac{e_k + e_{k-1}}{2} \right) - \frac{\tau_D}{T} (y_k - 2y_{k-1} + y_{k-2}) \right) \quad (7.1)$$

Table XXIV. Parameters values of the discrete PID controller.

Parameter	Value	Units
K_c	-0.7754	(mU/min)/(mg/dL)
τ_D	0	min
τ_i	60	min
T	10	min

Since the PID-based feedback control strategy did not function for the exercise issue, a complementary model based predictive controller is proposed, using the model obtained that is represented by equations 6.11, 6.12, 6.17 and tables XVII and XXI. Even though it has many autoregressive and exogenous input terms, all of them are fitted and therefore the implementation of the regulator can be done.

The basic principle of how the proposed predictive regulator works is:

After obtaining the measured glucose concentration, its rate of change is calculated with the knowledge of the sample time interval. Afterwards, knowing the exercise intensity (PAMM), the auxiliary variable (v_2) that depends on external glucagon infusion is calculated, and finally the external glucagon input (u_2) to produce the same glucose concentration rate but with opposite sign is predicted

Since the solution of equation 6.4 involves quadratic terms, there are two possible solutions. By trial and error in the simulations, it was stated that for values of time below 45 minutes the smallest value (v_i) was used in the calculation for exogenous glucagon infusion; for values of time greater than 45 minutes, the biggest value of (v_i) was used.

In figure 73, a flow chart of the predictive algorithm is depicted. It can be seen that the variables mentioned above are used; figure 74 illustrates the block diagram of complete automatic system including the predictive control strategy. The implementation of this strategy was done using Simulink®; figure 75 shows the resulting schematic of this software.

Even though the model to use in this strategy had some errors, these are compensated in the program file by making a fine readjustment in the parameters.

After implementing the predictor, several tests were executed with the system in a close loop mode, in order to see its performance. Table XXV indicates the value of the variables involved in these tests.

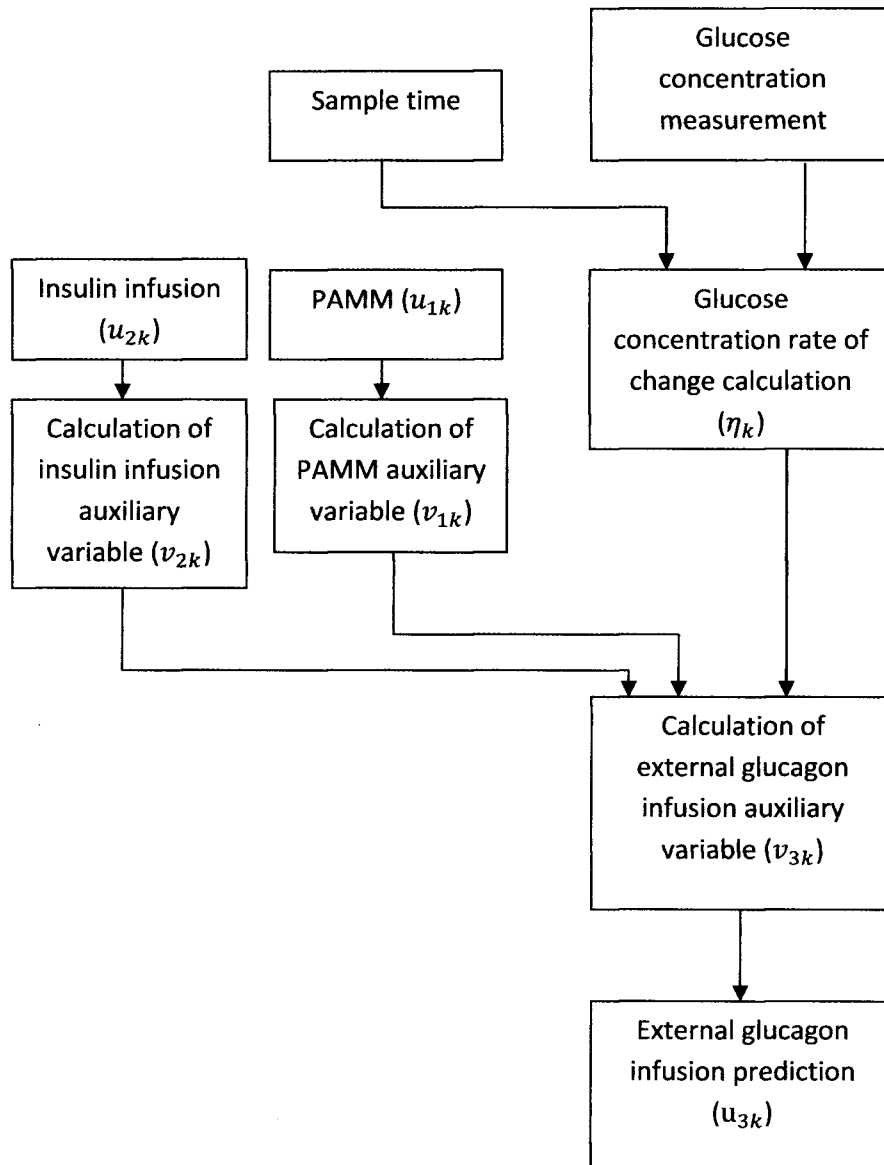


Figure 73. Flow chart of the predictive control algorithm for exercise effects compensation.

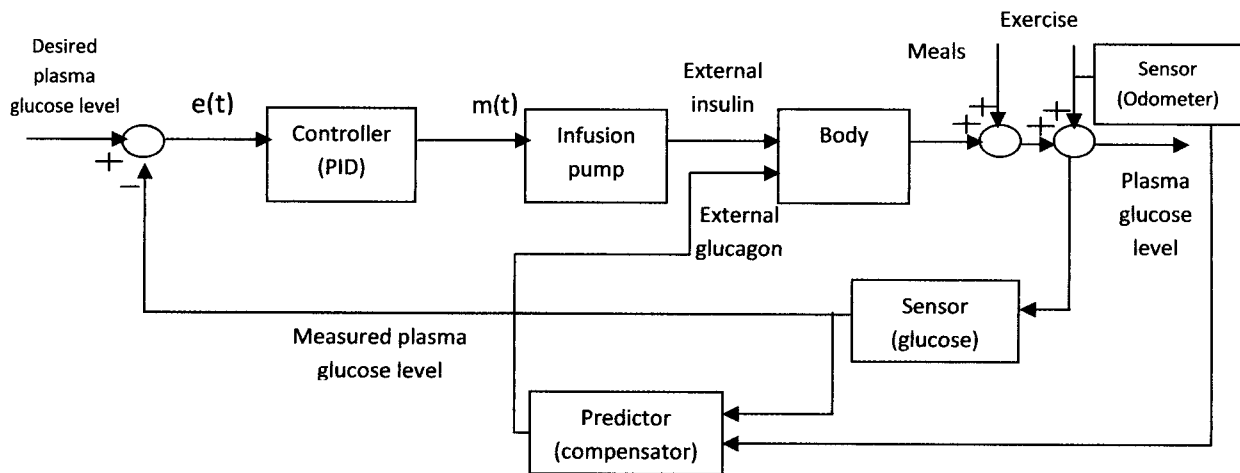


Figure 74. Block diagram of complete glucose level control system with compensation of exercise effects

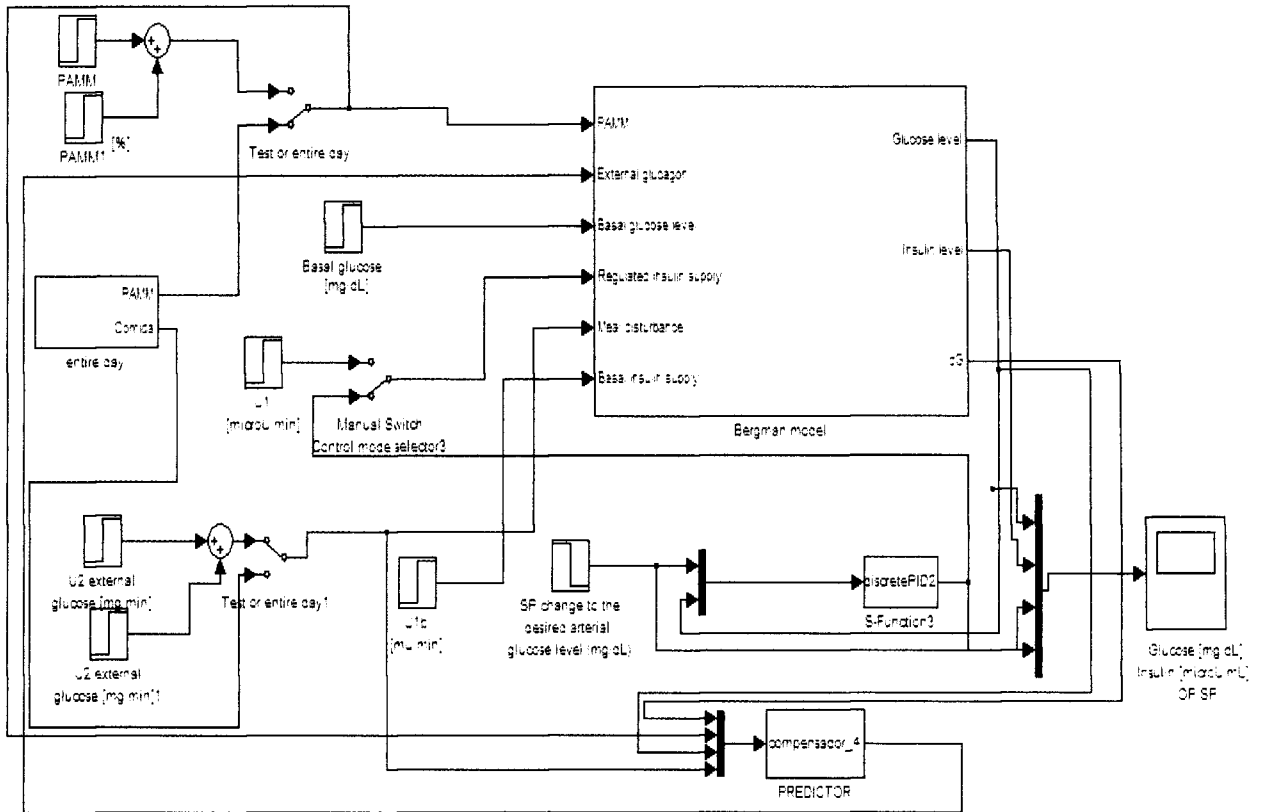


Figure 75. Implementation schematic of complete automatic system with predictive control strategy for compensation of exercise effects.

Table XXV. Test done in with the designed predictive regulator.

Test	Exercise duration (min)	PAMM (%)	Basal Glucose level (mg/dL)	Maximum glucose level deviation (mg/dL)
1	120	10	80	+0.5
2	120	15	80	-0.4
3	120	20	80	-2
4	120	25	80	+0.6
5	120	30	80	+0.8
6	120	35	80	-0.7
7	120	40	80	-0.8

8	45	40	90	+0.4
9	45	10	90	+0.5
10	45	30	90	+0.4
11	60	40	100	+1.5
12	60	10	100	+0.6
13	60	30	100	+0.8
14	30	40	70	+0.5
15	30	10	70	+0.5

In graphs 76 to 90, with a time scale in minutes, the performance of the predictive control is shown. Where, it can be stated that for any intensity of exercise from 0 to 40% PAMM, exercise duration from 0 to 120 minutes and any initial glucose level, the predictive controller will regulate in an excellent form, compensating the negative effect of exercise in glucose level. In these tests, the predictive compensator and the PID controller act on the system; like it is explained in chapter 2, the body's nature allows it because when blood glucose level rises only insulin is secreted and not glucagon and vice versa when blood glucose drops. This means that both control actions will not interfere with each other.

The final test done was combining both control strategies, feedback PID and feedforward predictive controller, with the purpose to react to meal disturbances and anticipate exercise disturbance, respectively.

To quantify the carbohydrate intake, information from Sánchez was taken, where the meals are represented by pulse functions for the carbohydrate consumption rate. The pulse durations is fixed in 30 min. and the pulse area represents the ingestion of 66 g of carbohydrates. The carbohydrates total in three meals accounts for 53% of the energy from a 1,500 kcal diet, close to the minimum daily recommended energy percentage from carbohydrates (Sánchez-Chávez, 2008).

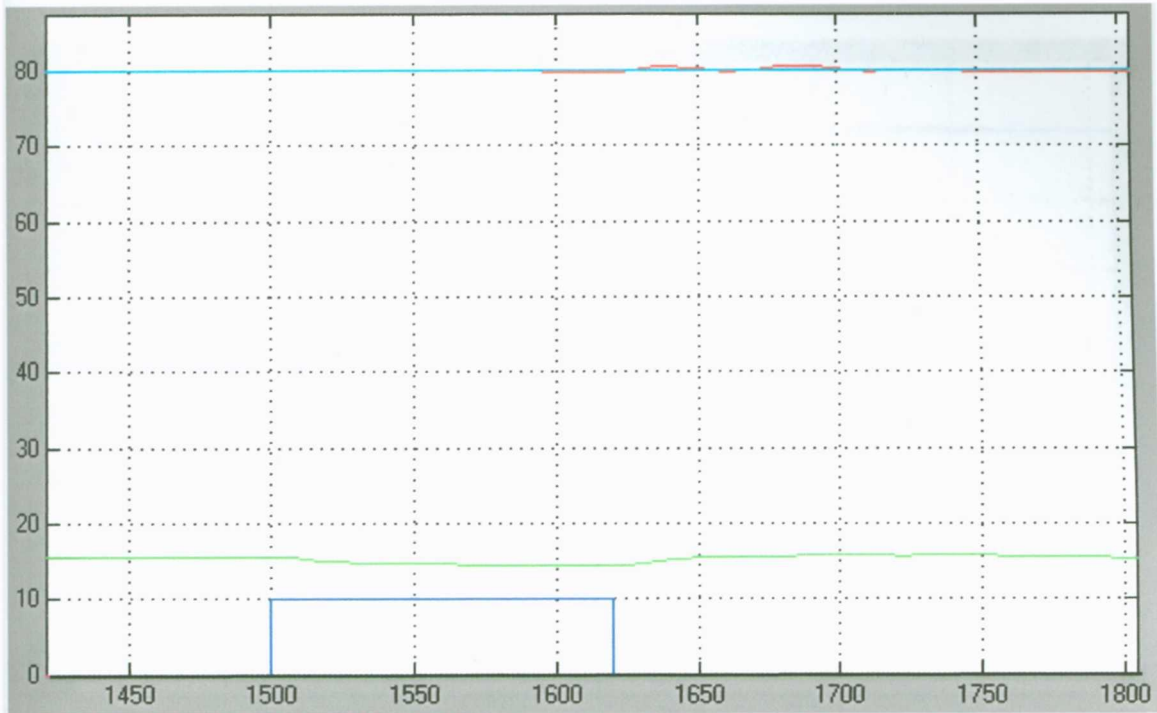


Figure 76. Performance of predictive control strategy, with 10% PAMM (blue) and a duration of 120 minutes. Glucose steady state level at 80 mg/dL(cyan), its response is the red graph and blood Insulin concentration(mU/L) is represented by the green graph.

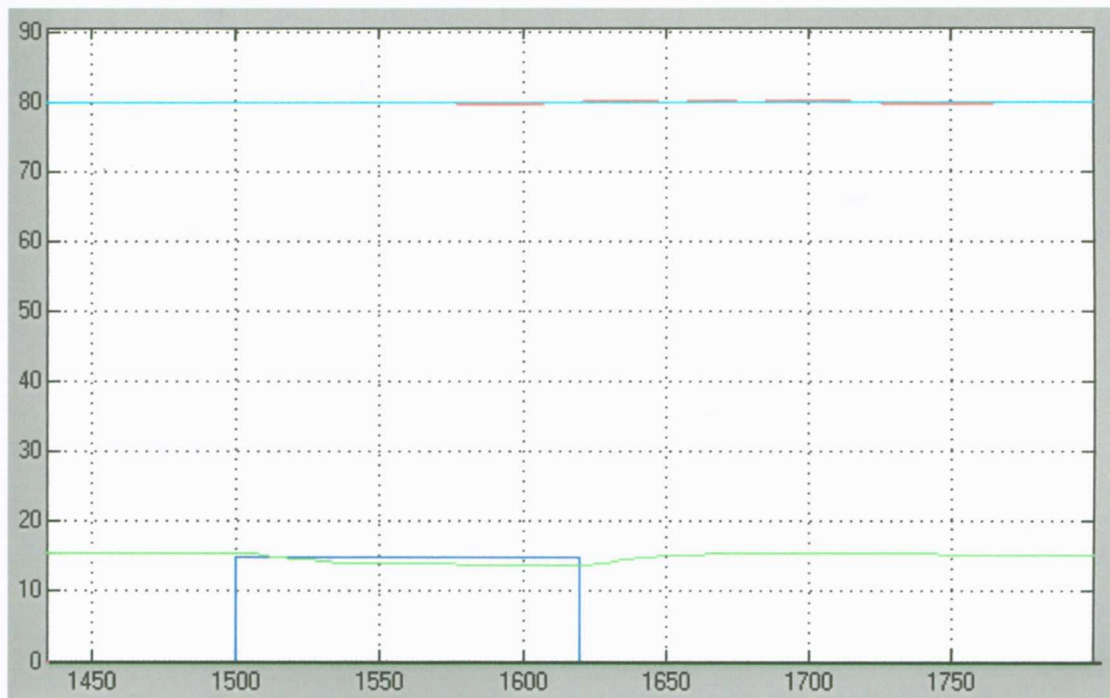


Figure 77. Performance of predictive control strategy, with 15% PAMM (blue) and a duration of 120 minutes. Glucose steady state level at 80 mg/dL(cyan), its response is the red graph and blood Insulin concentration(mU/L) is represented by the green graph.

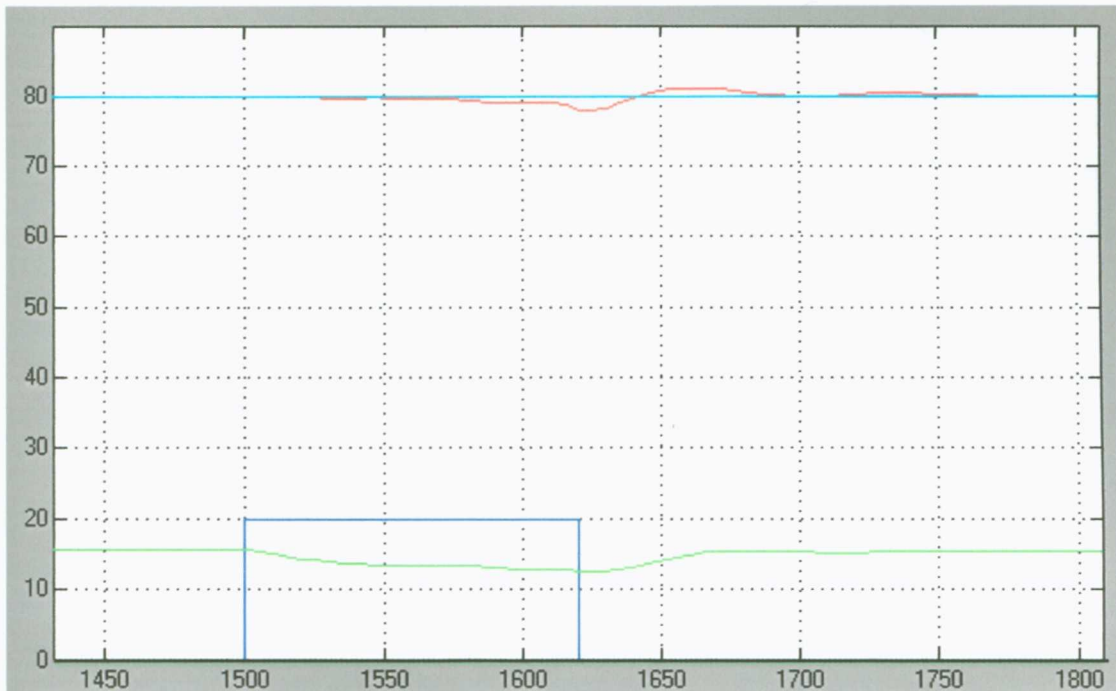


Figure 78. Performance of predictive control strategy, with 20% PAMM (blue) and a duration of 120 minutes. Glucose steady state level at 80 mg/dL(cyan), its response is the red graph and blood Insulin concentration(mU/L) is represented by the green graph.

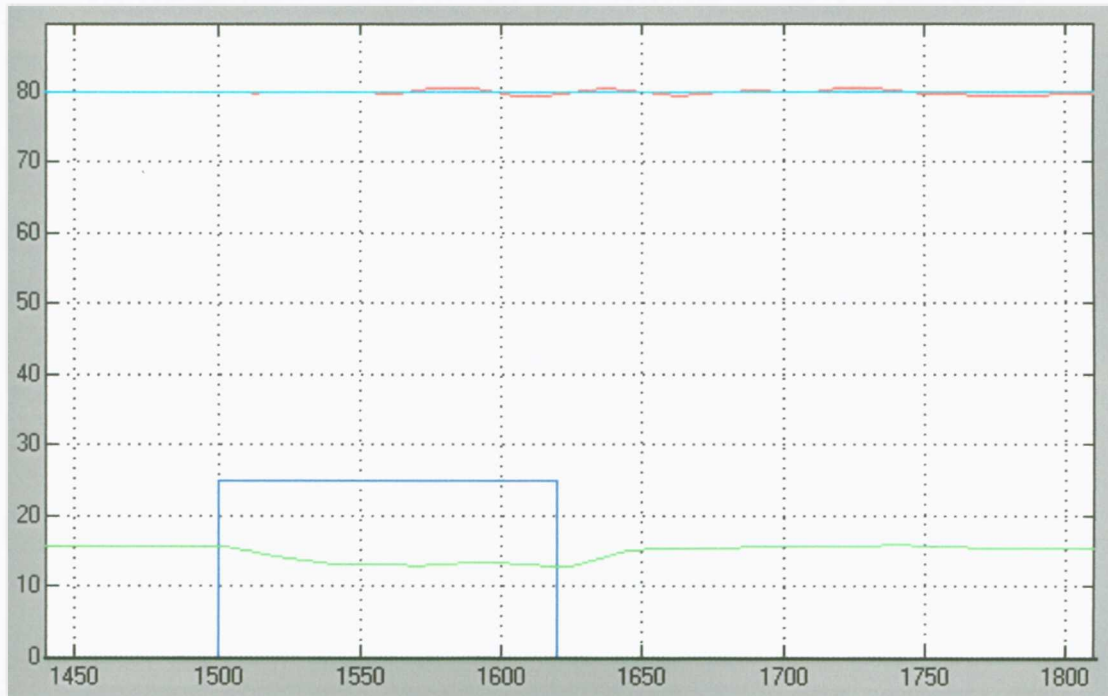


Figure 79. Performance of predictive control strategy, with 25% PAMM (blue) and a duration of 120 minutes. Glucose steady state level at 80 mg/dL(cyan), its response is the red graph and blood Insulin concentration(mU/L) is represented by the green graph.

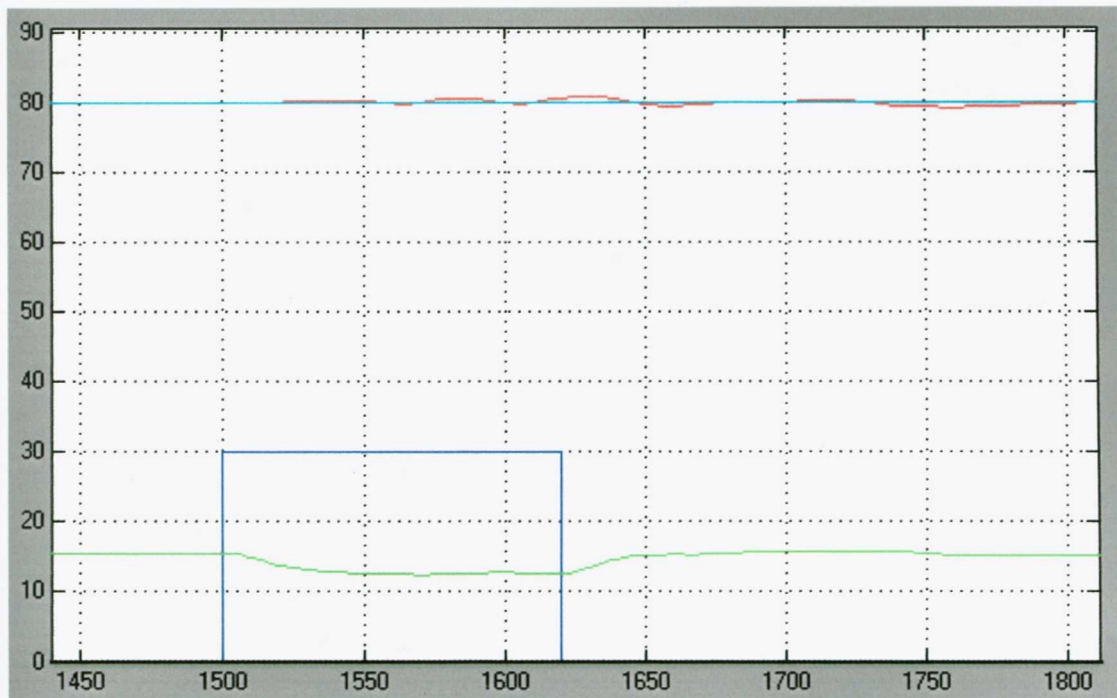


Figure 80. Performance of predictive control strategy, with 30% PAMM (blue) and a duration of 120 minutes. Glucose steady state level at 80 mg/dL(cyan), its response is the red graph and blood Insulin concentration(mU/L) is represented by the green graph.

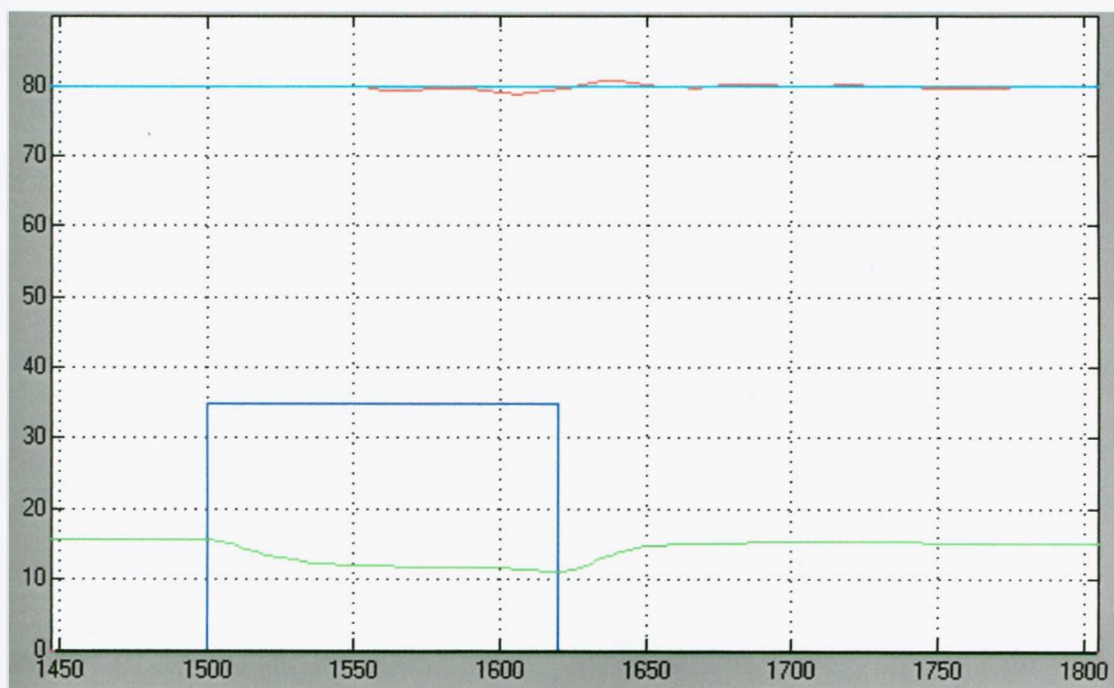


Figure 81. Performance of predictive control strategy, with 35% PAMM (blue) and a duration of 120 minutes. Glucose steady state level at 80 mg/dL(cyan), its response is the red graph and blood Insulin concentration(mU/L) is represented by the green graph.

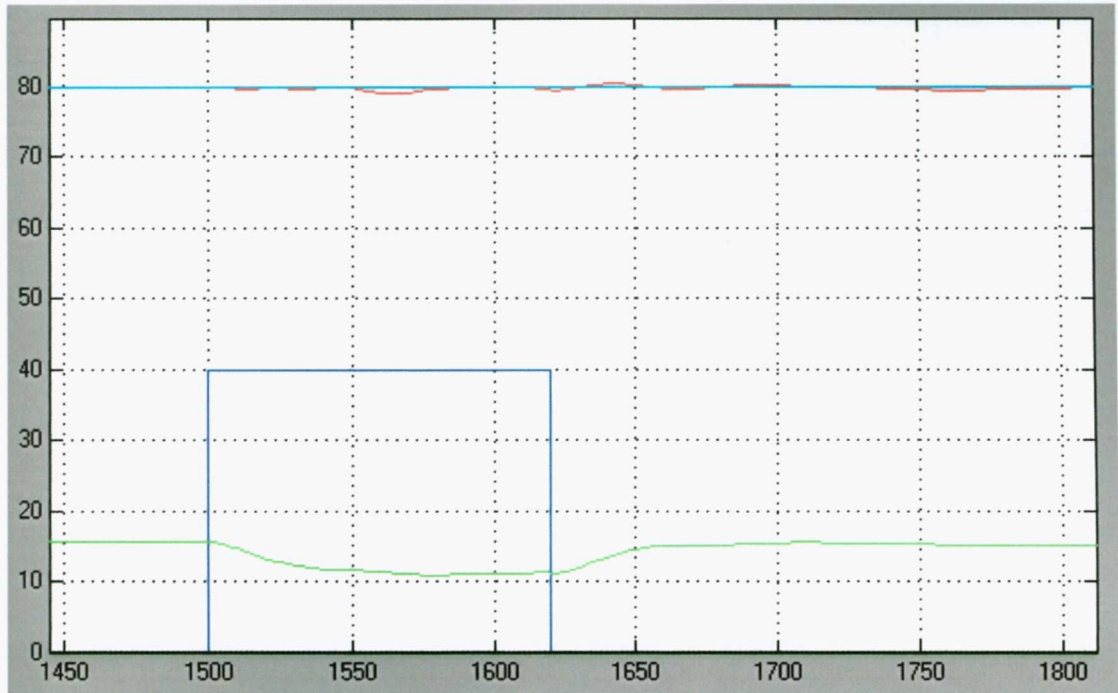


Figure 82. Performance of predictive control strategy, with 40% PAMM (blue) and a duration of 120 minutes. Glucose steady state level at 80 mg/dL(cyan), its response is the red graph and blood Insulin concentration(mU/L) is represented by the green graph.

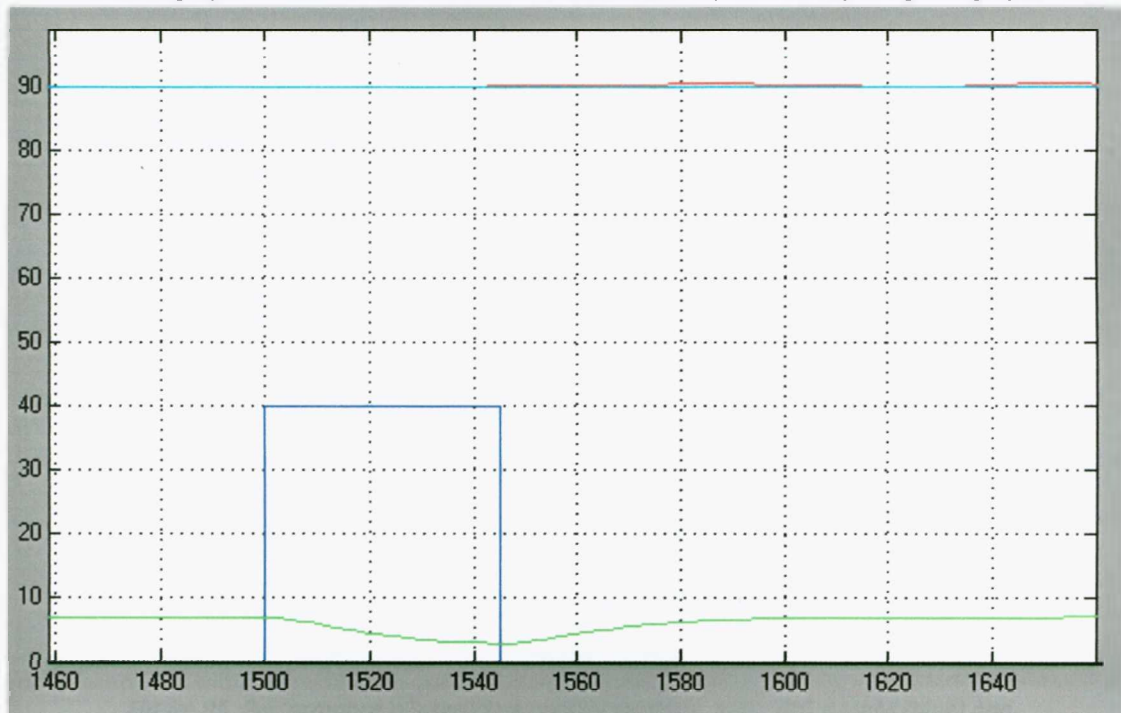


Figure 83. Performance of predictive control strategy, with 40% PAMM (blue) and a duration of 45 minutes. Glucose steady state level at 90 mg/dL(cyan), its response is the red graph and blood Insulin concentration(mU/L) is represented by the green graph.

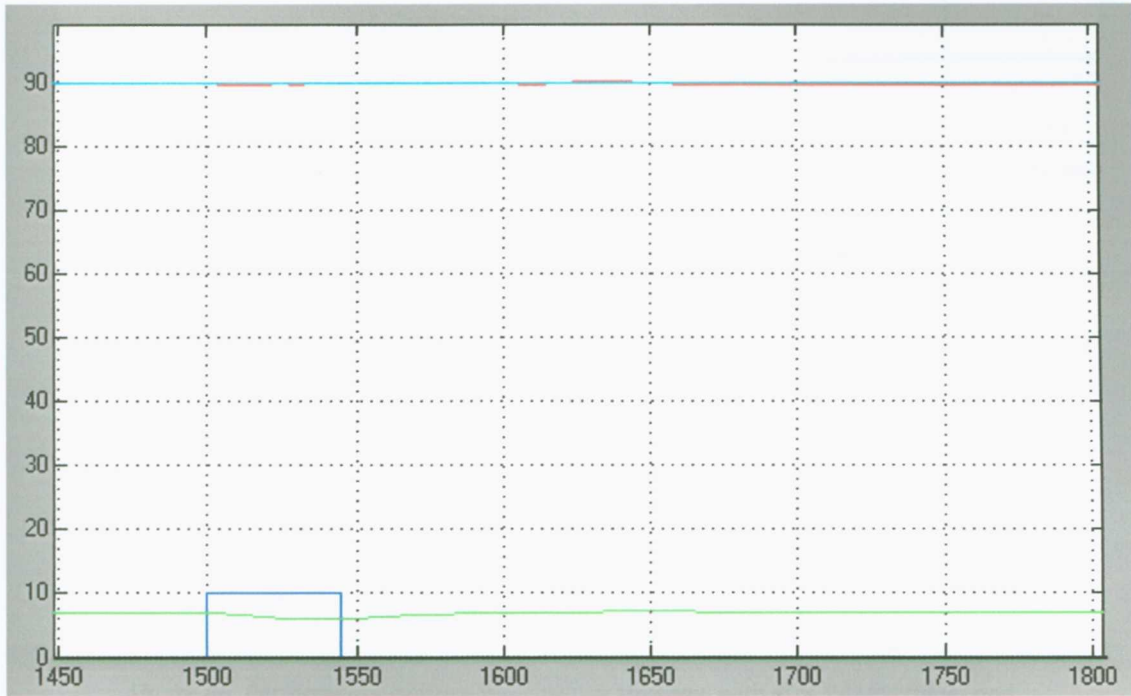


Figure 84. Performance of predictive control strategy, with 10% PAMM (blue) and a duration of 45 minutes. Glucose steady state level at 90 mg/dL(cyan) , its response is the red graph and blood Insulin concentration(mU/L) is represented by the green graph.

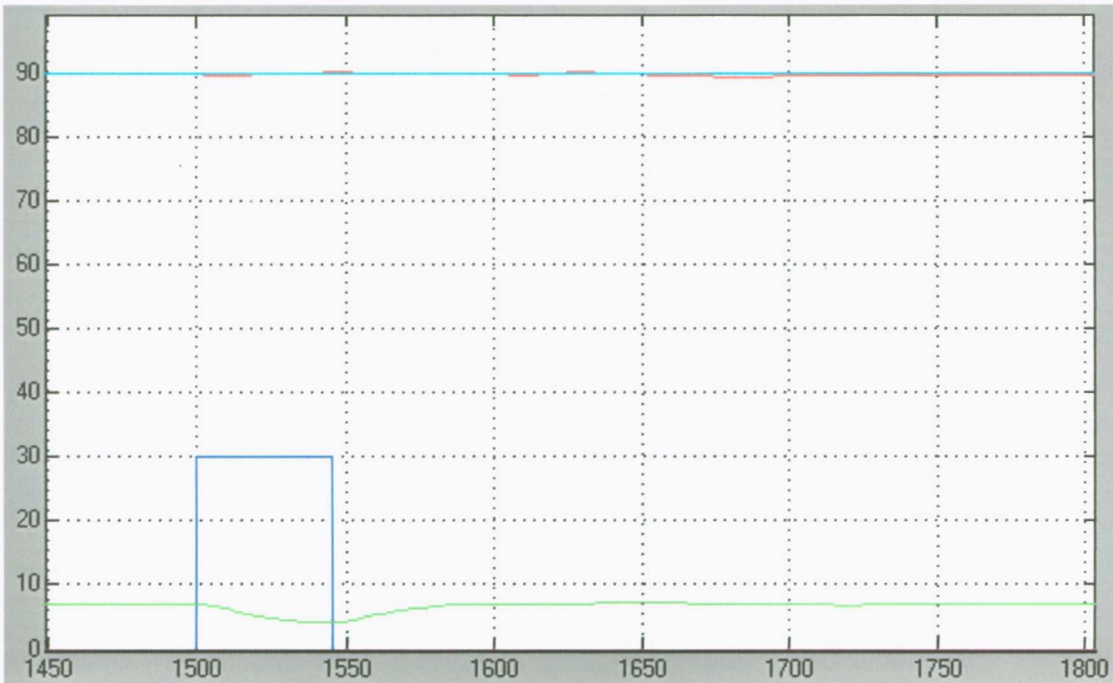


Figure 85. Performance of predictive control strategy, with 30% PAMM (blue) and a duration of 45 minutes. Glucose steady state level at 90 mg/dL(cyan), its response is the red graph and blood Insulin concentration(mU/L) is represented by the green graph.

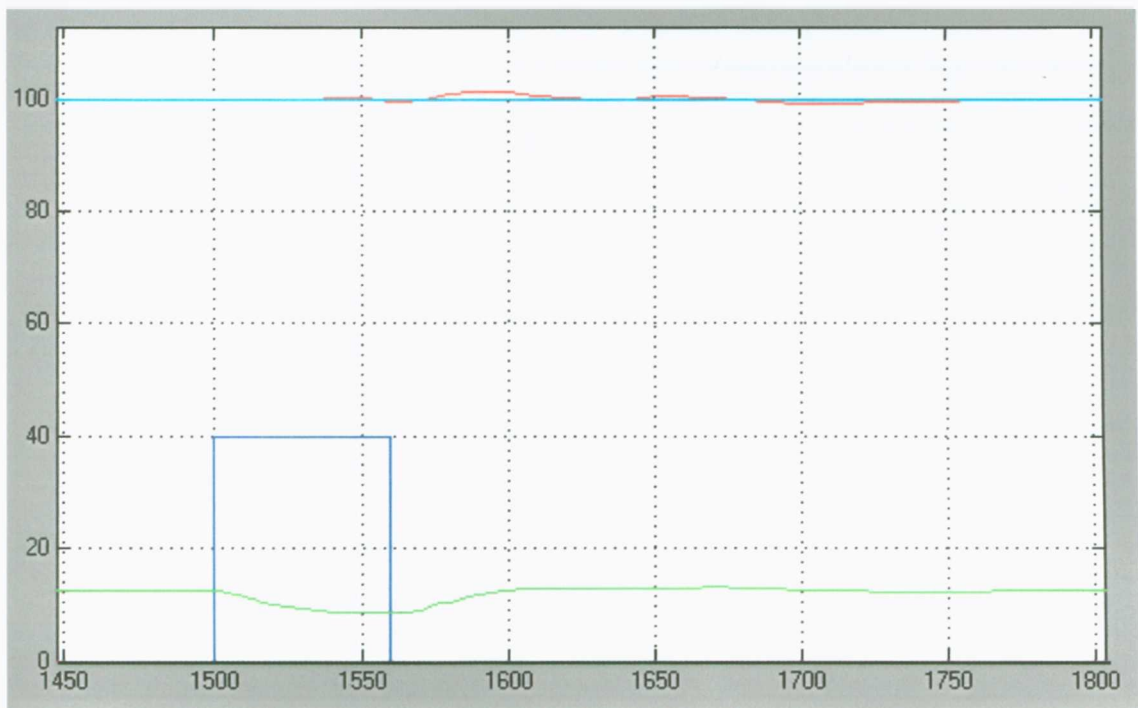


Figure 86. Performance of predictive control strategy, with 40% PAMM (blue) and a duration of 60 minutes. Glucose steady state level at 100 mg/dL(cyan), its response is the red graph and blood Insulin concentration(mU/L) is represented by the green graph.

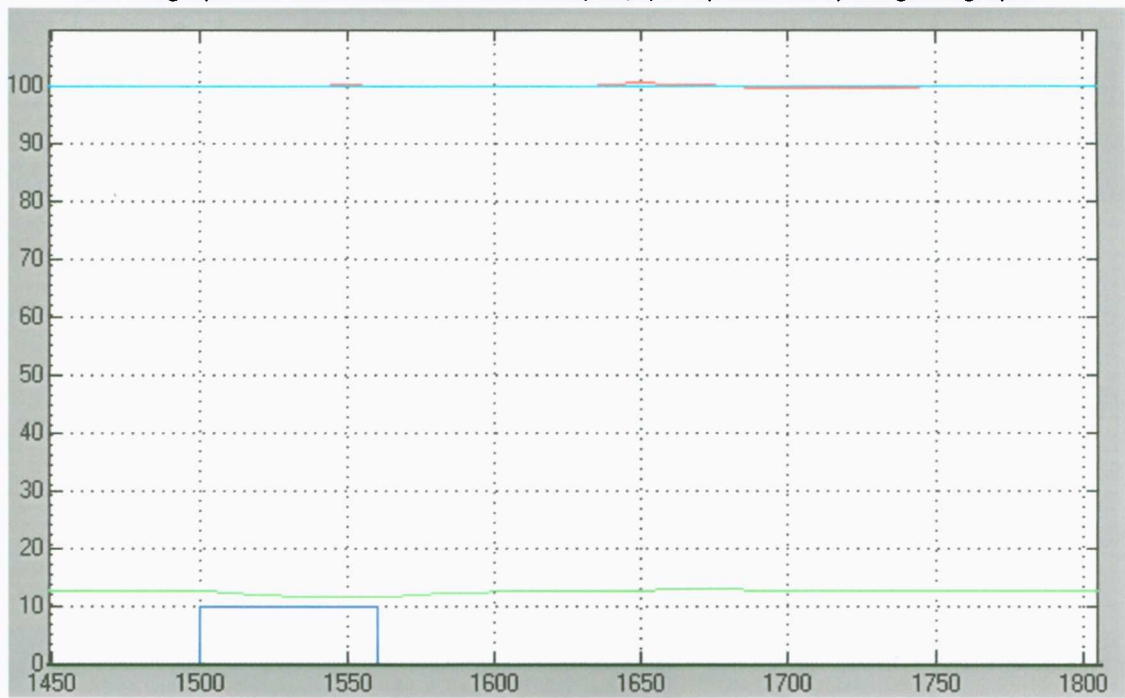


Figure 87. Performance of predictive control strategy, with 10% PAMM (blue) and a duration of 60 minutes. Glucose steady state level at 100 mg/dL(cyan), its response is the red graph and blood Insulin concentration(mU/L) is represented by the green graph.

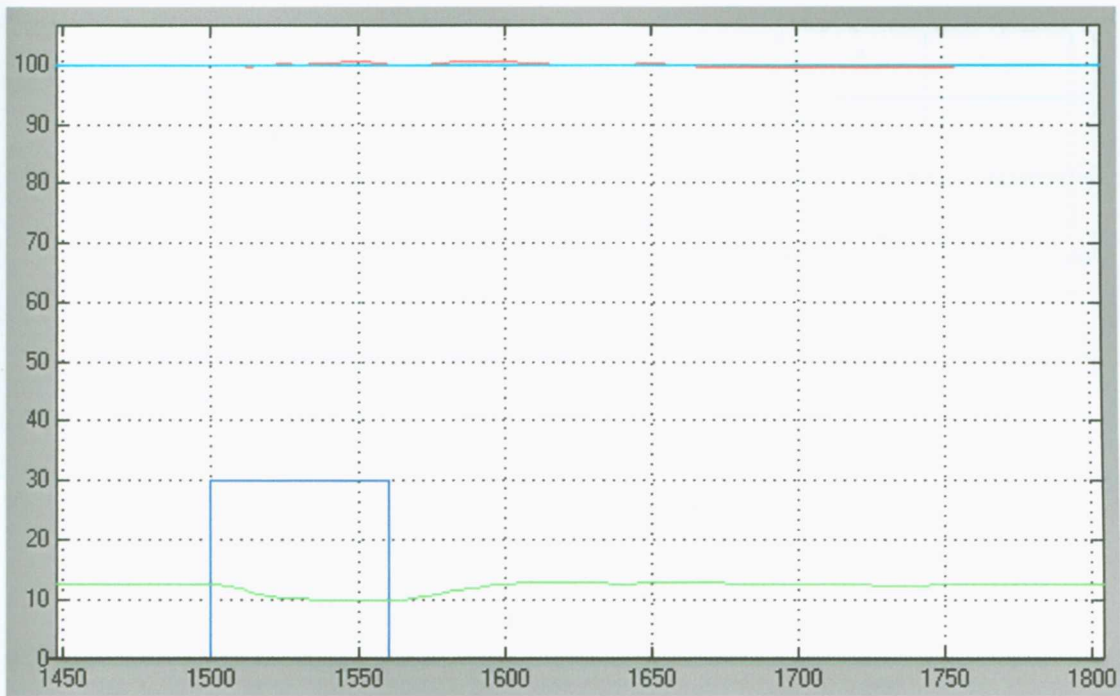


Figure 88. Performance of predictive control strategy, with 30% PAMM (blue) and a duration of 60 minutes. Glucose steady state level at 100 mg/dL(cyan), its response is the red graph and blood Insulin concentration(mU/L) is represented by the green graph.

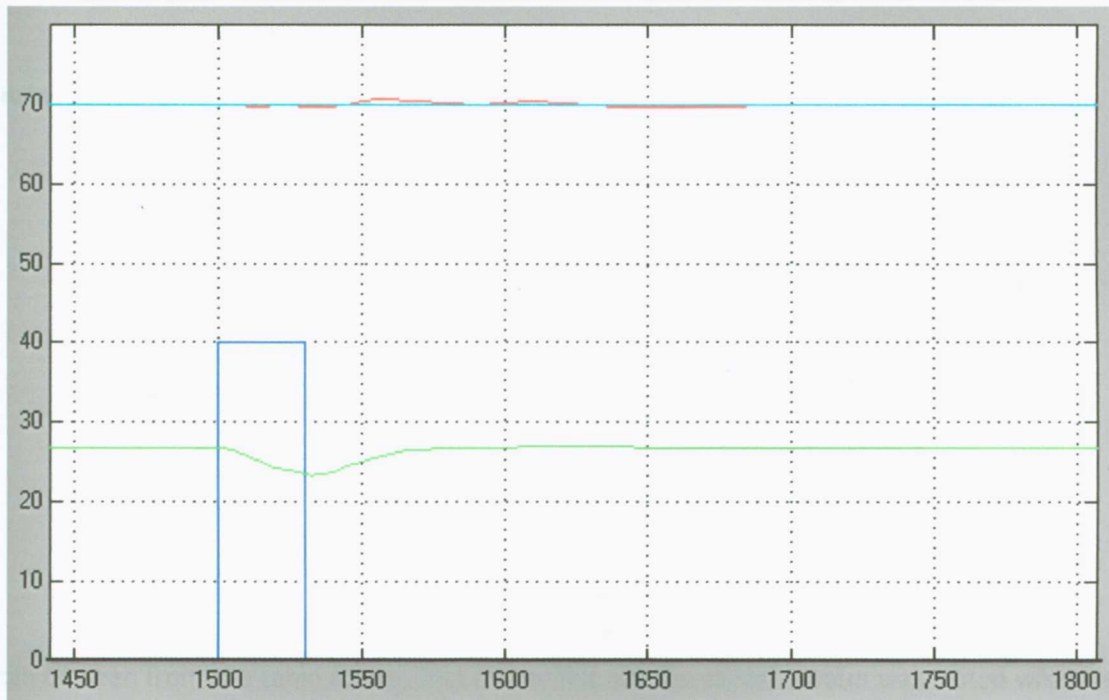


Figure 89. Performance of predictive control strategy, with 40% PAMM (blue) and a duration of 30 minutes. Glucose steady state level at 70 mg/dL(cyan), its response is the red graph and blood Insulin concentration(mU/L) is represented by the green graph.

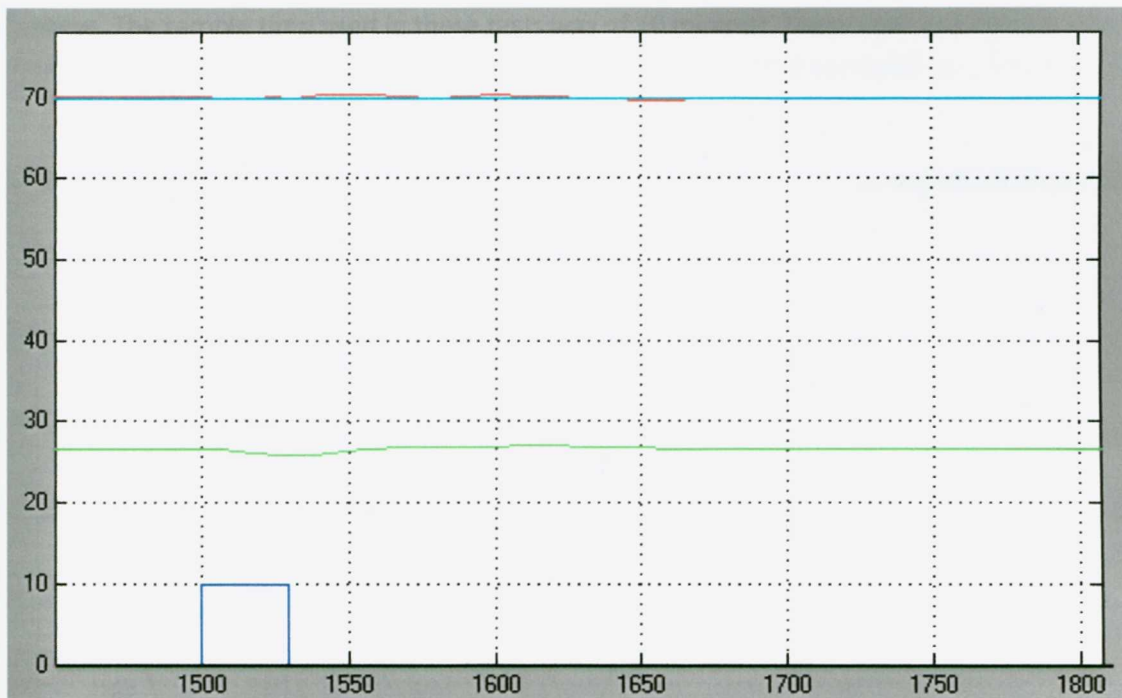


Figure 90. Performance of predictive control strategy, with 10% PAMM (blue) and a duration of 30 minutes. Glucose steady state level at 70 mg/dL(cyan), its response is the red graph and blood Insulin concentration(mU/L) is represented by the green graph.

The final test was done as follows:

Table XXVI. Final test done, combining meal and exercise disturbances.

Test	Basal Glucose level (mg/dL)	% PAMM	Exercise initial time (min)	Exercise end time (min.)	Meal time (min.)
1	90	40	1500	1620	1620
2	90	30	2200	2245	2000
3	90	20	2700	2820	2800

It can be seen from the table above, that in the first run the closed system was tested when exercise is first done and afterwards the patient has a meal. In the second run the person eats before he starts any physical activity, and finally, a run to explore the system response when exercise and eating are done in the same time interval. The latter test is proposed to experiment a third possibility in the timing of different disturbances, even though such timing may be less common in a person's routine. The set of the 3 tests do not represent a one-day routine, but only independent and isolated combinations of

disturbances. The sample time used in these tests was of 10 minutes. These trails are illustrated in figure 91; external insulin and glucagon infusion, which are the manipulated variables, are depicted in figure 92.

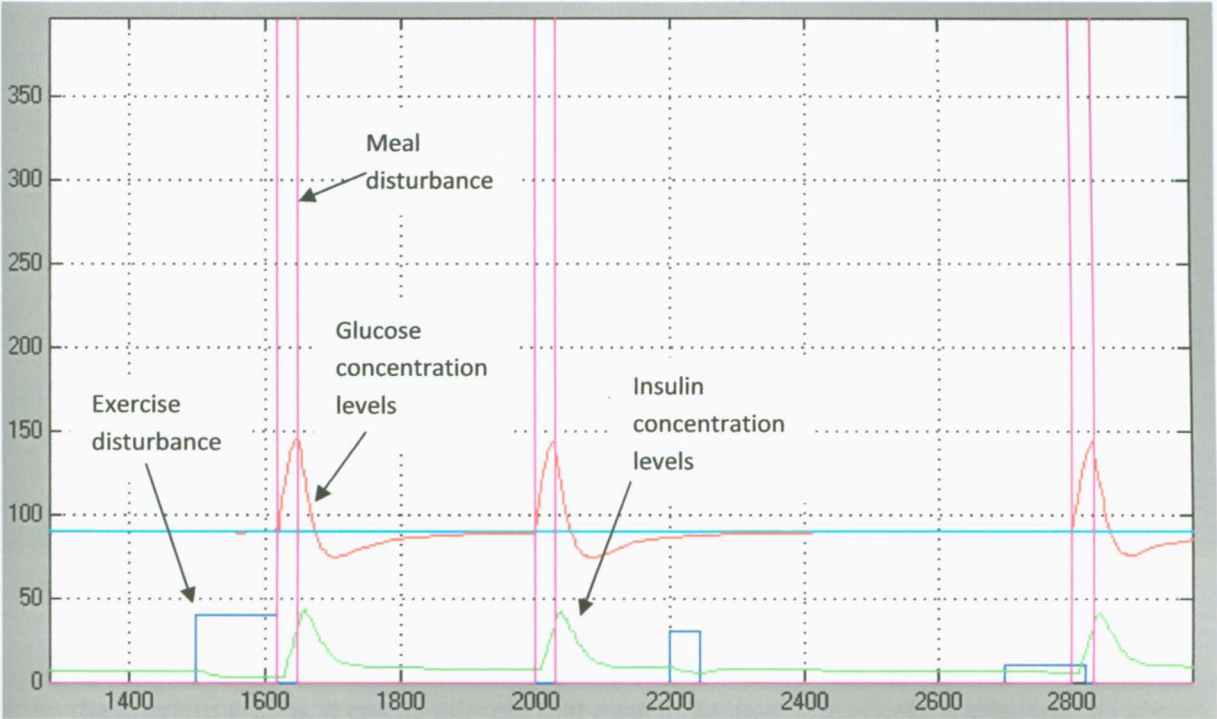


Figure 91. Performance of glucose level when meal and exercise disturbance excite the system And PID and predictive strategies are applied.

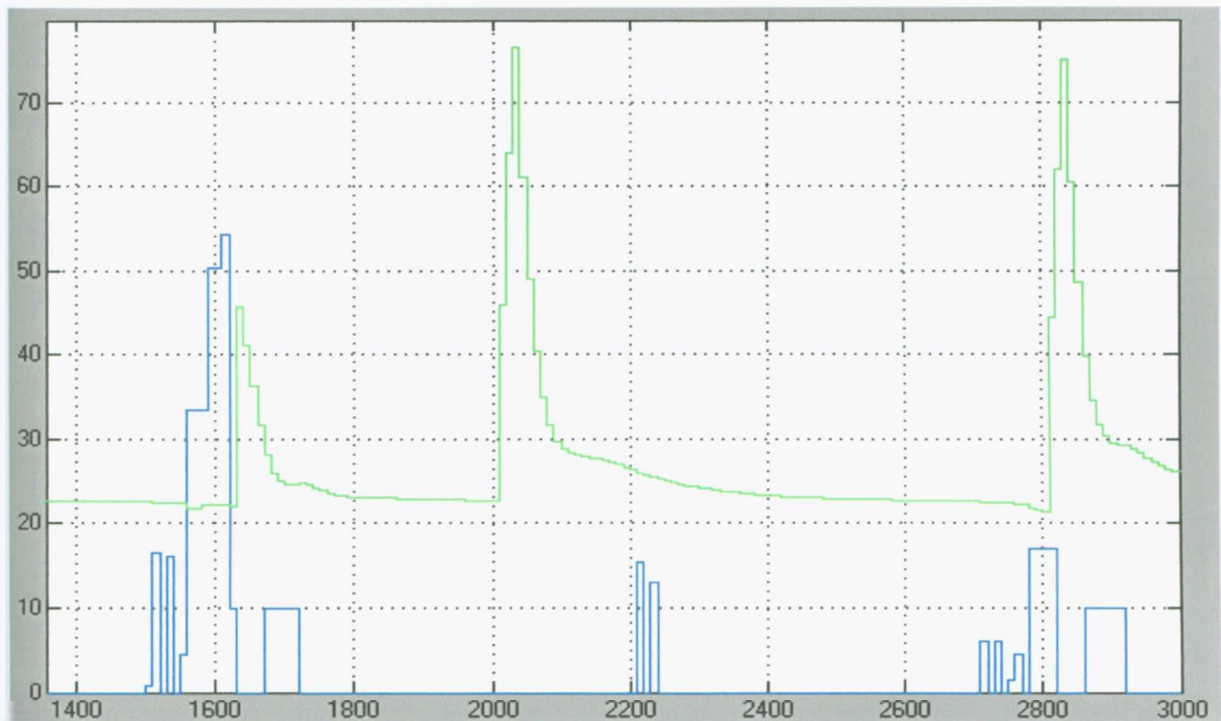


Figure 92. Manipulated variables of the feedback PID controller (external insulin in mU/min)(green) and feedforward predictive compensator (external glucagon in pg/min)((blue).

From the previous graphs, it can be inferred that even if the meal disturbance is affecting the system, the predictive controller impedes glucose level to decrease due to exercise. Conversely, the response of the glucose levels in the same is the three cases since the 3 meals are identical and the exercise disturbances have a null net effect thanks to the action of the predictive compensator. Nevertheless, the PID controller performance is not satisfactory because hypoglycemic levels can be observed in the response. As it was stated in chapter 3, this is one of the disadvantages of applying the integral action in glucose – insulin PID based control system.

It is important to remark, that since the implementation of the predictive control strategy was done in a discrete time form some restrictions were easily considered. Prior to the external glucagon infusion prediction, if the glucose level is above its steady state, the manipulation of external glucagon administration was set to zero; on the other hand, if it was under its normal value, external glucagon infusion was held constant between sample times as it is done with discrete controllers.

A manual mode test was done, which considers a constant insulin bolus administration and no external glucagon infusion, so the advantages of the feedback PID controller and feedforward predictive compensator can be observed; figure 93 illustrates open loop response.

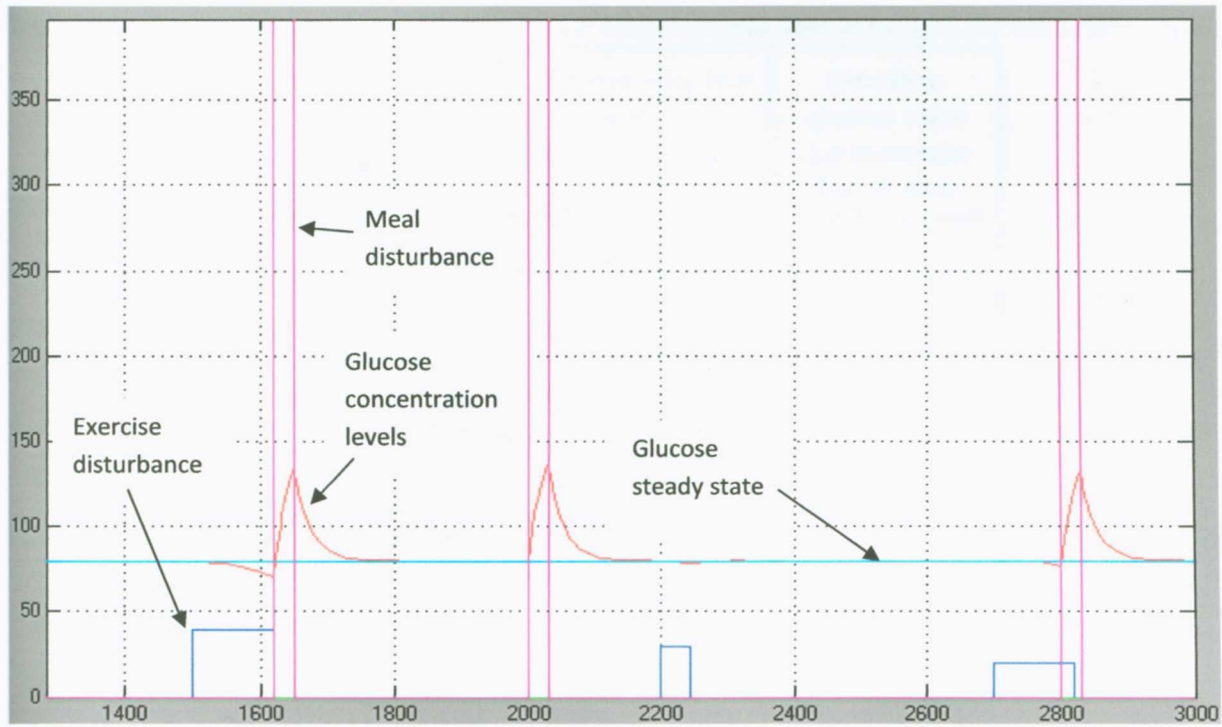


Figure 93. Response of blood glucose level when meal and exercise disturbance excite the system in manual mode.

For comparison issues, the glucose postprandial time due to meal disturbances and the deviation glucose level due to exercise were considered. Table XXVII shows these comparison indices. The hypoglycemic episode due to the integral action was omitted.

Table XXVII. Comparison in the system's behavior when it is operated in manual and automatic mode.

Test	System mode	Postprandial time due to meal disturbances (min)	Deviation glucose value due to exercise disturbances
1	Manual	84	10
	Automatic	25.86	-0.9
2	Manual	82	1.9
	Automatic	25.86	-
3	Manual	82	-3
	Automatic	26.85	-0.4

From the information in table XXVII, it can be concluded that the control strategy with feedback PID and feedforward predictive compensation makes a great performance improvement in blood glucose regulation. The postprandial time is shortened approximately 3.5 times than in manual mode and the deviation of glucose level decreased from 7.4 to 11.1 times, depending on exercise intensity and duration, than operating in manual mode.

7.2. Physical implementation of the feedforward predictive compensator

An important aspect when designing control strategies is the feasibility of their physical implementation. In addition to the instruments required for feedback control, the proposed automated system must have a sensor that measures the disturbance of interest, an actuator to produce a compensation of its effects and a reservoir of the drug to use.

In the next sections a description of the required elements, in order to operate in a close loop mode, is done. An explanation of how exercise intensity can be measured is also covered.

7.2.1. Disturbance measurement and sensor technology

As stated in chapter 3, an essential step for applying the feedforward strategy is that the disturbance that affects the system must be measured and quantified. In this thesis, the disturbance is the exercise done (*PAMM*) by the patient.

Nowadays, there is not a sensor that can directly measure *PAMM*. The only available method is by measuring the arterial blood gasses while the person is doing physical activity. This is done with a very sophisticated and non-portable device.

Nevertheless, it was found in the literature, an equation that relates the *heart rate* with PVO_2^{max} . This discovery combined with the developed equation (4.1) will allow an indirect measurement of *PAMM*.

Swain (1994) established two equations that relate the *heart rate* with PVO_2^{max} , one is for men and the other for women. The difference relies on the basis that the cardio vascular system does not behaves in the same form in men and women; this is due to a variation in the heart's size. (Guyton & Hall, 2001).

$$\%HR_{max} = (0.643 \pm 0.010)PVO_2^{max} + 36.8 \pm 1 \quad \text{for men} \quad (7.1)$$

$$\%HR_{max} = (0.628 \pm 0.014)PVO_2^{max} + 39 \pm 1.3 \quad \text{for women} \quad (7.2)$$

It is important to remark, that equations 7.1 and 7.2 are only valid for steady state values. This cannot be seen as a drawback, since the minimum sample time of today's glucose sensors is of 5 minutes and the settling of the PVO_2^{max} and *PAMM* system is faster. This means that when glucose is measured, PVO_2^{max} will already be at its steady state and therefore equations 7.1, 7.2 and 4.1 can be used to quantify *PAMM*. In other words, the procedure in order to quantify *PAMM* is

*Measure heart rate variations due to physical activity only, then equations 7.1 and 7.2 are used to calculate the corresponding PVO_2^{max} , the resulting value is introduced in equation 4.1 and *PAMM* is quantified.*

For measuring *heart rate* variations due to physical activity only, an odometer has to be used. It was found that there is a commercial odometer (Omron HJ-720ITC Pocket Pedometer with Advanced Omron

Health Management Software) that differentiates *heart rate* variations due to physical activity from other factors.

The characteristics of the chosen odometer are

- It has an integrated accelerometer to detect motion
- Measures steps, aerobic steps and minutes, calories and distance
- Separately displays aerobic steps and minutes walked more than 10 minutes continuously
- 7 day history allows a review of a full week of exercise
- Measures blood pressure
- Measures heart rate

7.2.2. Actuator and reservoir

The actuation principle to follow for glucagon infusion is the same as for exogenous insulin infusion, which typically corresponds to the use of an external pump that doses a specified drug amount to the patient.

Since glucagon is not used when glucose level rises and only insulin must be secreted when it drops; both exogenous hormones could be administrated through the same infusion site. Therefore glucagon and insulin could be placed in two different reservoirs inside one pumping device engineered to administer both substances by a single catheter.

Chapter 8

Conclusions

This chapter summarizes the results obtained from chapter 4 through chapter 7, as well the final conclusions that can be inferred from this thesis work and the challenges for future investigations in order to improve what has been obtained.

8.1. Discussion of results

The results from analytical and statistical modeling and from the simulations of the predictive controller of exercise effects are summarized in this section, although a more detailed presentation can be found in the previous chapters.

8.1.1. Results from analytical modeling

In the analytical modeling issue the principal contribution is the inclusion of all exercise effects in the Sorensen's model. This implies the quantification of exercise, blood flow rate in the main organs, glucose and insulin consumption and the addition of the input of external glucagon infusion.

Regarding to exercise quantification, several differential equations that represent the dynamics involved in the system were developed, such as peripheral glucose uptake (PGU_A), hepatic glucose production (HGP_A), percentage of maximum oxygen volume consumption rate (PVO_2^{max}), percentage of active muscular mass ($PAMM$), rate of glycogenolysis depletion ($\frac{dG_{gly}}{dt}$), kidney insulin uptake (KIU) and peripheral insulin uptake (PIU).

From the simulations done with the modified Sorensens system, it was concluded that even the glucose level had an accurate performance; insulin concentration did not behave as it is reported in the literature. This was the main reason why it was discarded for its use in the predictive control strategy. So

another model was implemented, this was the modified Bergman's minimal order model. Unlike Sorensen's model, this had a response that matched the reported clinical data.

Nevertheless, Bergman's model had a major drawback, it did not have an external glucagon infusion input, which is fundamental in impeding glucose level to decrease in the presence of exercise disturbance. In order to solve this problem, another innovation was implemented, which was the combination of Sorensen's and Bergman's models. The glucagon compartment of the Sorensen model modified with an input of exogenous glucagon was combined with the Bergman model with exercise caused PVO_2^{max} input. A more detailed explanation is described in chapter 4.

When the combined Sorensen – Bergman systems was simulated, the response obtained was in the range that the medical literature predicts.

8.1.2. Results from statistical modeling

In this section, the followed statistical procedure to obtain a Wiener model representing glucose behavior to exercise, glucagon and insulin inputs is described.

After getting sufficient data, near 5000 points from the experimental design the analytical system was modeled in a statistical form using the Wiener modeling technique, in order to develop a predictive regulator.

There were four data conditioning criterions involved in the statistical modeling, which were normalization of the data in a theoretical form, scaling of data with respect to its maximum value and without normalization. These criterions rose because the inputs were of very different order of magnitude.

As it is stated in chapter six, the first objective when using Wiener modeling is to find the multiple nonlinear regression parameters that describe the static nonlinear gain of the system; in this case these parameters were obtained via least squares algorithm.

Afterwards, the linear parameters of each of the dynamic ARX models are obtained using the generalized reduced gradient algorithm, which optimizes the parameters that will make a minimum error between the predicted and real output. This mathematical tool was used because the nonlinear parameters must constrain, according to the algorithm described by Rollins.

From the obtained models, it was concluded that the one with the minimum square error (mse) results when the inputs are normalized with respect to its maximum value, which gave an acceptable magnitude of 3.6098 with a sample time of 10 minutes. Nevertheless, this model was modified in order to have the external glucagon infusion regression starting from the first iteration. This adjustment lowered the mse to 3.1.

Also, it was observed that the sample time had a significant impact in the system. Although the control literature reports that using a smaller sample time will lead to a better identification, in this case a bigger one gave the best response. The model with a sample time of 10 minutes had a better response than the one with a sample time of 5 minutes.

Even though, there was an error between the system and the obtained model; this error was compensated in the predictive control development by making a small adjustment in the parameters.

8.1.3. Results from the predictive control implementation

The final goal of this thesis was the development of a regulator that could compensate the nonlinear and unstable effect of exercise over glucose level. This achievement was accomplished by designing a model based predictor controller, which has glucose concentration level and PAMM as inputs and a predicted external glucagon infusion as the output. The exogenous insulin input was ignored in the compensator because this hormone will not interfere for raising the blood glucose level that is the goal of the feedforward predictive compensator. Another reason is that exogenous insulin infusion will be considered as the manipulated variable in the feedback PID controller.

From the previous chapter, it was concluded that for a limited range of 0 - 40% PAMM and exercise duration from 0 to 120 minutes the performance of this strategy is excellent. The maximum glucose level deviation value from its steady state was +2 mg/dL, and this magnitude occurs at extreme conditions, meaning that the patient is exercising at the highest intensity and duration level.

In chapter 6, it was established that the intensity range was limited to 40% PAMM due to the results thrown by the testing phase. Also, from trials done to the controller, it was obtained that for values beyond 120 minutes, its performance failed. Figures 92 to 94, illustrates the behavior of the closed loop system when the limited range is exceeded.

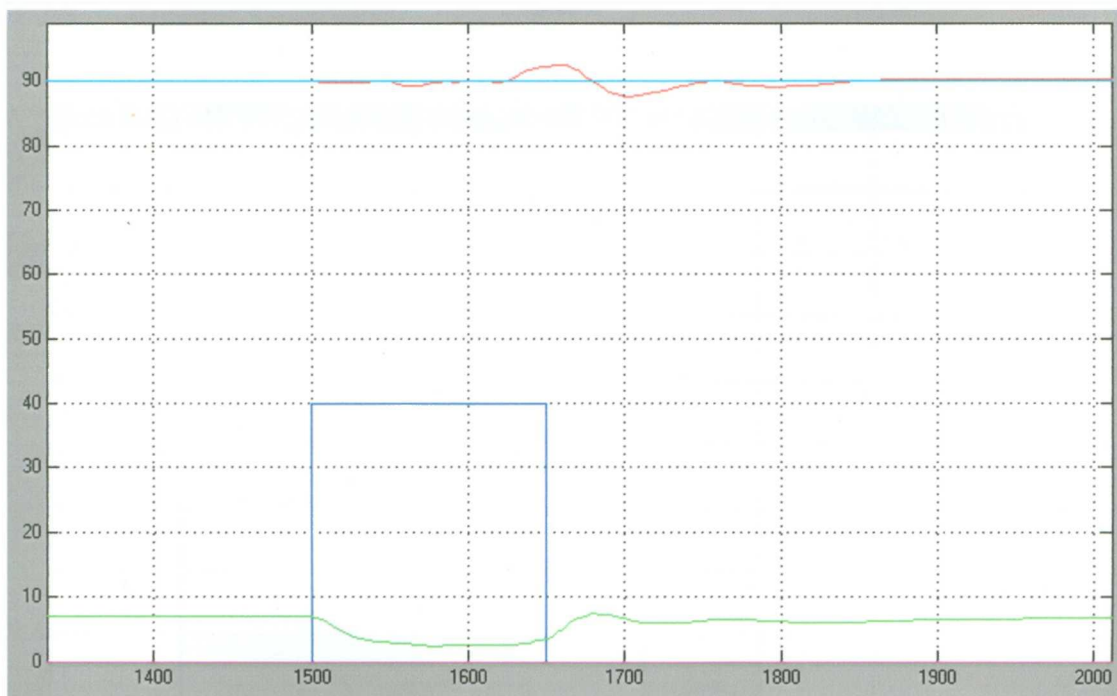


Figure 94. Performance of predictive control strategy. With 40% PAMM (blue) and a duration of 150 minutes. Glucose steady state level at 90 mg/dL(cyan).Glucose concentration response in red. Insulin concentration level in green.

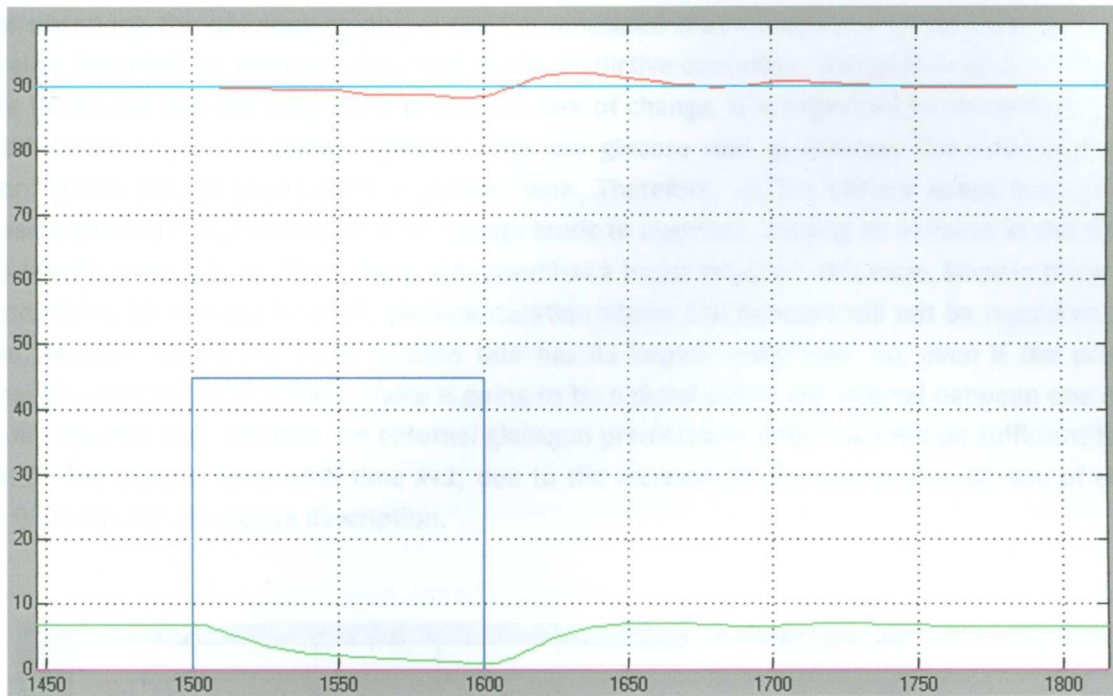


Figure 95. Performance of predictive control strategy. With 45% PAMM (blue) and a duration of 100 minutes. Glucose steady state level at 90 mg/dL(cyan).Glucose concentration response in red. Insulin concentration level in green.

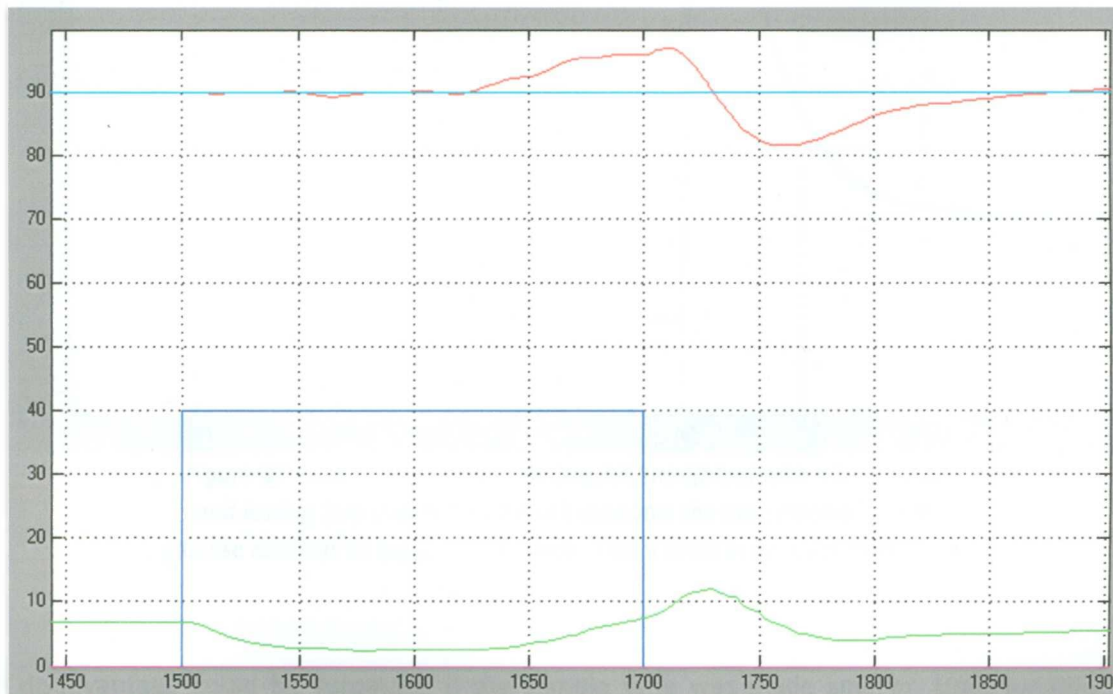


Figure 96. Performance of predictive control strategy. With 40% PAMM (blue) and a duration of 200 minutes. Glucose steady state level at 90 mg/dL(cyan).Glucose concentration response in red. Insulin concentration level in green.

After observing the previous graphs, it can be concluded that if exercise lasts beyond the duration constraint, there will be a serious drawback in the predictive controller. This performance is due to the sample time used and the magnitude of glucose rate of change. It is important to remember, that the selected model in the predictive algorithm uses the glucose rate to estimate the external glucagon infusion, which also depends on the sample time. Therefore, as the patient keeps exercising, his decreasing glucose concentration rate of change tends to augment, causing an increase in the difficulty to regulate its glucose level. The sample time used has a major impact in this issue. Since in this thesis it was considered a 10 minutes interval, exercise duration above 120 minutes will not be regulated as it is desired, because above this limit, glucose rate has its largest magnitude. So, even if the predicted external glucagon infusion is right, there is going to be a drawback in the interval between one sample time and the next one, because the external glucagon predicted at time k will not be sufficient to keep regulating the glucose level until time $k+1$, due to the increase of decreasing glucose rate of change. Graph 95 illustrates the above description.

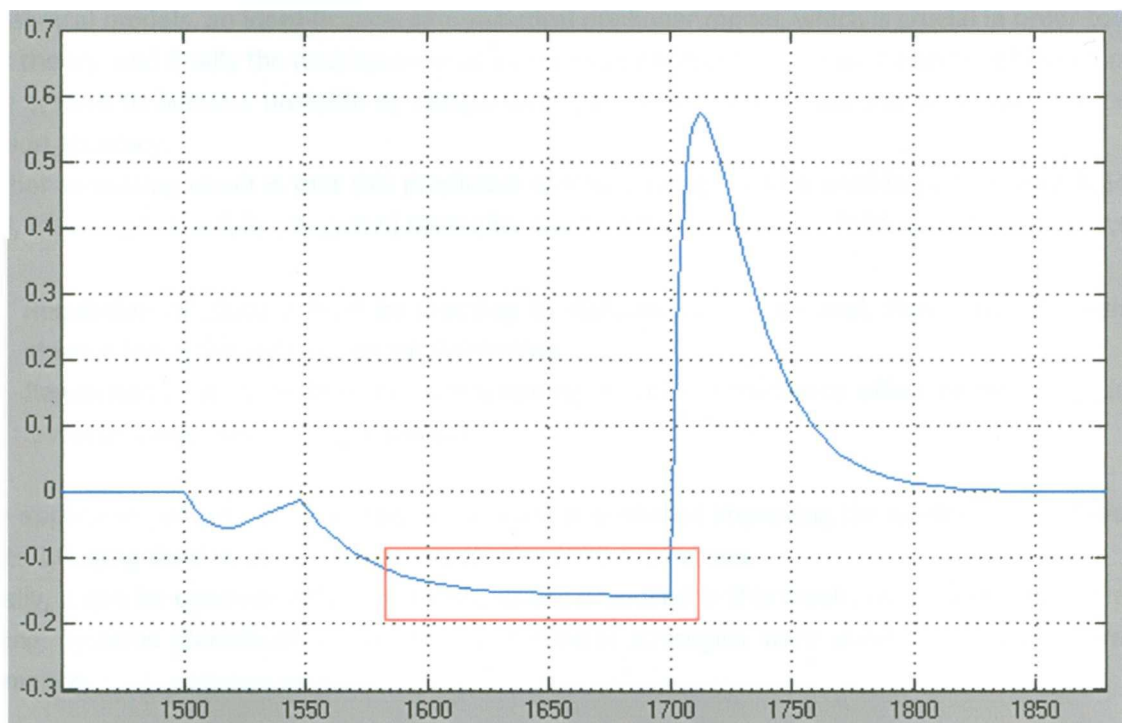


Figure 97. Glucose rate of change (mg/dL/min)(blue) with 40% PAMM and lasting 200 minutes. Red block indicates the time interval where glucose rate has its biggest magnitude. This is done in an open loop mode.

This disadvantage could be surpassed if the sample time was made smaller. Unfortunately, today glucose sensors generally measure this molecule every 5 minutes and it was demonstrated in chapter 6, that a model with this sample time does not work as well as with a sample time of 10 minutes.

Nevertheless, before this work, there was no report of a controller that compensated this disturbance, the results obtained are very promising in order to develop a fully integrated glucose regulator.

8.2. Conclusions and future challenges

8.2.1. Conclusions

The study of physiological systems is a hard issue due to their nonlinear behavior, as well as the lack of mathematical models that represent their dynamics. A more difficult problem arises when it is desired to regulate these systems, because advanced control strategies must be applied and sometimes, there is no technology to accomplish this.

Nonetheless, in this thesis research, potential outcomes have been obtained, from a modification of two analytical models, an identification of a statistical nonlinear model, which is crucial in order to apply control theory, and finally the development of a predictive controller that has the ability of impeding the glucose system to become unstable by compensating the effect of exercise and achieving an excellent regulation accuracy.

Another promising result is that this predictive control strategy can be used in parallel with feedback control, meaning that a fully integrated controller can be achieved with the following characteristics:

- Regulation of glucose level by reacting to disturbances, in general, that cause the rising of glucose levels through insulin administration
- Regulation of glucose level by compensating exercise disturbance effect of decaying glucose levels by exogenous glucagon infusion.

The application of both control schemes has the potential of improving the quality of life of diabetic patients, bringing their lifestyle to resemble that of a healthy person.

Finally, it can be concluded that all the objectives proposed in this thesis, which involve the areas of modeling, systems identification and advanced control strategies were achieved with a satisfactory performance.

8.2.2. Future challenges

As stated in the previous sections, the major drawbacks in the system identification and control implementation were the limitation of the exercise intensity and duration, which are consequences of the sample time used.

For surpassing these problems, two approaches can be done, which are

- Decreasing the sample time approximately to 1 minute or less.
- Applying other modeling technique.

Decreasing the sample time has several advantages, such as obtaining more information of the system dynamics from the experimental design which will make a better adjustment of the parameters, causing that the PAMM range could be broaden. However, its major improvement will be in the predictive controller implementation. A smaller sample time will allow an increment in the exercise duration range. When a sample time of 10 minutes was used and exercise lasted more than 120, even when the predicted external glucagon infusion was right at time k , glucose level tended to drop because the manipulated variable was not enough for compensating the effect of the disturbance, since the system needed to react faster and this was not possible within one long sampling period of 10 minutes (the next sample time $k+1$ lags 10 minutes from the previous one). So, by shortening the sample time this drawback can be surpassed.

Nevertheless, as it was stated before, up to these days there has not been a commercial sensor for obtaining quick measurements of arterial glucose concentration. However, promising results were obtained by Carvajal (2009), who successfully began to study a blood glucose sensing method based on Yamakoshi's work. Carvajal's work shows it is possible to obtain a reliable measure within the required parameters for this thesis research, without interferences from other analytes and tissues.

Nonetheless, if sensor technology does not improve in the next few years, other modeling techniques can be used for compensating exercise effect on glucose level. Artificial neural networks (ANN) could compete in performance with Wiener modeling. Their disadvantages are that they must be trained for all possible inputs combinations, and this may be a difficult issue; also, they will not provide a system structure, as it is done with Wiener modeling. So, basically the modeler would not know its internal behavior. However, if the ANN is well trained, its performance can be as good as Wiener modeling method.

Appendix 1. Sorensen's equations and parameter's values

The following nomenclature and equations describe the compartmental model by Sorensen for the glucose-insulin metabolism for either a healthy person or a diabetic patient. Taken from Sánchez.

Model variables

- A: auxiliary equation state (dimensionless)
 - B: fractional clearance (I, dimensionless; N, L/min)
 - G: glucose concentration (mg/dL)
 - I: insulin concentration (mU/L)
 - N: glucagons concentration (normalized, dimensionless)
 - Q: vascular plasma flow rate (L/min)
 - q: vascular blood flow rate (dL/min)
 - T: transcapillary diffusion time constant (min)
 - V: volume (L)
 - v : volume (dL)
 - ⊠ : metabolic source or sink rate (mg/min or mU/min)
- Variables in pancreatic insulin release model in healthy body:
- W: potentiator (dimensionless)
 - Y: inhibitor (dimensionless)
 - R: labile insulin (U)
 - Z: secretion rate (U/min)
 - X, W_{∞} : intermediate variables (dimensionless)

Model sub and superscripts

- A: hepatic artery
- B: brain / basal value in insulin pancreatic release model
- BU: brain uptake
- G: glucose
- H: heart and lungs
- HGP: hepatic glucose production
- HGU: hepatic glucose uptake
- I: insulin
- IHGP: insulin effect on HGP
- IHGU: insulin effect on HGU
- IVI: intravenous insulin infusion
- K: kidney
- KC: kidney clearance
- KE: kidney excretion
- L: liver
- LC: liver clearance

N: glucagon
NHGP: glucagons effect on HGP
P: periphery (muscle/adipose tissue)
PC: peripheral clearance
PGU: peripheral glucose uptake
PIR: pancreatic insulin release
PNC: pancreatic glucagon clearance
PNR: pancreatic glucagon release (normalized)
RBCU: red blood cell uptake
S: gut (stomach/intestine)
SIA: insulin absorption into blood stream from subcutaneous depot
SU: gut uptake
T: tissue or interstitial space

Glucose mass balance equations

$$v_B \frac{dG_B(t)}{dt} = (G_H(t) - G_B(t))q_B - (G_B(t) - G_B^T(t)) \frac{v_B^T}{T_B} \quad (\text{a1.1})$$

$$v_B^T \frac{dG_B^T(t)}{dt} = (G_B(t) - G_B^T(t)) \frac{v_B^T}{T_B} - \Gamma_{BU} \quad (\text{a1.2})$$

$$v_H \frac{dG_H(t)}{dt} = G_B(t)q_B + G_L(t)q_L + G_K(t)q_K + G_P(t)q_P - G_H(t)q_H - \Gamma_{RBCU} \quad (\text{a1.3})$$

$$v_S \frac{dG_S(t)}{dt} = (G_H(t) - G_S(t))q_S + \Gamma_{meal} - \Gamma_{SU} \quad (\text{a1.4})$$

$$v_L \frac{dG_L(t)}{dt} = G_H(t)q_A + G_S(t)q_S - G_L(t)q_L + \Gamma_{HGP} - \Gamma_{HGU} \quad (\text{a1.5})$$

$$v_K \frac{dG_K(t)}{dt} = (G_H(t) - G_K(t))q_K - \Gamma_{KE} \quad (\text{a1.6})$$

$$v_P \frac{dG_P(t)}{dt} = (G_H(t) - G_P(t))Q_P + (G_P^T(t) - G_P(t)) \frac{v_P^T}{T_P^G} \quad (\text{a1.7})$$

$$v_P^T \frac{dG_P^T(t)}{dt} = (G_P(t) - G_P^T(t)) \frac{v_P^T}{T_P^G} - \Gamma_{PGU} \quad (\text{a1.8})$$

Glucose metabolic sinks and sources (mg/min):

$$\Gamma_{BC} = 70 \quad (\text{a1.9})$$

$$\Gamma_{RBCU} = 10 \quad (\text{a1.10})$$

$$\Gamma_{SU} = 20 \quad (\text{a1.11})$$

$$\Gamma_{HGHP} = 155A_{IHGP}(t) \left[2.7 \tanh(0.388N(t)) - A_{NHGP}(t) \right] \times \left[1.425 - 1.406 \tanh \left\{ 0.6199 \left(\frac{G_L(t)}{101} - 0.4969 \right) \right\} \right] \quad (\text{a1.12})$$

$$\frac{dA_{IHGP}(t)}{dt} = \frac{1}{25} \left[1.2088 - 1.138 \tanh \left(1.669 \frac{I_L(t)}{21.43} - 0.8885 \right) - A_{IHGP}(t) \right] \quad (\text{a1.13})$$

$$\frac{dA_{NHGP}(t)}{dt} = \frac{1}{65} \left[\frac{2.7 \tanh(0.388N(t)) - 1}{2} - A_{NHGP}(t) \right] \quad (\text{a1.14})$$

$$\Gamma_{HGU}(t) = 20A_{IHGU}(t) \left[5.6648 + 5.6589 \tanh \left\{ 2.4375 \left(\frac{G_L(t)}{101} - 1.48 \right) \right\} \right] \quad (\text{a1.15})$$

$$\frac{dA_{IHGU}(t)}{dt} = \frac{1}{25} \left[2 \tanh \left(0.549 \frac{I_L(t)}{21.43} \right) - A_{IHGU}(t) \right] \quad (\text{a1.16})$$

$$\Gamma_{KE}(t) = \begin{cases} 71 + 71 \tanh[0.011(G_K(t) - 460)], & \text{for } G_K < 460 \text{ mg/dL} \\ 0.872G_K(t) - 300, & \text{for } G_K > 460 \text{ mg/dL} \end{cases} \quad (\text{a1.17})$$

$$\Gamma_{PGU}(t) = \frac{35G_P^T(t)}{86.81} \left[7.035 + 6.51623 \tanh \left\{ 0.33827 \left(\frac{I_P^T(t)}{5.304} - 5.82113 \right) \right\} \right] \quad (\text{a1.18})$$

Insulin mass balance equations

$$V_B \frac{dI_B(t)}{dt} = (I_H(t) - I_B(t))Q_B \quad (\text{a1.19})$$

$$v_H \frac{dI_H(t)}{dt} = I_B(t)Q_B + I_L(t)Q_L + I_K(t)Q_K + I_P(t)Q_P - I_H(t)Q_H + \Gamma_{IVI} \quad (\text{a1.20})$$

$$V_S \frac{dI_S(t)}{dt} = (I_H(t) - I_S(t))Q_S \quad (\text{a1.21})$$

$$V_L \frac{dI_L(t)}{dt} = I_H(t)Q_A + I_S(t)Q_S - I_L(t)Q_L + \Gamma_{PIR} - \Gamma_{LC} \quad (\text{a1.22})$$

$$V_K \frac{dI_K(t)}{dt} = (I_H(t) - I_K(t))Q_K - \Gamma_{KC} \quad (\text{a1.23})$$

$$V_P \frac{dI_P(t)}{dt} = (I_H(t) - I_P(t))Q_P - (I_P(t) - I_P^T(t)) \frac{V_P^T}{T_P^I} \quad (\text{a1.24})$$

$$V_P^T \frac{dI_P^T(t)}{dt} = (I_P(t) - I_P^T(t)) \frac{V_P^T}{T_P^I} + \Gamma_{SIA} - \Gamma_{PC} \quad (\text{a1.25})$$

Insulin metabolic sources and sinks (mU/min)

Γ_{IVI} and Γ_{SIA} are the terms for insulin administration in medical treatments using the intravenous and the subcutaneous routes, respectively.

$$\Gamma_{LC}(t) = F_{LC}(I_H(t)Q_A + I_S(t)Q_S + \Gamma_{PIR}) \quad (\text{a1.26})$$

$$\Gamma_{KC}(t) = F_{KC} I_K(t) Q_K \quad (\text{a1.27})$$

$$\Gamma_{PC}(t) = \frac{I_P^T(t)}{\frac{1 - F_{PC}}{F_{PC}} \frac{1}{Q_P} - \frac{T_P^I}{V_P^T}} \quad (\text{a1.28})$$

$$\Gamma_{PIR} = 0 \quad \text{no pancreatic insulin release in diabetic patient} \quad (\text{a1.29})$$

$$\Gamma_{PIR}(t) = \frac{Z(G_H)}{Z(G_H^B)} \Gamma_{PIR}^B \quad \text{pancreatic insulin release for a healthy person} \quad (\text{a1.30a})$$

$$\frac{dW(t)}{dt} = \alpha [W_\infty(t) - W(t)] \quad (\text{a1.30b})$$

$$\frac{dY(t)}{dt} = \beta [X(t) - Y(t)] \quad (\text{a1.30c})$$

$$\frac{dR(t)}{dt} = k [R_0 - R(t)] + \gamma W(t) - Z(t) \quad (\text{a1.30d})$$

$$Z(t) = \{M_1 W_\infty(t) + M_2 [X(t) - Y(t)]\} R(t) \quad (\text{a8.1.30e})$$

$$X(t) = \frac{[G_H(t)]^{3.27}}{132^{3.27} + 5.93 [G_H(t)]^{3.02}} \quad (\text{a1.30f})$$

$$W_\infty(t) = [X(t)]^{1.11} \quad (\text{a1.30g})$$

Glucagon mass balance

$$V_N \frac{dN(t)}{dt} = (\Gamma_{PNR}(t) - N(t)) F_{PNC} \quad (\text{a1.31})$$

Glucagon metabolic source (dimensionless)

$$\Gamma_{\text{PNR}}(t) = \left[1.3102 - 0.61016 \tanh \left\{ 1.0571 \left(\frac{I_H(t)}{15.15} - 0.46981 \right) \right\} \right] \times \left[2.9285 - 2.095 \tanh \left\{ 4.18 \left(\frac{G_H(t)}{91.89} - 0.6191 \right) \right\} \right] \quad (\text{a1.32})$$

Parameter values

Volumes	Flows	Diffusion time constants	Dimensionless factors
$v_B=3.5$ dL	$q_B=5.9$ dL/min	$T_B=2.1$ min	
$v_R^I = 4.5$ dL			
$v_H=13.8$ dL	$q_H=43.7$ dL/min		
$v_S=11.2$ dL	$q_S=10.1$ dL/min		
$v_L=25.1$ dL	$q_L=12.6$ dL/min		
	$q_A=2.5$ dL/min		
$v_K=6.6$ dL	$q_K=10.1$ dL/min		
$v_P=10.4$ dL	$q_P=15.1$ dL/min	$T_P^G = 5.0$ min	
$v_P^I = 67.4$ dL			
$V_B=0.265$ L	$Q_B=0.45$ L/min		
$V_H=0.985$ L	$Q_H=3.12$ L/min		
$V_S=0.945$ L	$Q_S=0.72$ L/min		
$V_L=1.14$ L	$Q_L=0.9$ L/min		$F_{LC}=0.4$
	$Q_A=0.18$ L/min		
$V_K=0.505$ L	$Q_K=0.72$ L/min		$F_{KC}=0.3$

$V_p=0.735$ L	$Q_p=1.05$ L/min	$T_p^I = 20$ min	$F_{PC}=0.15$
$V_p^I = 6.3$ dL			
$V_N=11.31$ L	$F_{PNC}=0.0091$ L/min		

Constants for insulin release model in healthy body:

$$\alpha=0.0482 \text{ min}^{-1}$$

$$\beta=0.931 \text{ min}^{-1}$$

$$k=0.00794 \text{ min}^{-1}$$

$$M_1=0.00747 \text{ min}^{-1}$$

$$M_2=0.0958 \text{ min}^{-1}$$

$$\gamma=0.575 \text{ U/min}$$

$$R_0=6.33 \text{ U}$$

Appendix 2. Data results of the experiment

The following appendix includes the data obtained from the experimental designed that is described in chapter 5.

Time [min]	PAMM [%]	INSULIN [mU/min]	GLUCAGON [pg/min]	dGlucose [mg/dl/min]
1500	0	0	0	0
1500	30	0	0	0
1505.167	30	0	0	-0.0196
1510	30	0	0	-0.0335
1516.8148	30	0	0	-0.0362
1520	30	0	0	-0.0329
1524.3173	30	0	0	-0.026
1530	30	0	0	-0.0151
1535	30	0	0	-0.0059
1540	30	0	0	0.0022
1545	30	0	0	0.0086
1550	30	0	0	0.0134
1555	30	0	0	0.0166
1560	30	0	0	0.0079
1565.0754	30	0	0	-0.0197
1570	30	0	0	-0.0431
1575	30	0	0	-0.0638
1580	30	0	0	-0.0818
1585	30	0	0	-0.0974
1590	30	0	0	-0.111
1595	30	0	0	-0.1228
1600	30	0	0	-0.133
1605	30	0	0	-0.1418
1610	30	0	0	-0.1494
1615	30	0	0	-0.1559
1620	30	0	0	-0.1615
1625	30	0	0	-0.1664
1630	30	0	0	-0.1705
1635	30	0	0	-0.174
1640	30	0	0	-0.177
1645	30	0	0	-0.1796
1650	30	0	0	-0.1818
1655	30	0	0	-0.1837
1660	30	0	0	-0.1853
1665	30	0	0	-0.1866
1670	30	0	0	-0.1878

1675	30	0	0	-0.1888
1680	30	0	0	-0.1896
1685	30	0	0	-0.1903
1690	30	0	0	-0.1909
1695	30	0	0	-0.1914
1700	30	0	10000	-0.1918
1705	30	0	10000	-0.155
1710	30	0	10000	-0.1392
1715	30	0	10000	-0.1353
1720	30	0	10000	-0.1378
1725	30	0	10000	-0.1434
1730	30	0	10000	-0.1504
1735	30	0	10000	-0.1575
1740	30	0	10000	-0.1643
1745	30	0	10000	-0.1704
1750	30	0	10000	-0.1758
1755	30	0	10000	-0.1804
1760	30	0	10000	-0.1843
1765	30	0	10000	-0.1876
1770	30	0	10000	-0.1902
1775	30	0	10000	-0.1924
1780	30	0	10000	-0.1942
1785	30	0	10000	-0.1956
1790	30	0	10000	-0.1967
1795	30	0	10000	-0.1976
1800	30	0	10000	-0.1982
1805	30	0	10000	-0.1987
1810	30	0	10000	-0.1991
1815	30	0	10000	-0.1993
1820	30	0	10000	-0.1995
1825	30	0	10000	-0.1996
1830	30	0	10000	-0.1996
1835	30	0	10000	-0.1996
1840	30	0	10000	-0.1996
1845	30	0	10000	-0.1995
1850	30	0	10000	-0.1994
1855	30	0	10000	-0.1994
1860	30	0	10000	-0.1993
1865	30	0	10000	-0.1992
1870	30	0	10000	-0.1991
1875	30	0	10000	-0.1991
1880	30	0	10000	-0.199
1885	30	0	10000	-0.199

1890	30	0	10000	-0.199
1895	30	0	10000	-0.1989
1900	0	0	0	-0.1989
1904.9806	0	0	0	0.9505
1910	0	0	0	1.3028
1915.111	0	0	0	1.3192
1920	0	0	0	1.2118
1926.528	0	0	0	1.0177
1930	0	0	0	0.9139
1933.1289	0	0	0	0.8255
1940	0	0	0	0.6535
1945	0	0	0	0.5484
1950	0	0	0	0.459
1955	0	0	0	0.3836
1960	0	0	0	0.3204
1965	0	0	0	0.2675
1970	0	0	0	0.2235
1975	0	0	0	0.1868
1980	0	0	0	0.1563
1985	0	0	0	0.1309
1990	0	0	0	0.1098
1995	0	0	0	0.0923
2000	0	0	0	0.0777
2005	0	0	0	0.0655
2010	0	0	0	0.0553
2015	0	0	0	0.0468
2020	0	0	0	0.0397
2025	0	0	0	0.0337
2030	0	0	0	0.0287
2035	0	0	0	0.0245
2040	0	0	0	0.021
2045	0	0	0	0.018
2050	0	0	0	0.0155
2055	0	0	0	0.0134
2060	0	0	0	0.0115
2065	0	0	0	0.01
2070	0	0	0	0.0087
2075	0	0	0	0.0076
2080	0	0	0	0.0066
2085	0	0	0	0.0058
2090	0	0	0	0.0051
2095	0	0	0	0.0045
2100	60	0	0	0.004

2105.2809	60	0	0	-0.0365
2110	60	0	0	-0.0639
2115.0602	60	0	0	-0.0714
2120	60	0	0	-0.0637
2124.116	60	0	0	-0.051
2130	60	0	0	-0.0423
2136.3138	60	0	0	-0.0541
2140	60	0	0	-0.0597
2145	60	0	0	-0.0672
2150	60	0	0	-0.075
2155	60	0	0	-0.0833
2160	60	0	0	-0.0921
2165	60	0	0	-0.1011
2170	60	0	0	-0.1102
2175	60	0	0	-0.1191
2180	60	0	0	-0.1278
2185	60	0	0	-0.136
2190	60	0	0	-0.1436
2195	60	0	0	-0.1507
2200	60	0	0	-0.1571
2205	60	0	0	-0.163
2210	60	0	0	-0.1683
2215	60	0	0	-0.1729
2220	60	0	0	-0.1771
2225	60	0	0	-0.1808
2230	60	0	0	-0.184
2235	60	0	0	-0.1868
2240	60	0	0	-0.1893
2245	60	0	0	-0.1915
2250	60	0	0	-0.1933
2255	60	0	0	-0.1949
2260	60	0	0	-0.1963
2265	60	0	0	-0.1975
2270	60	0	0	-0.1986
2275	60	0	0	-0.1995
2280	60	0	0	-0.2003
2285	60	0	0	-0.2009
2290	60	0	0	-0.2015
2295	60	0	0	-0.202
2300	60	0	10000	-0.2024
2305	60	0	10000	-0.1662
2310	60	0	10000	-0.1505

2315	60	0	10000	-0.1464
2320	60	0	10000	-0.1485
2325	60	0	10000	-0.1538
2330	60	0	10000	-0.1605
2335	60	0	10000	-0.1674
2340	60	0	10000	-0.174
2345	60	0	10000	-0.1801
2350	60	0	10000	-0.1854
2355	60	0	10000	-0.1901
2360	60	0	10000	-0.194
2365	60	0	10000	-0.1974
2370	60	0	10000	-0.2001
2375	60	0	10000	-0.2024
2380	60	0	10000	-0.2043
2385	60	0	10000	-0.2058
2390	60	0	10000	-0.2071
2395	60	0	10000	-0.208
2400	60	0	10000	-0.2088
2405	60	0	10000	-0.2094
2410	60	0	10000	-0.2099
2415	60	0	10000	-0.2102
2420	60	0	10000	-0.2104
2425	60	0	10000	-0.2106
2430	60	0	10000	-0.2107
2435	60	0	10000	-0.2108
2440	60	0	10000	-0.2108
2445	60	0	10000	-0.2109
2450	60	0	10000	-0.2109
2455	60	0	10000	-0.2109
2460	60	0	10000	-0.2109
2465	60	0	10000	-0.2109
2470	60	0	10000	-0.2108
2475	60	0	10000	-0.2109
2480	60	0	10000	-0.2109
2485	60	0	10000	-0.2109
2490	60	0	10000	-0.2109
2495	60	0	10000	-0.2109
2500	0	0	10000	-0.211
2505.1433	0	0	10000	1.1243
2510	0	0	10000	1.5278
2515.1158	0	0	10000	1.5697
2520	0	0	10000	1.4596
2526.3794	0	0	10000	1.2455

2530	0	0	10000	1.1181
2534.2731	0	0	10000	0.9746
2540	0	0	10000	0.801
2543.6346	0	0	10000	0.7035
2550	0	0	10000	0.5567
2555	0	0	10000	0.461
2560	0	0	10000	0.3807
2565	0	0	10000	0.3137
2570	0	0	10000	0.2582
2575	0	0	10000	0.2122
2580	0	0	10000	0.1744
2585	0	0	10000	0.1432
2590	0	0	10000	0.1176
2595	0	0	10000	0.0966
2600	0	0	10000	0.0794
2605	0	0	10000	0.0653
2610	0	0	10000	0.0537
2615	0	0	10000	0.0441
2620	0	0	10000	0.0363
2625	0	0	10000	0.0299
2630	0	0	10000	0.0246
2635	0	0	10000	0.0202
2640	0	0	10000	0.0166
2645	0	0	10000	0.0137
2650	0	0	10000	0.0113
2655	0	0	10000	0.0093
2660	0	0	10000	0.0076
2665	0	0	10000	0.0062
2670	0	0	10000	0.0051
2675	0	0	10000	0.0042
2680	0	0	10000	0.0034
2685	0	0	10000	0.0028
2690	0	0	10000	0.0023
2695	0	0	10000	0.0018
2700	30	0	20000	0.0015
2705.2807	30	0	20000	0.0187
2710	30	0	20000	0.019
2713.7339	30	0	20000	0.0188
2720	30	0	20000	0.0201
2725	30	0	20000	0.0225
2730	30	0	20000	0.0253
2735	30	0	20000	0.0278
2740	30	0	20000	0.0296

2745	30	0	20000	0.0304
2750	30	0	20000	0.0303
2755	30	0	20000	0.0294
2760	30	0	20000	0.0173
2765.0754	30	0	20000	-0.0132
2770	30	0	20000	-0.0389
2775	30	0	20000	-0.0615
2780	30	0	20000	-0.081
2785	30	0	20000	-0.0979
2790	30	0	20000	-0.1125
2795	30	0	20000	-0.125
2800	30	0	20000	-0.1358
2805	30	0	20000	-0.145
2810	30	0	20000	-0.1529
2815	30	0	20000	-0.1597
2820	30	0	20000	-0.1654
2825	30	0	20000	-0.1703
2830	30	0	20000	-0.1744
2835	30	0	20000	-0.1779
2840	30	0	20000	-0.1808
2845	30	0	20000	-0.1833
2850	30	0	20000	-0.1854
2855	30	0	20000	-0.1871
2860	30	0	20000	-0.1886
2865	30	0	20000	-0.1898
2870	30	0	20000	-0.1908
2875	30	0	20000	-0.1917
2880	30	0	20000	-0.1924
2885	30	0	20000	-0.1929
2890	30	0	20000	-0.1934
2895	30	0	20000	-0.1938
2900	30	10.45	0	-0.1941
2905.3936	30	10.45	0	-0.2942
2910	30	10.45	0	-0.3628
2914.912	30	10.45	0	-0.4109
2920	30	10.45	0	-0.4353
2923.9783	30	10.45	0	-0.4401
2930	30	10.45	0	-0.4307
2935	30	10.45	0	-0.4131
2940	30	10.45	0	-0.3909
2945	30	10.45	0	-0.3668
2950	30	10.45	0	-0.3426
2955	30	10.45	0	-0.3195

2960	30	10.45	0	-0.2981
2965	30	10.45	0	-0.2787
2970	30	10.45	0	-0.2615
2975	30	10.45	0	-0.2464
2980	30	10.45	0	-0.2333
2985	30	10.45	0	-0.2221
2990	30	10.45	0	-0.2126
2995	30	10.45	0	-0.2046
3000	30	10.45	0	-0.1979
3005	30	10.45	0	-0.1924
3010	30	10.45	0	-0.1878
3015	30	10.45	0	-0.184
3020	30	10.45	0	-0.181
3025	30	10.45	0	-0.1785
3030	30	10.45	0	-0.1765
3035	30	10.45	0	-0.175
3040	30	10.45	0	-0.1738
3045	30	10.45	0	-0.1728
3050	30	10.45	0	-0.1721
3055	30	10.45	0	-0.1716
3060	30	10.45	0	-0.1712
3065	30	10.45	0	-0.1709
3070	30	10.45	0	-0.1708
3075	30	10.45	0	-0.1707
3080	30	10.45	0	-0.1707
3085	30	10.45	0	-0.1707
3090	30	10.45	0	-0.1707
3095	30	10.45	0	-0.1708
3100	0	0	20000	-0.1709
3105.9555	0	0	20000	1.2091
3110	0	0	20000	1.4842
3111.2654	0	0	20000	1.5153
3113.7005	0	0	20000	1.5311
3120	0	0	20000	1.4201
3124.2475	0	0	20000	1.2945
3130	0	0	20000	1.114
3135	0	0	20000	0.9644
3140	0	0	20000	0.8281
3145	0	0	20000	0.707
3150	0	0	20000	0.6008
3155	0	0	20000	0.5087
3160	0	0	20000	0.4294
3165	0	0	20000	0.3614

3170	0	0	20000	0.3034
3175	0	0	20000	0.2541
3180	0	0	20000	0.2123
3185	0	0	20000	0.177
3190	0	0	20000	0.1472
3195	0	0	20000	0.1221
3200	0	0	20000	0.1011
3205	0	0	20000	0.0834
3210	0	0	20000	0.0686
3215	0	0	20000	0.0562
3220	0	0	20000	0.0459
3225	0	0	20000	0.0373
3230	0	0	20000	0.0302
3235	0	0	20000	0.0243
3240	0	0	20000	0.0193
3245	0	0	20000	0.0153
3250	0	0	20000	0.0119
3255	0	0	20000	0.0092
3260	0	0	20000	0.0069
3265	0	0	20000	0.0051
3270	0	0	20000	0.0036
3275	0	0	20000	0.0024
3280	0	0	20000	0.0014
3285	0	0	20000	0.0007
3290	0	0	20000	0.0001
3295	0	0	20000	-0.0004
3300	60	0	20000	-0.0008
3305.3279	60	0	20000	-0.0415
3310	60	0	20000	-0.0686
3316.5062	60	0	20000	-0.0754
3320	60	0	20000	-0.0688
3324.8946	60	0	20000	-0.0534
3330	60	0	20000	-0.0471
3336.3138	60	0	20000	-0.0582
3340	60	0	20000	-0.0634
3345	60	0	20000	-0.0702
3350	60	0	20000	-0.0774
3355	60	0	20000	-0.0852
3360	60	0	20000	-0.0935
3365	60	0	20000	-0.1021
3370	60	0	20000	-0.1108
3375	60	0	20000	-0.1195
3380	60	0	20000	-0.1279

3385	60	0	20000	-0.136
3390	60	0	20000	-0.1435
3395	60	0	20000	-0.1505
3400	60	0	20000	-0.1569
3405	60	0	20000	-0.1627
3410	60	0	20000	-0.168
3415	60	0	20000	-0.1727
3420	60	0	20000	-0.1768
3425	60	0	20000	-0.1805
3430	60	0	20000	-0.1838
3435	60	0	20000	-0.1866
3440	60	0	20000	-0.1891
3445	60	0	20000	-0.1913
3450	60	0	20000	-0.1932
3455	60	0	20000	-0.1948
3460	60	0	20000	-0.1963
3465	60	0	20000	-0.1975
3470	60	0	20000	-0.1986
3475	60	0	20000	-0.1995
3480	60	0	20000	-0.2003
3485	60	0	20000	-0.201
3490	60	0	20000	-0.2016
3495	60	0	20000	-0.2021
3500	60	10.45	0	-0.2025
3505.3936	60	10.45	0	-0.2998
3510	60	10.45	0	-0.3661
3514.912	60	10.45	0	-0.4126
3520	60	10.45	0	-0.4364
3523.9783	60	10.45	0	-0.4414
3530	60	10.45	0	-0.4328
3535	60	10.45	0	-0.4163
3540	60	10.45	0	-0.3952
3545	60	10.45	0	-0.3722
3550	60	10.45	0	-0.349
3555	60	10.45	0	-0.3267
3560	60	10.45	0	-0.3059
3565	60	10.45	0	-0.287
3570	60	10.45	0	-0.2701
3575	60	10.45	0	-0.2553
3580	60	10.45	0	-0.2424
3585	60	10.45	0	-0.2312
3590	60	10.45	0	-0.2218
3595	60	10.45	0	-0.2137

3600	60	10.45	0	-0.207
3605	60	10.45	0	-0.2014
3610	60	10.45	0	-0.1968
3615	60	10.45	0	-0.193
3620	60	10.45	0	-0.1899
3625	60	10.45	0	-0.1874
3630	60	10.45	0	-0.1854
3635	60	10.45	0	-0.1838
3640	60	10.45	0	-0.1826
3645	60	10.45	0	-0.1816
3650	60	10.45	0	-0.1809
3655	60	10.45	0	-0.1804
3660	60	10.45	0	-0.18
3665	60	10.45	0	-0.1797
3670	60	10.45	0	-0.1796
3675	60	10.45	0	-0.1795
3680	60	10.45	0	-0.1794
3685	60	10.45	0	-0.1794
3690	60	10.45	0	-0.1795
3695	60	10.45	0	-0.1795
3700	0	10.45	0	-0.1796
3705.1433	0	10.45	0	1.1396
3710	0	10.45	0	1.5142
3715.1158	0	10.45	0	1.5265
3720	0	10.45	0	1.3948
3726.5144	0	10.45	0	1.1582
3730	0	10.45	0	1.0307
3733.2392	0	10.45	0	0.9188
3740	0	10.45	0	0.7123
3745	0	10.45	0	0.5848
3750	0	10.45	0	0.4775
3755	0	10.45	0	0.3884
3760	0	10.45	0	0.315
3765	0	10.45	0	0.255
3770	0	10.45	0	0.2061
3775	0	10.45	0	0.1664
3780	0	10.45	0	0.1344
3785	0	10.45	0	0.1085
3790	0	10.45	0	0.0876
3795	0	10.45	0	0.0708
3800	0	10.45	0	0.0572
3805	0	10.45	0	0.0463
3810	0	10.45	0	0.0375

3815	0	10.45	0	0.0304
3820	0	10.45	0	0.0247
3825	0	10.45	0	0.0201
3830	0	10.45	0	0.0164
3835	0	10.45	0	0.0134
3840	0	10.45	0	0.0109
3845	0	10.45	0	0.009
3850	0	10.45	0	0.0074
3855	0	10.45	0	0.006
3860	0	10.45	0	0.005
3865	0	10.45	0	0.0041
3870	0	10.45	0	0.0034
3875	0	10.45	0	0.0028
3880	0	10.45	0	0.0024
3885	0	10.45	0	0.002
3890	0	10.45	0	0.0016
3895	0	10.45	0	0.0014
3900	30	10.45	10000	0.0012
3905.2806	30	10.45	10000	0.023
3910	30	10.45	10000	0.0244
3913.9274	30	10.45	10000	0.0237
3920	30	10.45	10000	0.0229
3925	30	10.45	10000	0.023
3930	30	10.45	10000	0.0234
3935	30	10.45	10000	0.0238
3940	30	10.45	10000	0.0238
3945	30	10.45	10000	0.0233
3950	30	10.45	10000	0.0223
3955	30	10.45	10000	0.0209
3960	30	10.45	10000	0.0085
3965.0754	30	10.45	10000	-0.0216
3970	30	10.45	10000	-0.0462
3975	30	10.45	10000	-0.0674
3980	30	10.45	10000	-0.0853
3985	30	10.45	10000	-0.1003
3990	30	10.45	10000	-0.113
3995	30	10.45	10000	-0.1236
4000	30	10.45	10000	-0.1326
4005	30	10.45	10000	-0.14
4010	30	10.45	10000	-0.1463
4015	30	10.45	10000	-0.1515
4020	30	10.45	10000	-0.1558
4025	30	10.45	10000	-0.1594

4030	30	10.45	10000	-0.1623
4035	30	10.45	10000	-0.1648
4040	30	10.45	10000	-0.1668
4045	30	10.45	10000	-0.1684
4050	30	10.45	10000	-0.1697
4055	30	10.45	10000	-0.1708
4060	30	10.45	10000	-0.1717
4065	30	10.45	10000	-0.1724
4070	30	10.45	10000	-0.173
4075	30	10.45	10000	-0.1734
4080	30	10.45	10000	-0.1737
4085	30	10.45	10000	-0.174
4090	30	10.45	10000	-0.1742
4095	30	10.45	10000	-0.1744
4100	30	10.45	20000	-0.1745
4105	30	10.45	20000	-0.1364
4110	30	10.45	20000	-0.1207
4115	30	10.45	20000	-0.1174
4120	30	10.45	20000	-0.1206
4125	30	10.45	20000	-0.127
4130	30	10.45	20000	-0.1345
4135	30	10.45	20000	-0.142
4140	30	10.45	20000	-0.149
4145	30	10.45	20000	-0.1552
4150	30	10.45	20000	-0.1605
4155	30	10.45	20000	-0.165
4160	30	10.45	20000	-0.1688
4165	30	10.45	20000	-0.1718
4170	30	10.45	20000	-0.1743
4175	30	10.45	20000	-0.1762
4180	30	10.45	20000	-0.1778
4185	30	10.45	20000	-0.179
4190	30	10.45	20000	-0.1799
4195	30	10.45	20000	-0.1806
4200	30	10.45	20000	-0.1811
4205	30	10.45	20000	-0.1815
4210	30	10.45	20000	-0.1818
4215	30	10.45	20000	-0.182
4220	30	10.45	20000	-0.1821
4225	30	10.45	20000	-0.1822
4230	30	10.45	20000	-0.1823
4235	30	10.45	20000	-0.1823
4240	30	10.45	20000	-0.1823

4245	30	10.45	20000	-0.1823
4250	30	10.45	20000	-0.1824
4255	30	10.45	20000	-0.1824
4260	30	10.45	20000	-0.1824
4265	30	10.45	20000	-0.1824
4270	30	10.45	20000	-0.1825
4275	30	10.45	20000	-0.1825
4280	30	10.45	20000	-0.1826
4285	30	10.45	20000	-0.1826
4290	30	10.45	20000	-0.1827
4295	30	10.45	20000	-0.1827
4300	0	10.45	10000	-0.1828
4305.9555	0	10.45	10000	1.0638
4310	0	10.45	10000	1.2908
4315.2691	0	10.45	10000	1.2891
4320	0	10.45	10000	1.1728
4326.2706	0	10.45	10000	0.9762
4330	0	10.45	10000	0.8606
4334.9924	0	10.45	10000	0.7194
4340	0	10.45	10000	0.5963
4345.9501	0	10.45	10000	0.4739
4350	0	10.45	10000	0.4043
4355	0	10.45	10000	0.3316
4360	0	10.45	10000	0.2716
4365	0	10.45	10000	0.2223
4370	0	10.45	10000	0.1819
4375	0	10.45	10000	0.1489
4380	0	10.45	10000	0.1219
4385	0	10.45	10000	0.0999
4390	0	10.45	10000	0.082
4395	0	10.45	10000	0.0674
4400	0	10.45	10000	0.0554
4405	0	10.45	10000	0.0457
4410	0	10.45	10000	0.0377
4415	0	10.45	10000	0.0312
4420	0	10.45	10000	0.0259
4425	0	10.45	10000	0.0215
4430	0	10.45	10000	0.018
4435	0	10.45	10000	0.015
4440	0	10.45	10000	0.0126
4445	0	10.45	10000	0.0106
4450	0	10.45	10000	0.0089
4455	0	10.45	10000	0.0076

4460	0	10.45	10000	0.0064
4465	0	10.45	10000	0.0055
4470	0	10.45	10000	0.0047
4475	0	10.45	10000	0.004
4480	0	10.45	10000	0.0035
4485	0	10.45	10000	0.003
4490	0	10.45	10000	0.0026
4495	0	10.45	10000	0.0023
4500	60	10.45	10000	0.002
4505.3279	60	10.45	10000	-0.0385
4510	60	10.45	10000	-0.0658
4516.8776	60	10.45	10000	-0.0739
4520	60	10.45	10000	-0.0691
4524.9032	60	10.45	10000	-0.056
4530	60	10.45	10000	-0.0523
4536.3138	60	10.45	10000	-0.0657
4540	60	10.45	10000	-0.0717
4545	60	10.45	10000	-0.079
4550	60	10.45	10000	-0.0861
4555	60	10.45	10000	-0.0932
4560	60	10.45	10000	-0.1004
4565	60	10.45	10000	-0.1077
4570	60	10.45	10000	-0.1148
4575	60	10.45	10000	-0.1217
4580	60	10.45	10000	-0.1283
4585	60	10.45	10000	-0.1345
4590	60	10.45	10000	-0.1402
4595	60	10.45	10000	-0.1454
4600	60	10.45	10000	-0.1501
4605	60	10.45	10000	-0.1543
4610	60	10.45	10000	-0.1581
4615	60	10.45	10000	-0.1614
4620	60	10.45	10000	-0.1642
4625	60	10.45	10000	-0.1668
4630	60	10.45	10000	-0.1689
4635	60	10.45	10000	-0.1708
4640	60	10.45	10000	-0.1725
4645	60	10.45	10000	-0.1739
4650	60	10.45	10000	-0.1751
4655	60	10.45	10000	-0.1761
4660	60	10.45	10000	-0.177
4665	60	10.45	10000	-0.1778
4670	60	10.45	10000	-0.1784

4675	60	10.45	10000	-0.179
4680	60	10.45	10000	-0.1795
4685	60	10.45	10000	-0.1799
4690	60	10.45	10000	-0.1802
4695	60	10.45	10000	-0.1806
4700	60	10.45	20000	-0.1808
4705	60	10.45	20000	-0.1442
4710	60	10.45	20000	-0.1289
4715	60	10.45	20000	-0.1256
4720	60	10.45	20000	-0.1287
4725	60	10.45	20000	-0.1348
4730	60	10.45	20000	-0.1421
4735	60	10.45	20000	-0.1495
4740	60	10.45	20000	-0.1564
4745	60	10.45	20000	-0.1626
4750	60	10.45	20000	-0.1681
4755	60	10.45	20000	-0.1727
4760	60	10.45	20000	-0.1765
4765	60	10.45	20000	-0.1797
4770	60	10.45	20000	-0.1823
4775	60	10.45	20000	-0.1845
4780	60	10.45	20000	-0.1862
4785	60	10.45	20000	-0.1876
4790	60	10.45	20000	-0.1887
4795	60	10.45	20000	-0.1895
4800	60	10.45	20000	-0.1902
4805	60	10.45	20000	-0.1908
4810	60	10.45	20000	-0.1912
4815	60	10.45	20000	-0.1915
4820	60	10.45	20000	-0.1918
4825	60	10.45	20000	-0.192
4830	60	10.45	20000	-0.1921
4835	60	10.45	20000	-0.1923
4840	60	10.45	20000	-0.1924
4845	60	10.45	20000	-0.1924
4850	60	10.45	20000	-0.1925
4855	60	10.45	20000	-0.1926
4860	60	10.45	20000	-0.1926
4865	60	10.45	20000	-0.1927
4870	60	10.45	20000	-0.1927
4875	60	10.45	20000	-0.1928
4880	60	10.45	20000	-0.1928
4885	60	10.45	20000	-0.1928

4890	60	10.45	20000	-0.1928
4895	60	10.45	20000	-0.1927
4900	0	10.45	20000	-0.1927
4905.1433	0	10.45	20000	1.1299
4910	0	10.45	20000	1.5153
4915.1158	0	10.45	20000	1.5405
4920	0	10.45	20000	1.4179
4926.5144	0	10.45	20000	1.1872
4930	0	10.45	20000	1.0603
4933.1537	0	10.45	20000	0.9507
4940	0	10.45	20000	0.7379
4945	0	10.45	20000	0.6068
4950	0	10.45	20000	0.4957
4955	0	10.45	20000	0.4029
4960	0	10.45	20000	0.3261
4965	0	10.45	20000	0.263
4970	0	10.45	20000	0.2115
4975	0	10.45	20000	0.1697
4980	0	10.45	20000	0.1358
4985	0	10.45	20000	0.1085
4990	0	10.45	20000	0.0865
4995	0	10.45	20000	0.0689
5000	0	10.45	20000	0.0547
5005	0	10.45	20000	0.0433
5010	0	10.45	20000	0.0342
5015	0	10.45	20000	0.027
5020	0	10.45	20000	0.0212
5025	0	10.45	20000	0.0165
5030	0	10.45	20000	0.0128
5035	0	10.45	20000	0.0099
5040	0	10.45	20000	0.0076
5045	0	10.45	20000	0.0057
5050	0	10.45	20000	0.0042
5055	0	10.45	20000	0.0031
5060	0	10.45	20000	0.0022
5065	0	10.45	20000	0.0015
5070	0	10.45	20000	0.0009
5075	0	10.45	20000	0.0005
5080	0	10.45	20000	0.0001
5085	0	10.45	20000	-0.0001
5090	0	10.45	20000	-0.0003
5095	0	10.45	20000	-0.0004
5100	30	20.9	0	-0.0005

5105.2807	30	20.9	0	-0.1286
5110	30	20.9	0	-0.2171
5116.1144	30	20.9	0	-0.2785
5120	30	20.9	0	-0.2914
5124.831	30	20.9	0	-0.2876
5130	30	20.9	0	-0.268
5135.0712	30	20.9	0	-0.2404
5140	30	20.9	0	-0.2107
5145	30	20.9	0	-0.1807
5150	30	20.9	0	-0.1524
5155	30	20.9	0	-0.1269
5160	30	20.9	0	-0.1149
5165.0754	30	20.9	0	-0.1228
5170	30	20.9	0	-0.1284
5175	30	20.9	0	-0.1325
5180	30	20.9	0	-0.1355
5185	30	20.9	0	-0.1379
5190	30	20.9	0	-0.1397
5195	30	20.9	0	-0.1411
5200	30	20.9	0	-0.1423
5205	30	20.9	0	-0.1433
5210	30	20.9	0	-0.1442
5215	30	20.9	0	-0.145
5220	30	20.9	0	-0.1457
5225	30	20.9	0	-0.1463
5230	30	20.9	0	-0.1469
5235	30	20.9	0	-0.1475
5240	30	20.9	0	-0.1481
5245	30	20.9	0	-0.1486
5250	30	20.9	0	-0.1491
5255	30	20.9	0	-0.1495
5260	30	20.9	0	-0.1499
5265	30	20.9	0	-0.1504
5270	30	20.9	0	-0.1507
5275	30	20.9	0	-0.1511
5280	30	20.9	0	-0.1515
5285	30	20.9	0	-0.1518
5290	30	20.9	0	-0.1521
5295	30	20.9	0	-0.1524
5300	30	20.9	10000	-0.1527
5305	30	20.9	10000	-0.1108
5310	30	20.9	10000	-0.0945
5315	30	20.9	10000	-0.0923

5320	30	20.9	10000	-0.0974
5325	30	20.9	10000	-0.1057
5330	30	20.9	10000	-0.115
5335	30	20.9	10000	-0.124
5340	30	20.9	10000	-0.1321
5345	30	20.9	10000	-0.1392
5350	30	20.9	10000	-0.145
5355	30	20.9	10000	-0.1498
5360	30	20.9	10000	-0.1536
5365	30	20.9	10000	-0.1566
5370	30	20.9	10000	-0.1589
5375	30	20.9	10000	-0.1606
5380	30	20.9	10000	-0.1618
5385	30	20.9	10000	-0.1627
5390	30	20.9	10000	-0.1633
5395	30	20.9	10000	-0.1637
5400	30	20.9	10000	-0.1639
5405	30	20.9	10000	-0.164
5410	30	20.9	10000	-0.164
5415	30	20.9	10000	-0.1639
5420	30	20.9	10000	-0.1638
5425	30	20.9	10000	-0.1636
5430	30	20.9	10000	-0.1634
5435	30	20.9	10000	-0.1633
5440	30	20.9	10000	-0.1631
5445	30	20.9	10000	-0.1629
5450	30	20.9	10000	-0.1627
5455	30	20.9	10000	-0.1625
5460	30	20.9	10000	-0.1623
5465	30	20.9	10000	-0.1622
5470	30	20.9	10000	-0.162
5475	30	20.9	10000	-0.1618
5480	30	20.9	10000	-0.1617
5485	30	20.9	10000	-0.1615
5490	30	20.9	10000	-0.1614
5495	30	20.9	10000	-0.1612
5500	0	20.9	20000	-0.1611
5504.6766	0	20.9	20000	0.9942
5510	0	20.9	20000	1.3759
5515.2691	0	20.9	20000	1.3586
5520	0	20.9	20000	1.2228
5526.2706	0	20.9	20000	1.0008
5530	0	20.9	20000	0.872

5535.4192	0	20.9	20000	0.7037
5540	0	20.9	20000	0.5813
5545	0	20.9	20000	0.4684
5550	0	20.9	20000	0.375
5555	0	20.9	20000	0.2987
5560	0	20.9	20000	0.2368
5565	0	20.9	20000	0.1869
5570	0	20.9	20000	0.1468
5575	0	20.9	20000	0.1148
5580	0	20.9	20000	0.0894
5585	0	20.9	20000	0.0691
5590	0	20.9	20000	0.0531
5595	0	20.9	20000	0.0405
5600	0	20.9	20000	0.0305
5605	0	20.9	20000	0.0227
5610	0	20.9	20000	0.0166
5615	0	20.9	20000	0.0119
5620	0	20.9	20000	0.0082
5625	0	20.9	20000	0.0054
5630	0	20.9	20000	0.0032
5635	0	20.9	20000	0.0015
5640	0	20.9	20000	0.0003
5645	0	20.9	20000	-0.0006
5650	0	20.9	20000	-0.0013
5655	0	20.9	20000	-0.0018
5660	0	20.9	20000	-0.0021
5665	0	20.9	20000	-0.0023
5670	0	20.9	20000	-0.0025
5675	0	20.9	20000	-0.0025
5680	0	20.9	20000	-0.0025
5685	0	20.9	20000	-0.0025
5690	0	20.9	20000	-0.0024
5695	0	20.9	20000	-0.0024
5700	60	20.9	10000	-0.0023
5705.328	60	20.9	10000	-0.0847
5710	60	20.9	10000	-0.1266
5713.893	60	20.9	10000	-0.1384
5720	60	20.9	10000	-0.13
5724.9303	60	20.9	10000	-0.1109
5730	60	20.9	10000	-0.1002
5736.3138	60	20.9	10000	-0.1044
5740	60	20.9	10000	-0.1052
5745	60	20.9	10000	-0.106

5750	60	20.9	10000	-0.1071
5755	60	20.9	10000	-0.1088
5760	60	20.9	10000	-0.1112
5765	60	20.9	10000	-0.1142
5770	60	20.9	10000	-0.1176
5775	60	20.9	10000	-0.1212
5780	60	20.9	10000	-0.1249
5785	60	20.9	10000	-0.1286
5790	60	20.9	10000	-0.1321
5795	60	20.9	10000	-0.1354
5800	60	20.9	10000	-0.1385
5805	60	20.9	10000	-0.1413
5810	60	20.9	10000	-0.1439
5815	60	20.9	10000	-0.1462
5820	60	20.9	10000	-0.1482
5825	60	20.9	10000	-0.15
5830	60	20.9	10000	-0.1517
5835	60	20.9	10000	-0.1531
5840	60	20.9	10000	-0.1544
5845	60	20.9	10000	-0.1555
5850	60	20.9	10000	-0.1565
5855	60	20.9	10000	-0.1573
5860	60	20.9	10000	-0.1581
5865	60	20.9	10000	-0.1588
5870	60	20.9	10000	-0.1594
5875	60	20.9	10000	-0.16
5880	60	20.9	10000	-0.1605
5885	60	20.9	10000	-0.1609
5890	60	20.9	10000	-0.1614
5895	60	20.9	10000	-0.1617
5900	0	20.9	10000	-0.1621
5905.319	0	20.9	10000	0.4903
5910	0	20.9	10000	0.669
5915.8715	0	20.9	10000	0.6751
5920	0	20.9	10000	0.6194
5927.841	0	20.9	10000	0.481
5930	0	20.9	10000	0.4427
5935	0	20.9	10000	0.3602
5940	0	20.9	10000	0.2884
5945	0	20.9	10000	0.228
5950	0	20.9	10000	0.1785
5955	0	20.9	10000	0.1386
5960	0	20.9	10000	0.1068

5965	0	20.9	10000	0.0817
5970	0	20.9	10000	0.0621
5975	0	20.9	10000	0.047
5980	0	20.9	10000	0.0354
5985	0	20.9	10000	0.0265
5990	0	20.9	10000	0.0197
5995	0	20.9	10000	0.0146
6000	0	20.9	10000	0.0107
6005	0	20.9	10000	0.0078
6010	0	20.9	10000	0.0057
6015	0	20.9	10000	0.0041
6020	0	20.9	10000	0.0029
6025	0	20.9	10000	0.002
6030	0	20.9	10000	0.0014
6035	0	20.9	10000	0.0009
6040	0	20.9	10000	0.0006
6045	0	20.9	10000	0.0004
6050	0	20.9	10000	0.0002
6055	0	20.9	10000	0.0001
6060	0	20.9	10000	0
6065	0	20.9	10000	0
6070	0	20.9	10000	-0.0001
6075	0	20.9	10000	-0.0001
6080	0	20.9	10000	-0.0001
6085	0	20.9	10000	-0.0001
6090	0	20.9	10000	-0.0001
6095	0	20.9	10000	-0.0001
6100	60	20.9	0	-0.0001
6105.3281	60	20.9	0	-0.084
6110	60	20.9	0	-0.1262
6113.8933	60	20.9	0	-0.138
6120	60	20.9	0	-0.1293
6124.9302	60	20.9	0	-0.1098
6130	60	20.9	0	-0.0989
6136.3138	60	20.9	0	-0.103
6140	60	20.9	0	-0.1038
6145	60	20.9	0	-0.1046
6150	60	20.9	0	-0.1058
6155	60	20.9	0	-0.1076
6160	60	20.9	0	-0.1102
6165	60	20.9	0	-0.1134
6170	60	20.9	0	-0.1169
6175	60	20.9	0	-0.1206

6180	60	20.9	0	-0.1244
6185	60	20.9	0	-0.1281
6190	60	20.9	0	-0.1317
6195	60	20.9	0	-0.135
6200	60	20.9	0	-0.1381
6205	60	20.9	0	-0.1409
6210	60	20.9	0	-0.1435
6215	60	20.9	0	-0.1457
6220	60	20.9	0	-0.1477
6225	60	20.9	0	-0.1495
6230	60	20.9	0	-0.1511
6235	60	20.9	0	-0.1525
6240	60	20.9	0	-0.1537
6245	60	20.9	0	-0.1547
6250	60	20.9	0	-0.1557
6255	60	20.9	0	-0.1565
6260	60	20.9	0	-0.1572
6265	60	20.9	0	-0.1578
6270	60	20.9	0	-0.1584
6275	60	20.9	0	-0.1588
6280	60	20.9	0	-0.1593
6285	60	20.9	0	-0.1596
6290	60	20.9	0	-0.16
6295	60	20.9	0	-0.1603
6300	0	20.9	0	-0.1605
6305.319	0	20.9	0	0.4916
6310	0	20.9	0	0.6694
6315.8715	0	20.9	0	0.6737
6320	0	20.9	0	0.617
6322.841	0	20.9	0	0.5681
6330	0	20.9	0	0.439
6335	0	20.9	0	0.3565
6340	0	20.9	0	0.2851
6345	0	20.9	0	0.2252
6350	0	20.9	0	0.1762
6355	0	20.9	0	0.1368
6360	0	20.9	0	0.1055
6365	0	20.9	0	0.0809
6370	0	20.9	0	0.0617
6375	0	20.9	0	0.0469
6380	0	20.9	0	0.0355
6385	0	20.9	0	0.0268
6390	0	20.9	0	0.0202

6395	0	20.9	0	0.0151
6400	0	20.9	0	0.0113
6405	0	20.9	0	0.0085
6410	0	20.9	0	0.0063
6415	0	20.9	0	0.0047
6420	0	20.9	0	0.0035
6425	0	20.9	0	0.0027
6430	0	20.9	0	0.002
6435	0	20.9	0	0.0015
6440	0	20.9	0	0.0011
6445	0	20.9	0	0.0009
6450	0	20.9	0	0.0007
6455	0	20.9	0	0.0005
6460	0	20.9	0	0.0004
6465	0	20.9	0	0.0003
6470	0	20.9	0	0.0003
6475	0	20.9	0	0.0002
6480	0	20.9	0	0.0002
6485	0	20.9	0	0.0002
6490	0	20.9	0	0.0001
6495	0	20.9	0	0.0001
6500	30	20.9	20000	0.0001
6505.2807	30	20.9	20000	0.0683
6510	30	20.9	20000	0.0849
6514.9442	30	20.9	20000	0.0856
6520	30	20.9	20000	0.0787
6526.6732	30	20.9	20000	0.0662
6530	30	20.9	20000	0.0598
6535	30	20.9	20000	0.0506
6540	30	20.9	20000	0.0423
6545	30	20.9	20000	0.0349
6550	30	20.9	20000	0.0283
6555	30	20.9	20000	0.0224
6560	30	20.9	20000	0.0067
6565.0754	30	20.9	20000	-0.0254
6570	30	20.9	20000	-0.0509
6575	30	20.9	20000	-0.0723
6580	30	20.9	20000	-0.0897
6585	30	20.9	20000	-0.104
6590	30	20.9	20000	-0.1157
6595	30	20.9	20000	-0.1252
6600	30	20.9	20000	-0.1329
6605	30	20.9	20000	-0.1391

6610	30	20.9	20000	-0.1441
6615	30	20.9	20000	-0.1481
6620	30	20.9	20000	-0.1514
6625	30	20.9	20000	-0.1539
6630	30	20.9	20000	-0.1559
6635	30	20.9	20000	-0.1574
6640	30	20.9	20000	-0.1586
6645	30	20.9	20000	-0.1595
6650	30	20.9	20000	-0.1602
6655	30	20.9	20000	-0.1607
6660	30	20.9	20000	-0.1611
6665	30	20.9	20000	-0.1613
6670	30	20.9	20000	-0.1615
6675	30	20.9	20000	-0.1616
6680	30	20.9	20000	-0.1616
6685	30	20.9	20000	-0.1616
6690	30	20.9	20000	-0.1616
6695	30	20.9	20000	-0.1616
6700	60	20.9	20000	-0.1615
6705.2853	60	20.9	20000	-0.1817
6710	60	20.9	20000	-0.1966
6714.9439	60	20.9	20000	-0.2037
6720	60	20.9	20000	-0.2045
6726.6836	60	20.9	20000	-0.1999
6730	60	20.9	20000	-0.1965
6735	60	20.9	20000	-0.1911
6740	60	20.9	20000	-0.1859
6745	60	20.9	20000	-0.1812
6750	60	20.9	20000	-0.1774
6755	60	20.9	20000	-0.1743
6760	60	20.9	20000	-0.1719
6765	60	20.9	20000	-0.1702
6770	60	20.9	20000	-0.169
6775	60	20.9	20000	-0.1681
6780	60	20.9	20000	-0.1677
6785	60	20.9	20000	-0.1675
6790	60	20.9	20000	-0.1674
6795	60	20.9	20000	-0.1676
6800	60	20.9	20000	-0.1678
6805	60	20.9	20000	-0.168
6810	60	20.9	20000	-0.1684
6815	60	20.9	20000	-0.1687
6820	60	20.9	20000	-0.169

6825	60	20.9	20000	-0.1694
6830	60	20.9	20000	-0.1697
6835	60	20.9	20000	-0.17
6840	60	20.9	20000	-0.1702
6845	60	20.9	20000	-0.1705
6850	60	20.9	20000	-0.1707
6855	60	20.9	20000	-0.1708
6860	60	20.9	20000	-0.171
6865	60	20.9	20000	-0.1711
6870	60	20.9	20000	-0.1712
6875	60	20.9	20000	-0.1712
6880	60	20.9	20000	-0.1712
6885	60	20.9	20000	-0.1713
6890	60	20.9	20000	-0.1712
6895	60	20.9	20000	-0.1712
6900	60	20.9	20000	-0.1711

Works cited

1. Ahlborg, G., & Felig, P. (1986). *Splanchnic and peripheral glucose and lactate metabolism during and after prolonged arm exercise*. *J. Clin. Invest.* , 77, 690-699.
2. Alberts, B. (2002). *Molecular biology of the cell (4 ed.)*. Garland Science.
3. Andersen, P., Adams, G., Sjogaard, A., & Saltin, B. (1985). *Dynamic knee extension as model for study of isolated exercising muscle in humans*. *J. Appl. Physiol.* , 59, 1647-1653.
4. Bhandari, N. (2003). *Continuous-time multiple-input, multiple-outputs Wiener modeling method*. *Ind. Eng. Chem. Res.* , 42, 5583-5595.
5. Campos-Delgado, D. U. (2008). *Extension of the Run-to-Run control to multi-boluses schemes*. 17th IEEE International Conference on Control Applications, (págs. 678-683). San Antonio, United States of America.
6. Carvajal, A. E. (2009). *Non-invasive glucose sensor*. M.S. Thesis, ITESM, Monterrey.
7. Chapman, C. B., & Mitchell, J. H. (1965). *The physiology of exercise*. *Sci. Am.* , 212, 88-96.
8. Doyle, F., Jovanic, L., & Seborg, D. (2007). *Glucose control strategies for treating type 1 diabetes mellitus*. *Journal of Process Control* , 17, 571-576.
9. Dvorkin, & Cardinali. (2003). *Best & Taylor: Bases fisiológicas de la práctica médica (13 ed.)*. México: Editorial médica panamericana.
10. Eskinat, E. (1991). *Use of Hammerstein models in identification of nonlinear systems*. *AIChE Journal* , 37 (2), 255-268.
11. Felig, P., & J., W. (1975). *Fuel homeostasis in exercise*. *N. Engl. J. Med.* , 293, 1078-1084.
12. Firman, G. (2005). *InterMEDICINA*. Recuperado el 1 de 2009, de http://www.intermedicina.com/Avances/Interes_General/AIG05.html
13. Guyton, A., & Hall, J. (2001). *Textbook of medical physiology (10 ed.)*. United States of America: Saunders.
14. Keinitz, K. H. (1993). *A robust controller for insulin pumps based on H-infinity theory*. *IEEE transactions on Biomedical Engineering* , 40 (11), 1133-1137.
15. Khoo, M. C. (1999). *Physiological control systems*. Wiley interscience.
16. Kronenber, H. M. (2002). *Williams textbook of endocrinology (10 ed.)*. Saunders.

17. Lenart, P. j., & Parker, R. S. (2002). *Modeling exercise effects in type I diabetic patients*. 15th Triennial World Congress. Barcelona.
18. Ljung, L. (1999). *System identification: Theory for the user* (2 ed.). Prentice Hall.
19. LSU. (s.f.). Recuperado el May de 2009, de <http://www.mpri.lsu.edu/textbook/Chapter6.htm>
20. McKee, T., & McKee, J. (2003). *Biochemistry, the molecular basis of life* (3 ed.). United States of America: McGraw Hill.
21. Montgomery, D. C. (1985). *Diseño y análisis de experimentos*. Iberoamérica.
22. Murray, R. K. (1993). *Harper's Biochemistry*. Appleton & Lange.
23. Ogata, K. (2002). *Modern control engineering* (4 ed.). Prentice Hall.
24. Palerm, C. c., Zisser, H., Jovanovic, L., & Doyle, F. J. (2008). A run-to-run control strategy to adjust basal insulin infusion rates in type 1 diabetes. *Journal of Process Control* , 258-263.
25. Parker, R. S. (2000). Robust H infinite glucose control in diabetes using a physiological model. *AIChE Journal* , 46 (12), 2537-2549.
26. Pruetz, E. (1970). Glucose and insulin during prolonged work stress in men living on different diets. *J. Appl. Physiol.* , 28 (2), 199-208.
27. Ritter, P. (1996). *Biochemistry, a foundation*. United States of America: Brooks/Cole Publishing Company.
28. Rollins, D. K. (2004). Constrained MIMO dynamic discrete-time modeling exploiting optimal experimentatl design. *Journal of Process Control* , 14, 671-683.
29. Rollins, D. K., Bhandari, N., & Kotz, K. R. (2008). Critical modeling issues for succesful feedforward control of blood glucose in insulin dependent diabetics. *American control conference*, (págs. 832-837). Seattle.
30. Roy, A., & Parker, R. S. (2007). Dynamic modeling of exercise effects on plasma glucose and insulin levels. *Journal of diabetes science and technology* , 1 (3), 338-347.
31. Sánchez, I. Y. (2008). Glucose optimal control system in diabetes treatment. *Appl. Math. Comput.*
32. Sánchez-Chávez, I. Y. (2008). Computer evaluation of hydrogel-based systems for diabetes closed loop treatment. *AIChE Journal* , 54 (7), 1901-1911.
33. Skogestad, S. (2005). *Multivariable feedback control. Analysis and design* (2 ed.). Wiley.
34. Slotine, J.-J. E., & Li, W. (1991). *Applied nonlinear control* (1 ed.). Prentice Hall.

35. Smith, C. A., & Corripio, A. (2006). *Principles and practice of automatic process control (3 ed.)*. United States of America: Wiley.
36. Snyder, W. S. (1975). *Report of the task group on reference man: a report prepared by a task group of committee 2 of the international commission on radiological protection*. Oxford.
37. Sorensen, J. (1985). *A physiologic model of glucose metabolism in man and its use to design and assess improved insulin therapies for diabetes*. MIT, Dept. of Chemical Engineering.
38. Swain, D. P., Abernathy, K. S., Smith, C. S., Lee, S. J., & Bunn, S. A. (1994). *Target heart rates for the development of cardiorespiratory fitness*. *Medicine and Science in Sports and Exercise* , 112-116.
39. Wolfe, R. R. (1986). *Role of changes in insulin and glucagon in glucose homeostasis in exercise*. *J. Clin. Invest.* , 77 (3).
40. Yipintso, T., Gatewood, L., Ackerman, E., & Spivak, P. (1973). *Mathematical analysis of blood glucose and plasma insulin responses to insulin infusion in healthy and diabetic subjects*. *Computer in biology in medicine* , 3 (1), 71-80.

Tecnológico de Monterrey, Campus Monterrey



30002007255821

<http://biblioteca.mty.itesm.mx>